UiT
THE ARCTIC UNIVERSITY OF NORWAY

Faculty of Medical Biology

Characterization of ATG8 Family Protein Binding to TRIM23 and TRIM31

—

Heidi Isaksen

Master thesis in Biomedicine … May 2018

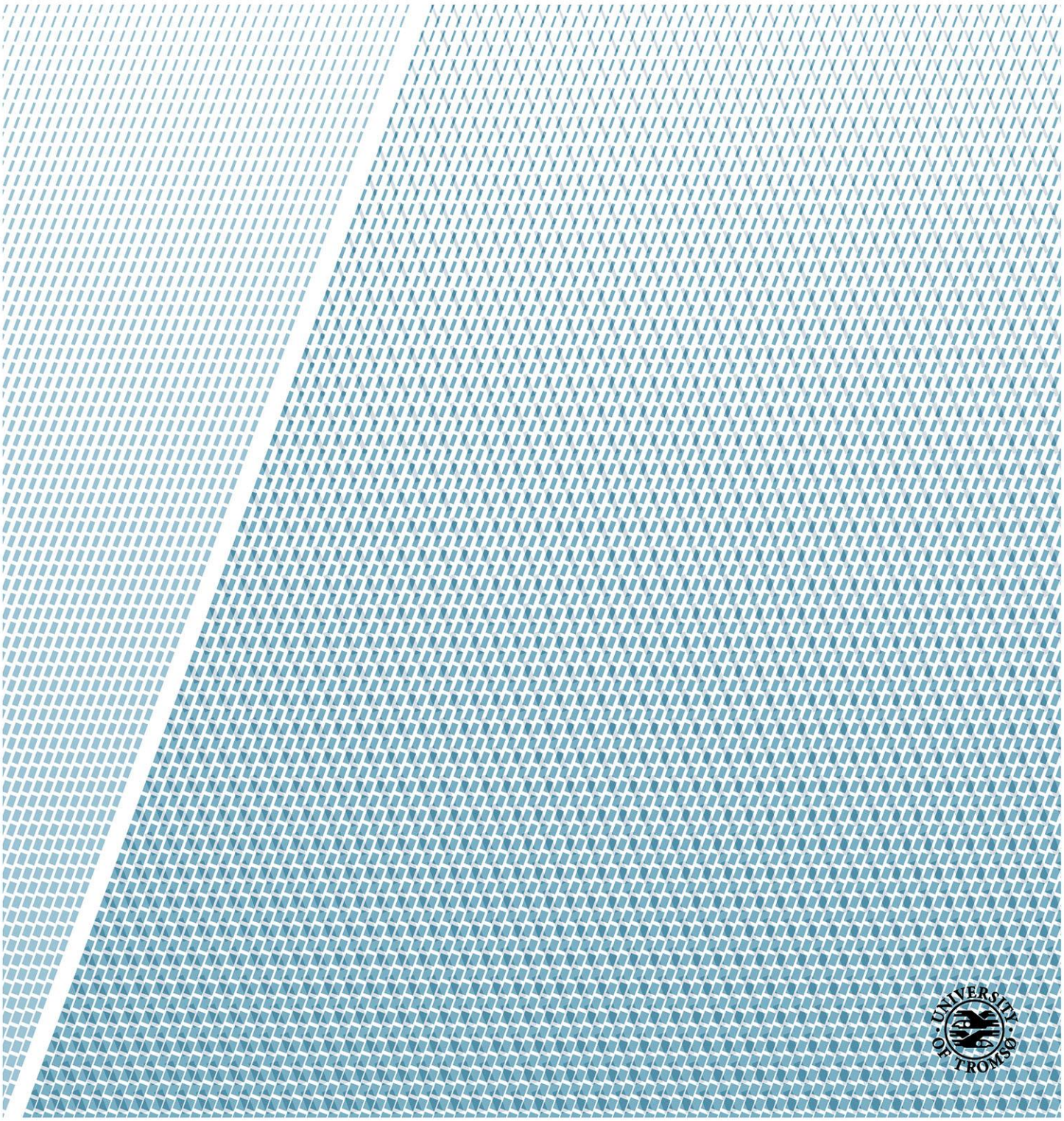

Acknowledgement

The work presented in this thesis was performed at Molecular Cancer Research Group, Institute of Medical Biology, University of Tromsø from August 2017 to May 2018.

First, I would like to thank my supervisor, Professor Terje Johansen, for all the help during and preliminary to this thesis, and my co-supervisor Associate Professor Eva Sjøttem for all help provided. You have both taught me a lot and been available for all my questions.

I will also thank all members of MCRG. There has always been someone at the laboratory, late nights, early mornings and weekends, you have all been very helpful. I never experienced a no when I needed help, and often I didn't even have to ask. A special thanks to Yakubu Abudu who gave me important insights in the experimental procedure of GST pulldown, Hanne Brenne who have helped me a lot with a variety of experimental procedures and always stayed positive, Aud Øvervatn who helped me with cell related experiments, Trond Lamark who are a great educator, and Apsana Lamsal, my fellow master student, which asked me questions I didn't even know I should have been asking. Gry Evjen deserves a lot more than a thank you. You have been amazing, always helping me, caring for my wellbeing and even been available for my questions outside of the lab.

At last I want to thank my fellow master student Sandra for all moments in the office, every laughs, discussions and friendship, and my mom who always picked up the phone, eased my worries and made sure I remembered to eat and sleep.

Summary

Macroautophagy (hereafter called autophagy) is a process where proteins, organelles and intracellular micro-organisms are degraded by the lysosome. The autophagosome engulfs a part of the cytoplasm where the cargo is, and transports it to the endosomal-lysosomal system for degradation. Autophagy can also be selective, where cargos are recognized directly by the autophagy receptors or by other proteins in which target a specific cargo for degradation and can bind to for example ATG8s via a LIR domain. There are many proteins involved in autophagy, and TRIM proteins represent some of them. TRIM proteins are classified in a family of E3 ligases because of their RING domain, even though not all TRIM proteins contain this RING domain. Some TRIM proteins have been shown to be of great importance in the process of autophagy and the selectivity of autophagy by binding to autophagy-related proteins. Recent studies show that TRIM23 and TRIM31 are important in autophagy. ATG8 family proteins have hydrophobic pockets which bind LIR motifs in other proteins. Here, the interaction of TRIM23 and TRIM31 with the ATG8 family proteins is studied, and moreover their interaction with human ATG8 family proteins and if the binding is LIR dependent. GST pulldown, and co-localization assays with confocal fluorescence microscope were methods used for this purpose. Furthermore, the mCherry-EYFP double-tag was used to monitor if TRIM23 and TRIM31 are degraded in the lysosome. The lysosomal inhibitor Bafilomycin A1 (Baf) and the proteosomal inhibitor MG132 were included in the assays performed in HeLa cells to determine the degradation pathway. The results showed that both TRIM23 and TRIM31 bind ATG8s in a LIR-dependent manner. Neither TRIM23 nor TRIM31 were found to be degraded by autophagy using the double-tag assay, even though both were degraded upon starvation. Confocal imaging showed that TRIM31 co-localizes with LC3A, LC3B and GABARAP in HeLa cells.

Abbreviations

Ab: Antibody

AMPK: AMP-activated protein kinase

ARF: ADP-ribosylation factor

ATG: AuTophaGy-related

Baf: Bafilomycin A1

Bcl-2: B-cell lymphoma 2

BNIP3: Aadenovirus E1B 19kDa-interacting protein 3 (also called Bcl-2)

CALCOCO2: Ca^{2+}-binding and coiled-coil domain 2 (also called NDP52)

CCD: Coiled-coil domain

CMA: Chaperone-mediated autophagy

DMEM: Dulbecco's Modified Eagle's Medium

DNA: Deoxyribonucleic acid

dNTP: Deoxyribonucleotide triphosphate

DRAM: Damaged-regulated autophagy modulator

DTT: DL-Dithiothreitol

ER: Endoplasmic reticulum

FADD: Fas-associated protein with death domain

FBS: Fetal bovine serum

FMF: Familial Mediterranean fever

FUNDC1: Fun14 domain-containing protein 1

GABARAP: γ-aminobutyric acid receptor-associated protein

GATE-16: Golgi-associated ATPase enhancer of 16kDa

GST: Glutathione S-transferase

HBSS: Hank's Balanced Salt Solution

HCC: Hepatocellular carcinoma

HeLa: Henrietta Lacks

His-tag: Hexa-histidine tag

HIV-1: Human immunodeficiency virus type 1

HP: Hydrophobic pocket

HRP: Horse raddish peroxidase

IFN-γ: Interferon-γ

Ig: Immunoglobulin

IPTG: Isopropyl β-D-1-thiogalactopyranoside

IP_3: Myo-inositol-1,4,5-triphosphate

IRF3: IFN regulatory factor 3

KIR: Keap-interacting region

LAMP-2A: Lysosome-associated membrane protein 2A

LB: Lysogeny broth or Luria-Bertani

LC3: Microtubule-associated protein 1 light chain 3

LIR: LC3-interacting region

mTORC1: Mechanistic (mammalian) target of rapamycin complex1

NBR1: Neighbor of BRCA1 gene 1

NDP52: Nuclear dot protein 52

NIX: Bcl-2/adenovirus E1B 19kDa-interacting protein 3-like

NLRP: Nucleotide-binding oligomerization domain, Leucine rich Repeat and Pyrin domain containing

O.D.: Optical density

PAS: Phagophore assembly site

PBS(-T): Phosphate-Buffered Saline (with Tween 20)

PB1: Phox and Bem1

PCNA: Anti-Proliferating Cell Nuclear Antigen Clone PC10

PCR: Polymerase chain reaction

PE: Phosphatidylethanolamine

PFA: Paraformaldehyde

PI3K: Phosphatidylinositol 3-phophate

$p19^{ARF}$: ARF tumor suppressor protein

PURE: Protein synthesis Using Recombinant Elements

RING: Really interesting new gene

ROS: Reactive oxygen species

Rpm: Rounds per minute

SDS-PAGE: Sodium Dodecyl Sulfate – PolyAcrylamide Gel Electrophoresis

SIV: Simian immunodeficiency virus

SLR: SQSTM1-like receptors

SNARE: Soluble N-ethylmaleimide-sensitive factor Attachment protein Receptor

SOC-medium: Super Optimal broth with Catabolite repression

STX17: N-ethylmaleimide-sensitive factor attachment protein receptor

TAXBP1: Tax-binding protein 1

TB: TRAF6 binding

TE-buffer: Tris-HCl and EDTA

TOR: Target of rapamycin

TRAIL: tumor necrosis factor-related apoptosis-inducing ligand

TRIM: Tripartite motif

TSC: Tuberous sclerosis complex

TX-TL: Transcription-translation

Ub: Ubiquitin

UBA: Ubiquitin-associated domain

ULK1: Uncoordinated 51-like kinase 1

UPS: Ubiquitin-proteasome system

VPS: Vacuolar protein sorting

WT: Wild type

ZZ: Zinc finger

Table of content

1 Introduction

1.1 Autophagy

Autophagy is a degradation process in cells, dependent on the lysosome. This process is used to replace the cytoplasm over time to maintain the functioning cell (Xie & Klionsky, 2007). This involves providing nutrients for the cell during starvation, and degradation of surplus and damaged organelles, misfolded proteins and invading micro-organisms (B. Levine & Kroemer, 2008). Many diseases have been shown to be associated with autophagy being deficient or functioning abnormally; polyglutamine diseases, Parkinson disease, frontotemporal dementia, Alzheimer's disease (Knaevelsrud & Simonsen, 2010) and cancer (Chude & Amaravadi, 2017) are some examples.

Autophagy is divided into three main pathways (Figure 1); chaperone-mediated autophagy (CMA), microautophagy and macroautophagy (Klionsky, 2005). CMA is activated during starvation and nutrient limitations, and functions to maintain the cell cytoplasm under these conditions (Majeski & Dice, 2004). The main difference of this autophagy pathway compared to the two other, is that the proteins to be degraded are directly transported to the lysosome and finally taken into the lysosome by the lysosome-associated membrane protein 2A (LAMP-2A) receptor (Cuervo & Dice, 1998; Zhang et al., 2017). Microautophagy is when part of the cytoplasm is taken up by invagination of the lysosomal membrane followed by inward budding. Both single soluble components and whole organelles can be degraded by this pathway (Kunz, Schwarz, & Mayer, 2004). Macroautophagy is the pathway where the autophagosome engulfs a part of the cytoplasm and transport organelles and macromolecules to the lysosome (Kunz et al., 2004).

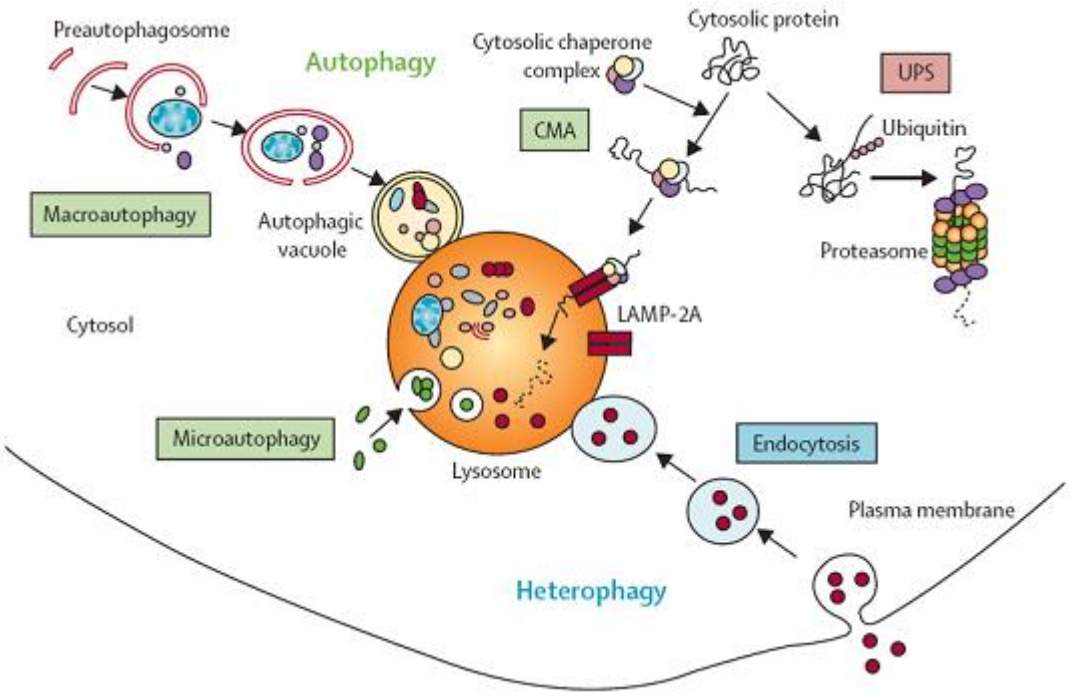

Figure 1: Overview of degradation pathways including autophagy (microautophagy, macroautophagy and CMA), endocytosis and UPS. There are three different types of autophagy; Macroautophagy, microautophagy and chaperonemediated autophagy (CMA). In macroautophagy, the cytoplasmic cargo is delivered to the lysosome in a double membrane-bound vesicle, called an autophagosome. Microautophagy is when the cytosolic cargos are taken up directly by the lysosomal membrane by invagination. In CMA, the cytosolic proteins are targeted by a cytosolic chaperone complex. This complex is recognized by the lysosomal membrane receptor lysosomal-associated membrane protein 2A (LAMP-2A), which transports the complex through the lysosomal membrane and unfolds it. Inside the lysosome, the cargos and proteins are degraded (Glick, Barth, & Macleod, 2010). The figure is reprinted with permission from Amsbio ("Autophagy," 2013).

The focus in this thesis will be on macroautophagy, hereafter called autophagy, because this is the main mechanism used by eukaryotes to degrade proteins and organelles with a long life-time (B. Levine & Kroemer, 2008).

1.1.1 Processes of Autophagy

Autophagy can be divided into different stages; induction, autophagosome formation (which is also mentioned under “Selective Autophagy”), degradation, and reuse. Many different signals and factors can initiate or inhibit autophagy in the cells (Mizushima, 2007). These factors include insulin- and amino acid signaling whereas in starvation autophagy is initiated (Jung, Ro, Cao,

Otto, & Kim, 2010), reactive oxygen species (ROS) which induces autophagy (Djavaheri-Mergny et al., 2006), free cytosolic calcium which induces autophagy (Hoyer-Hansen et al., 2007), AMP-activated protein kinase (AMPK) which are required for autophagy (Meley et al., 2006), Bcl-2/adenovirus E1B 19 kDa-interacting protein 3 (BNIP3) which induce autophagy in malignant glioma cells (Daido et al., 2004), the ARF tumor suppressor protein ($p19^{ARF}$) which induces autophagy (Reef et al., 2006), damaged-regulated autophagy modulator (DRAM) which induces autophagy via p53 (Crighton et al., 2006), calpain which induces autophagy (Demarchi et al., 2006), tumor necrosis factor-related apoptosis-inducing ligand (TRAIL) which induces autophagy during lumen formation (Mills, Reginato, Debnath, Queenan, & Brugge, 2004), Fas-associated protein with death domain (FADD) induced autophagy by interacting with Atg5 (Pyo et al., 2005), and myo-inositol-1,4,5-triphosphate (IP_3) which inhibit autophagy (Sarkar et al., 2005).

TOR (target of rapamycin) is a serine/threonine protein kinase. By responding to nutrients and growth factors, TOR regulates translation, metabolism, and transcription. Mammalian TOR, also called mechanistic target of rapamycin (mTOR), forms two complexes; mTORC1 (mTOR complex 1) and mTORC2 (mTOR complex 2) (Figure 2). Both complexes regulate autophagy, mTORC2 in skeletal muscles (Jung et al., 2010).

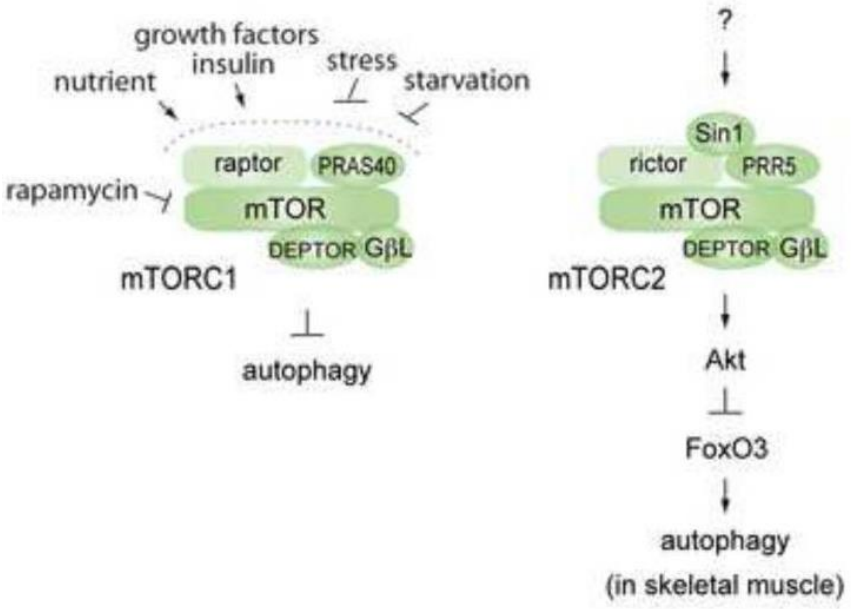

Figure 2: mTOR forms two complexes; mTORC1 and mTORC2. In response to nutrients and growth factors, mTORC1 is facilitated and inhibits autophagy. Stress and starvation inhibits mTORC1 and thereby facilitate autophagy. Rapamycin is an inhibitor of mTOR. mTORC2 regulates autophagy in skeletal muscles via Akt-FoxO3 (Jung et al., 2010).

ULK1 and Beclin-1 are important regulators of autophagy, as mentioned (Lamb, Yoshimori, & Tooze, 2013). Figure 3 shows the different proteins involved in the formation of the autophagosome. ULK1 is activated by AMP-activated protein kinase (AMPK) in a nutrient poor state of the cell, and Beclin-1 is activated by ULK1 phosphorylation (Nazarko & Zhong, 2013). Beciln-1, ATG14L, VPS15 and phosphatidylinositol 3-phosphate kinase (PI3K) VPS34 constitute the PI3K class III complex 1 required for autophagy (Funderburk, Wang, & Yue, 2010) (Figure 3).

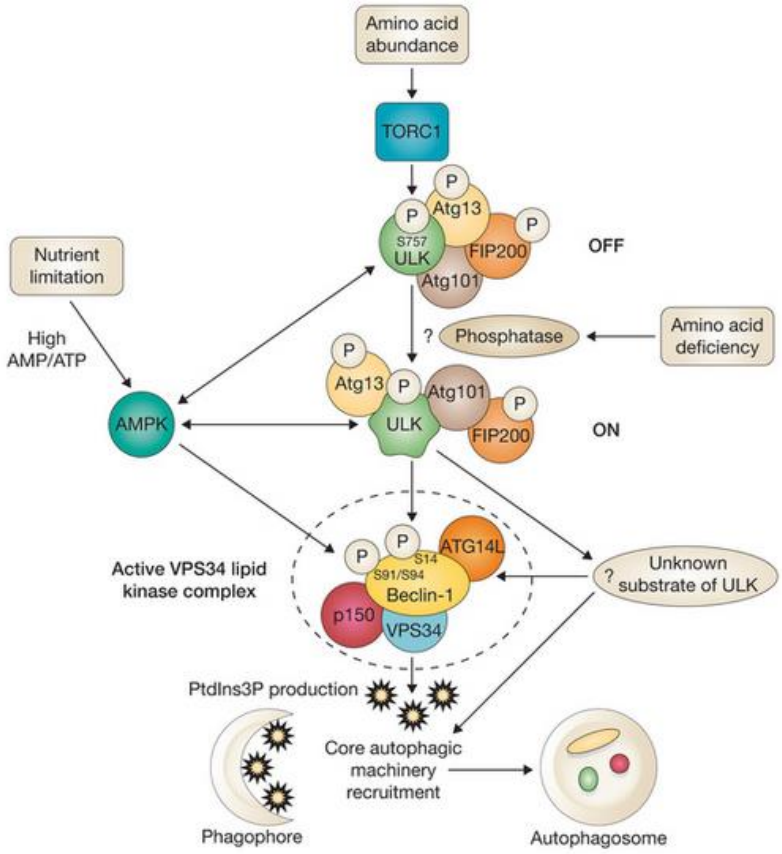

Figure 3: Overview over proteins involved in the formation of the autophagosome. ULK is negatively regulated by TORC1 in an amino acid abundance state and positively regulated by AMPK in an amino acid deficiency state. Beclin-1, in the PI3K class III complex I, is phosphorylated by both ULK and AMPK. This again, leads to the formation of the autophagosome from the phagophore. Figure reprinted with permission from (Nazarko & Zhong, 2013).

The second stage is the formation of the autophagosome which is made at the phagophore assembly site (PAS in yeast) (Xie & Klionsky, 2007). In higher eukaryotes, phagophores are created from several membrane sources including endoplasmic reticulum (ER), Golgi, mitochondria, endosomes and the plasma membrane, whereas the ER is the most likely main source (Lamb et al., 2013). Phagophores are membranes in the cytosol which, when fully enveloped or closed, becomes autophagosomes (Mizushima, 2007). Formation of the phagophores is dependent on specific complexes, and can be divided into three stages; initiation requiring the ULK complex and the PI3K class III complex I, nucleation involving phosphorylation and recruitment of additional ATG proteins, and expansion of the phagophore requiring ATG8 family proteins (LC3s and GABARAPs) and two conjugation systems including ATG7, ATG10, ATG3 and the ATG5-ATG12:ATG16L1 complex (Lamb et al., 2013). The autophagosome enwraps cytoplasm containing the cargos destined for autophagy, and takes it to the endosomal-lysosomal system for degradation (Lamb et al., 2013; Xie & Klionsky, 2007). At this maturation step of the autophagosome there is first a recruitment of the SNARE (Soluble N-ethylmaleimide-sensitive factor Attachment protein Receptor) syntaxin 17 (STX17), before the autophagosome fuses with the lysosomes. Thereafter the inner membrane of the autophagosome is degraded by the enzymes provided by the lysosomes. At the last stage of autophagosome maturation, STX17 is released. Even though STX17 is necessary, the autophagosomal complete closure and inner membrane degradation is also dependent on ATG3 (Tsuboyama et al., 2016). Products of the degradation, such as amino acids, are thereafter released into the cytosol for further use for the cell (Mizushima, 2007; Xie & Klionsky, 2007). This last stage, reuse or recycling, is not fully understood. An overview of autophagy with some of its modulators is illustrated in Figure 4.

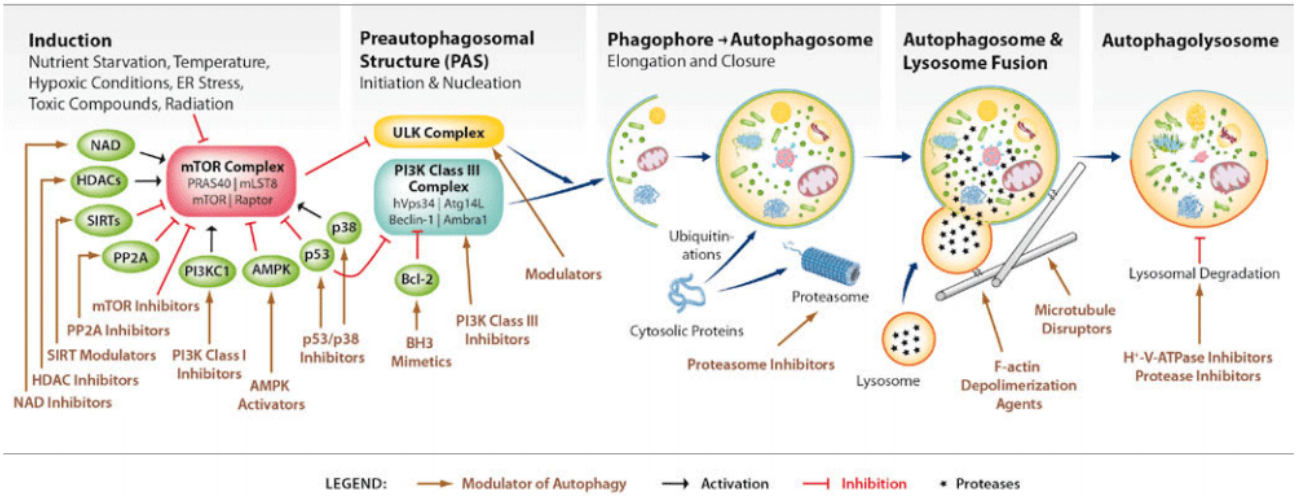

Figure 4: Schematic of autophagy with some of the modulators. Autophagy is induced by stress and starvation. An mTOR complex responds to these various signals, and, in a stressful condition, the autophagosome assembles from a preautophagosomal structure (PAS). Lysosomes fuses with the fully formed autophagosome, and the content is degraded by enzymes in the autophagolysosome. The figure is reprinted with permission from Bio-Connect ("Modulators of Autophagy Signaling,").

1.1.2 ATGs

ATG stands for AuTophaGy-related. The name is first mentioned by Klinonsky et al. in their publication in 2003 (Klionsky et al., 2003), and also reviewed in 2004 (Beth Levine & Klionsky, 2004). The name was developed to create a common nomenclature because of the confusion caused by different names of these ATGs in different publications (Klionsky et al., 2003). In 1993, Tsukada and Ohsumi discovered the first ATG in the yeast *Saccharomyces serevisiae*, and named it APG (AutoPhaGy). In this study, they concluded that at least 15 APG/ATG gene functions are required for the autophagic process in yeast, and that they are essential in the creation of autophagic bodies during starvation (Tsukada & Ohsumi, 1993). In 2003 there were 18 ATGs that are associated with autophagy in higher eukaryotes (Klionsky et al., 2003). In a review by van Beek, et al. this year (2018), 41 *ATG* genes have this far been isolated from yeast whereas many also have one or more counterparts in mammalian cells (van Beek, Klionsky, & Reggiori, 2018). In addition to ATG8 acting on the autophagosome (which are explained in detail under “ATG8”), Atg8 is also involved in a ubiquitination-like modification system. After processing, Atg4 processes Atg8. Atg7 (an E1 enzyme) then activates Atg8 which then are transferred to Atg3 (an E2 enzyme). In addition to activating Atg8, Atg7 also activates Atg12. The first The Atg1-Atg13 complex are involved in the TOR pathway, and are phosphorylated by

TORC1 under growing conditions. Other *ATG*s have been found to interact with each other; Atg17 with Atg1-Atg13, and Atg29 and Atg31 with Atg17. Atg9 have been found to be essential in the autophagosome formation by delivering membrane lipids from the Golgi apparatus. This transfer is also depending on Atg23 and Atg27 (Ohsumi, 2014).

1.1.3 The Selectivity of Autophagy

Autophagy was first thought to be a non-selective process, but more recent studies have suggested it to be more selective (Birgisdottir, Lamark, & Johansen, 2013; Johansen & Lamark, 2011; Rogov, Dotsch, Johansen, & Kirkin, 2014). Studies of the molecular mechanisms of autophagy began with the finding of *ATG* genes, and the family of Atg/ATG proteins have since grown. Atg8 is one of these protein families, consisting of several subfamilies. In animals, there are two subfamilies; microtubule-associated protein 1 light chain 3 (LC3), γ-aminobutyric acid receptor-associated protein (GABARAP) (Shpilka, Weidberg, Pietrokovski, & Elazar, 2011; van Beek et al., 2018). Within these two subclasses of ATG8, there are 7 homologs in humans; LC3A, LC3B, LC3B2, LC3C, GABARAP, GABARAPL1, and GABARAPL2/GATE-16 (Rogov et al., 2014). There has been discovered a number of human cargo receptors which have been shown to be important for the selectivity in autophagy (Johansen & Lamark, 2011; Rogov et al., 2014). The cargos may have conjugated ubiquitin (Ub) regions in which these autophagic cargo receptors recognize and bind. p62/SQSTM1 (hereafter only called p62), neighbor of BRCA1 gene 1 (NBR1), optineurin, and nuclear dot protein 52 (NDP52) are examples on receptors that recognize and bind to ubiquitinated cargos (Rogov et al., 2014). p62, NBR1, NDP52/Ca^{2+}-binding and coiled-coil domain 2 (CALCOCO2) and optineurin is in the class of SQSTM1-like receptors (SLRs) together with Tax1-binding protein 1 (TAX1BP1) (Hatakeyama, 2017). Other receptors are the mitophagy-specific receptors (BNIP3, NIX (Bcl-2/adenovirus E1B 19 kDa-interacting protein 3-like), FUNDC1 (Fun14 domain-containing protein 1) and FKBP8 (Rogov et al., 2014)) that is involved in autophagy of severely, damaged mitochondria, and pexophagy-specific receptors (methylotrophic yeast) where peroxisomes are degraded to generate energy. This recognition and binding by autophagic cargo receptors may induce autophagosome formation, but require two things from the cargo to do so; (1) Multiple receptors must be able to bind simultaneously to its surface, which requires that the cargo is large enough or oligomeric. (2) Atg8 must bind to the cargo in addition to the autophagy receptor,

simultaneously. A model for this selective autophagosome formation has been suggested by Rogov et al.: i) the cargo must be modified to be recognized, multiple receptors have to bind simultaneously either directly or via Ub for further modification of the cargo, ii) preexisting phagophores must be recruited (either by phosphatidylethanolamine (PE)-conjugated Atg8/LC3/GABARAPs and ATG5-ATG12-ATG16 bound to Ub or autophagic receptors), iii) ULK1 (uncoordinated 51-like kinase 1) must be recruited (by Atg8/LC3/GABARAPs and/or ATG16) so that VPS34 (vacuolar protein sorting 34) may be recruited, iv) the phagophore must be expanded around the cargo to become an autophagosome (performed by ATG5-ATG12-ATG16 complex and other ATG factors), and the autophagosome must fuse with lysosomes for degradation of cargo and receptors (Rogov et al., 2014).

The first SLR to be discovered was p62 (Bjorkoy et al., 2005; Pankiv et al., 2007). p62 is an important signaling protein and an autophagy receptor mediating selective degradation of various cargos (Lippai & Low, 2014). A schematic of p62 is illustrated in Figure 5, showing the domains important for the protein´s function in autophagy and other signal pathways.

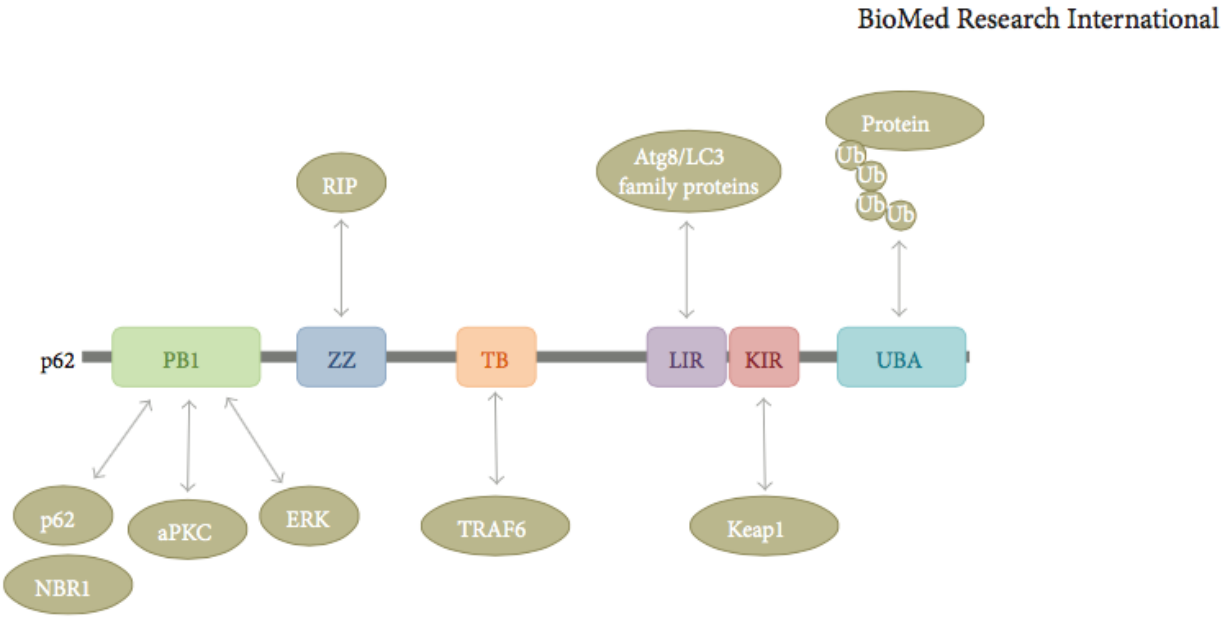

Figure 5: p62 domain structure with interacting partners. p62 has six functional domains; PB1 (N-terminal Phox and Bem1), ZZ (zinc finger), TB (for TRAF6 binding), LIR (the LC3-interacting domain), KIR (the Keap-interacting region) and UBA (C-terminal ubiquitin-associated domain). All these domains are important for p62 to function in autophagy and other signaling pathways. Figure reprinted with permission from (Lippai & Low, 2014).

LC3, encoded by the genes MAP1LC3A, MAP1LC3B, MAP1LC3B2 and MAP1LC3C in humans, is placed both on the inner membrane and on the outer membrane of the autophagosome. LC3B acts as a receptor for p62/SQSTM1 (Pankiv et al., 2007; Rogov et al., 2014). One major task for p62 is to gather components marked for autophagy in larger aggregates (Johansen & Lamark, 2011). The aggregates are then delivered to the autophagosomes by, in the case of p62, LC3B. In this way, Atg8s help with the selectivity of autophagosomal degradation (Shpilka et al., 2011).

1.1.4 ATG8s

In mammals, there are six different ATG8s divided in two subfamilies; LC3 and GABARAP/GABARAPL2. In conjugation with phosphatidylethanolamine (PE) LC3 and GABARAP contribute in autophagy by binding to other components in a LIR-dependent manner. This is illustrated in Figure 6. In a study performed by Nguyen et al. the complex was found not to be essential for the autophagosome formation. Though, the autophagosomes with LC3/GABARAP-PE present are bigger than they are without the ATG8s present. The ATG8s also seem to be important for the efficient formation of autophagosomes and the fusion between the autophagosome and lysosome (Nguyen et al., 2016).

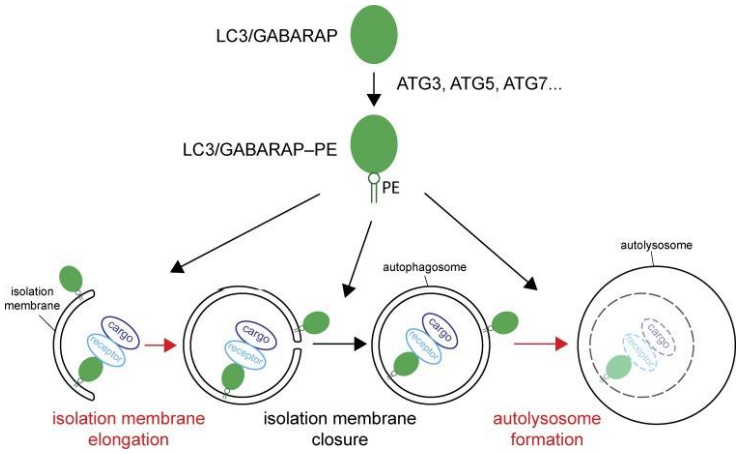

Figure 6: LC3/GABARAP regulates autophagy. LC3/GABARAP conjugation to the membrane lipid phosphatidylethanolamine (PE) is facilitated by several enzymes, including ATG3, ATG5 and ATG7. The LC3/GABARAP-PE complex is involved in the process of membrane elongation, autolysosome formation and membrane closure. The figure is reprinted with permission (Martens, 2016).

Proteins interact with ATG8s via their LIR (LC3-interacting region) (Birgisdottir et al., 2013; Shpilka et al., 2011). Even though LC3s and GABARAPs similarities, and they both participates in the processes of autophagy, they act in different parts of the process. GABARAP is crucial in the successful autophagosome-lysosome fusion, while the lack of LC3 did not significantly alter this fusion (Nguyen et al., 2016). Earlier studies have marked LC3B as the most prevalent and well-established marker for the autophagosome in mammals (Birgisdottir et al., 2013; Kabeya et al., 2000).

ATG8s have two hydrophobic pockets (HP1 and HP2) in which they interact with cargos or other proteins. It is these hydrophobic pockets that bind the LC3-interacting region (LIR) of other proteins (e.g. p62) (Noda et al., 2008).

1.1.5 LIR

LC3-interacting region (LIR) was first identified in p62 (Pankiv et al., 2007), and have later been found in a large amount of other proteins (Alemu et al., 2012). LIR-motif dependent binding between different proteins are essential in many different processes of autophagy. Phosphorylation of threonine/serine residues either in LIR itself or the surrounding regions may regulate the binding between LIR and the ATG8s. The LIR domain of different proteins does not consist of the same four amino acids, but some general rules have been shown to apply for many LIRs. The aromatic position in LIR that binds to the HP (hydrophobic) 1 pocket usually has a tryptophan (W) or a phenylalanine (F) for most proteins, and a few proteins have tyrosine (Y). F has a lower affinity for HP1 than W, and is therefore more dependent on the amino acid next to it in the LIR domain to compensate. Only the amino acids valine (V), cysteine (C), isoleucine (I), glutamic acid (E) and F were acceptable in these LIRs. An acidic charge has also seemed to be of importance at either the N- or the C-terminal of the conserved, aromatic residue; E, aspartic acid (D), serine (S) or threonine (T). As the general rule, the consensus of the LIR domain is (W/F/Y)XX(L/I/V) (Alemu et al., 2012; Birgisdottir et al., 2013).

1.2 Marking and detecting proteins for degradation

The most used methods for *in vivo* studies include microscopes, confocal fluorescence microscopes in most cases. By tagging the protein of interest with a fluorescing tag, e.g. GFP or

mCherry, the protein may be seen in the fluorescence microscope (Shashkova & Leake, 2017). Autophagy includes the lysosome for degradation of for example targeted proteins. Proteins involved in autophagy may also be degraded in the lysosome (Lamb et al., 2013; Xie & Klionsky, 2007). One important hallmark of the lysosomes, is that it has a pH of 5 or lower due to H^+ pumps in the membrane (Alberts et al., 2008). This hallmark can be taken advantage of when using confocal microscopy. While mCherry fusion tags are quite pH stable, the EGFP or EYFP fusion tags are not. In the acidic lysosomes, the EGFP loses its fluorescence, while mCherry maintains its fluorescence until it is proteolytically degraded. Therefore, it is possible to detect degradation of autophagy substrates and autophagy receptors by the lysosome and thereby monitor autophagy (Bjørkøy et al., 2009).

In eukaryotic cells, there are two systems for degradation of proteins; the ubiquitin-proteasome system (UPS) and autophagy. In both systems, the protein to be degraded is ubiquitinated and thereby recognized by receptors. UPS degradation of proteins through the 26S proteasome is almost solely dependent on this ubiquitination of the target for recognition and targeting (Schreiber & Peter, 2014).

For ubiquitination to occur, there is a need for three different enzymes; the E1 activating enzyme, the E2 conjugating enzyme, and the E3 ligase (Pickart, 2001). An overview of the ubiquitination process is illustrated in Figure 7.

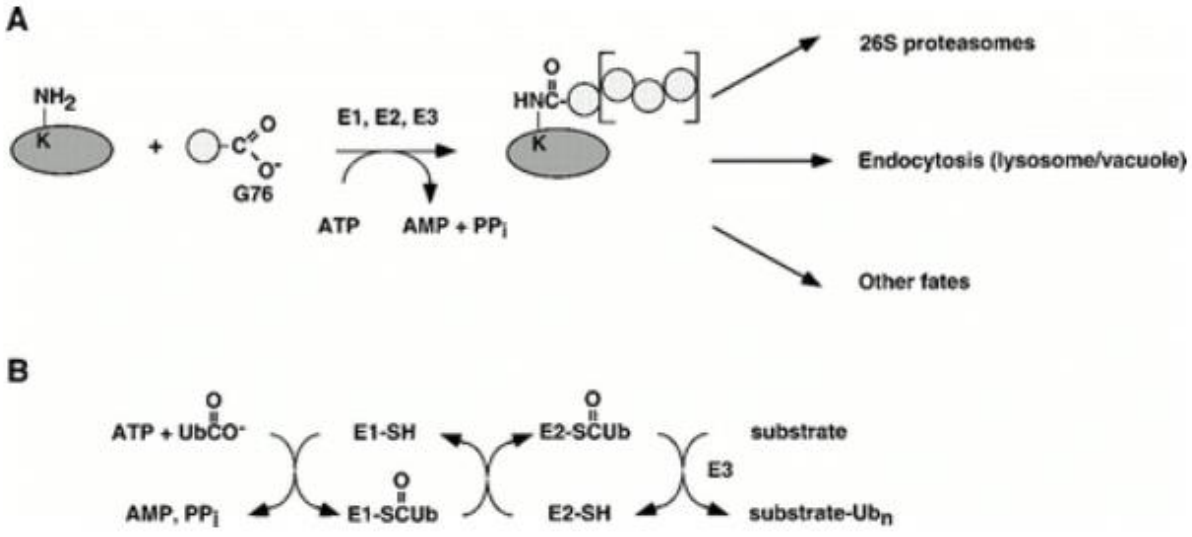

Figure 7: Overview of ubiquitin signaling. (A) The substrate (dark gray) is added ubiquitin (light gray) with the help from the enzymes E1, E2, and E3. Polyubiquitination may occur, in which the substrate is modified with a chain or chains of ubiquitin molecules. The fate of the substrate may be transport to the 26S proteasome, endocytosis or other fates. (B) shows a more detailed overview from the free ubiquitin molecule until it is added to the substrate with help from the three enzymes E1, E2, and E3. Figure is reprinted with permission from (Pickart, 2001).

1.3 TRIMs

Tripartite motif (TRIM) proteins are classified as a subfamily of the E3 ubiquitin ligase family. This is because most TRIM proteins contain a RING domain, even though some of them do not (Hatakeyama, 2017). The RING domain is cysteine-rich and binds to zinc (Borden, 2000), and is known for its interaction with E2 ubiquitin conjugating enzymes, and thereby, the proteins containing the RING (Really Interesting New Gene) finger domain, act as E3 ubiquitin protein ligases (Freemont, 2000). As for now, more than 80 different human TRIM proteins have been discovered, and their involvement demonstrated in processes like autophagy, immunity and carcinogenesis. In addition to the RING domain, TRIM proteins usually also possess one or two B-boxes and a coiled-coil domain (CCD) in their N-terminal part. Not all TRIM proteins have all these domains, and with different combination of functional domains in their C-terminal part they can act in different pathways binding to different substrates. The family of TRIM proteins are organized in subfamilies, C-I to C-XI, with the additional RING-less (UC) subfamily (Figure 8). This subfamily classification is due to their domain organization (Hatakeyama, 2017). Figure 8 shows the organization of the TRIM proteins, with their N- and C-terminal domains.

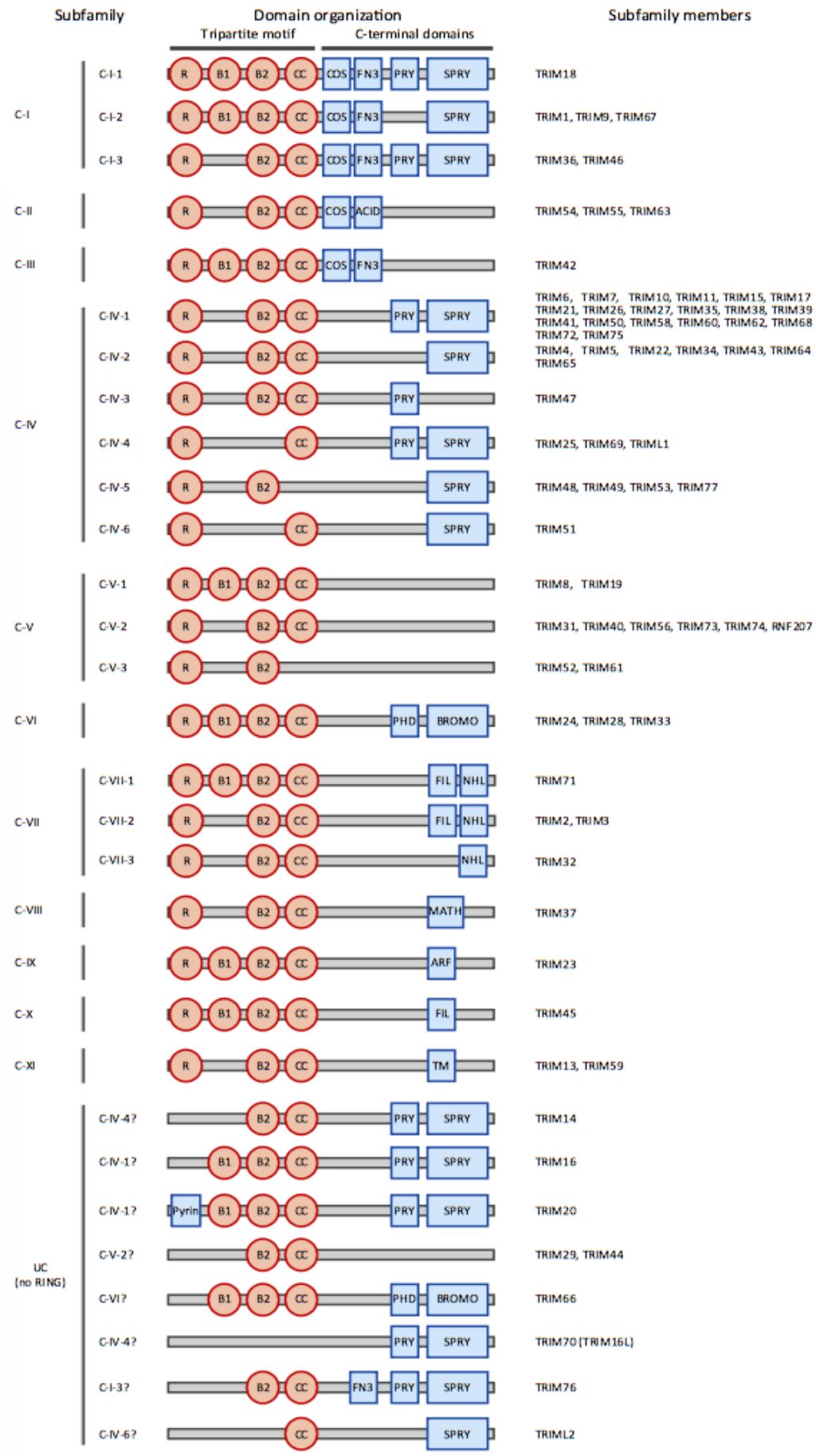
Subfamily
Domain organization
Tripartite motif
C-terminal domains
Subfamily members
C-I
C-I-1
R B1 B2 CC COS FN3 PRY SPRY
TRIM18
C-I-2
R B1 B2 CC COS FN3 SPRY
TRIM1, TRIM9, TRIM67
C-I-3
R B2 CC COS FN3 PRY SPRY
TRIM36, TRIM46
C-II
R B2 CC COS ACID
TRIM54, TRIM55, TRIM63
C-III
R B1 B2 CC COS FN3
TRIM42
C-IV
C-IV-1
R B2 CC PRY SPRY
TRIM6, TRIM7, TRIM10, TRIM11, TRIM15, TRIM17 TRIM21, TRIM26, TRIM27, TRIM35, TRIM38, TRIM39 TRIM41, TRIM50, TRIM58, TRIM60, TRIM62, TRIM68 TRIM72, TRIM75
C-IV-2
R B2 CC SPRY
TRIM4, TRIM5, TRIM22, TRIM34, TRIM43, TRIM64 TRIM65
C-IV-3
R B2 CC PRY
TRIM47
C-IV-4
R CC PRY SPRY
TRIM25, TRIM69, TRIML1
C-IV-5
R B2 SPRY
TRIM48, TRIM49, TRIM53, TRIM77
C-IV-6
R CC SPRY
TRIM51
C-V
C-V-1
R B1 B2 CC
TRIM8, TRIM19
C-V-2
R B2 CC
TRIM31, TRIM40, TRIM56, TRIM73, TRIM74, RNF207
C-V-3
R B2
TRIM52, TRIM61
C-VI
R B1 B2 CC PHD BROMO
TRIM24, TRIM28, TRIM33
C-VII
C-VII-1
R B1 B2 CC FIL NHL
TRIM71
C-VII-2
R B2 CC FIL NHL
TRIM2, TRIM3
C-VII-3
R B2 CC NHL
TRIM32
C-VIII
R B2 CC MATH
TRIM37
C-IX
R B1 B2 CC ARF
TRIM23
C-X
R B1 B2 CC FIL
TRIM45
C-XI
R B2 CC TM
TRIM13, TRIM59
UC (no RING)
C-IV-4?
B2 CC PRY SPRY
TRIM14
C-IV-1?
B1 B2 CC PRY SPRY
TRIM16
C-IV-1?
Pyrin B1 B2 CC PRY SPRY
TRIM20
C-V-2?
B2 CC
TRIM29, TRIM44
C-VI?
B1 B2 CC PHD BROMO
TRIM66
C-IV-4?
PRY SPRY
TRIM70 (TRIM16L)
C-I-3?
B2 CC FN3 PRY SPRY
TRIM76
C-IV-6?
CC SPRY
TRIML2

Figure 8: Structure of the different TRIMs. TRIM proteins are organized into different families according to the domain structure in their C-terminal part. In the N-terminal part there may be a RING domain (R), one or two B-boxes (B1 and B2), and a coiled-coil domain (CC). The C-terminal part may include a variety of domains, including the SPRY domain. Reprinted with permission from (Hatakeyama, 2017).

The review article by Kimura, Mandell and Deretic from 2016 lists the general physiology of TRIM proteins with their coherent diseases (Kimura, Mandell, & Deretic, 2016). For TRIM16L (alias TRIM70), TRIM42, TRIM43, TRIM48, TRIM49, TRIM51, TRIM52, TRIM60, TRIM64, TRIM67, TRIM69 and TRIM75, only their domain organization is known. Almost all of the remaining TRIMs listed in this table have been associated with a disease. Then there are some TRIMs that are extensively studied. Domain organization, binding partners, functional details, and disease/general physiology/mutations have been found for many of these TRIMs; TRIM5, TRIM13, TRIM19, TRIM20, TRIM21, TRIM22, TRIM28, TRIM50, and TRIM55 (Hatakeyama, 2017; Kimura, Mandell, et al., 2016).

1.3.1 TRIM E3 Ligases in Autophagy

Many TRIM proteins have been shown to be associated with autophagy by interacting with different known autophagy proteins and autophagy receptors. This is shown in Table 1. Here, the autophagy proteins are divided into three groups; human ATG8, SLRs, and others (Hatakeyama, 2017). Of these 20 different TRIM proteins listed in Table 1, half of them interact with p62, half interact with LC3A and/or GABARAP, and 9 interact with Beclin-1 and/or ULK1.

There are some of the TRIMs that lack the RING domain, e.g. TRIM20, but still interacts with autophagy-related proteins. This suggest that it is not only the E3 ligase activity of the TRIM proteins that is important for autophagy. Of the over 80 TRIM proteins found, all of them act in different pathways, and interact with different proteins/complexes. When studying autophagy, yeast is often used as a model organism. Therefore, it is quite interesting that no TRIM proteins, or some ancestral protein or gene encoding TRIM proteins, is found in yeast (Hatakeyama, 2017).

Table 1: TRIM proteins related to autophagy for their interaction with autophagy-related proteins. The autophagy-related proteins are divided into three groups; the human Atg8, the SLRs, and others. This table is modified from figure 3C in (Hatakeyama, 2017).

TRIM protein	**Interacting autophagy-related protein**
TRIM1 (Kimura et al., 2015)	SLR (NDP52)
TRIM5 (Mandell, Kimura, Jain, Johansen, & Deretic, 2015; Ribeiro et al., 2016)	Human Atg8 (LC3A, LC3C, GABARAP) SLR (p62), Others (Beclin-1, ULK1)
TRIM6 (Mandell et al., 2014)	Others (Beclin-1, ULK1)
TRIM13 (Tomar et al., 2013; Tomar & Singh, 2014; Tomar, Singh, Singh, Pandya, & Singh, 2012)	SLR (p62)
TRIM16 (Kimura, Jia, Claude-Taupin, et al., 2017; Kimura, Jia, Kumar, et al., 2017; Kumar et al., 2017; Mandell et al., 2014)	Human Atg8 (GABARAP)
TRIM17 (Mandell et al., 2016; Mandell et al., 2017)	Human Atg8 (LC3A, GABARAP) SLR (p62), Others (Beclin-1, ULK1)
TRIM20 (Kimura et al., 2015; Mandell et al., 2014)	Human Atg8 (LC3A, GABARAP) Others (Beclin-1, ULK1)
TRIM21 (Kimura, Jain, et al., 2016; Kimura et al., 2015)	Human Atg8 (LC3A, LC3B, GABARAPL2/GATE-16) SLR (p62), Others (Beclin-1, FIP200/RB1CC1, ULK1)
TRIM22 (Mandell et al., 2014)	Human Atg8 (LC3A, GABARAP) SLR (p62), Others (Beclin-1, ULK1)
TRIM28 (Pineda & Potts, 2015; Y. Yang et al., 2013)	Human Atg8 (LC3A, LC3B, GABARAP) SLR (p62), Other (ULK1)
TRIM33 (Gallouet et al., 2017)	Other (FIP200/RB1CC1)
TRIM40 (Noguchi et al., 2011)	Other (Beclin-1)
TRIM41 (Hatakeyama, 2017)	Human Atg8 (LC3A)
TRIM45 (Shibata, Sato, Nukiwa, Ariga, & Hatakeyama, 2012; Wang et al., 2004)	Human Atg8 (GABARAPL2/GATE-16)
TRIM49 (Mandell et al., 2014)	Human Atg8 (LC3A, GABARAP) SLR (p62), Others (Beclin-1, ULK1)
TRIM50 (Fusco et al., 2012)	SLR (p62)
TRIM55 (Mandell et al., 2014)	Human Atg8 (LC3A, GABARAP) SLRs (p62, NBR1)
TRIM61 (Hatakeyama, 2017)	Other (Beclin-1)
TRIM63 (Khan et al., 2014)	SLR (p62)
TRIM76 (Blandin et al., 2013)	SLR (Optineurin)

There are some of the TRIMs that lack the RING domain, e.g. TRIM20, but still interacts with autophagy-related proteins. This suggest that it is not only the E3 ligase activity of the TRIM proteins that is important for autophagy. Of the over 80 TRIM proteins found, all of them act in different pathways, and interact with different proteins/complexes. When studying autophagy, yeast is often used as a model organism. Therefore, it is quite interesting that no TRIM proteins, or some ancestral protein or gene encoding TRIM proteins, is found in yeast (Hatakeyama, 2017).

TRIMs involved in autophagy differ from many other autophagy receptors by acting as platforms to assemble compounds involved in formation of the autophagosome, in addition to act as receptors and E3 ligases. These proteins do not need their cargos to be ubiquitinated or subjected to any other modification, and they bind to their cargo by direct protein-protein interactions. After binding with their cargo, they serve as assembly platforms for important autophagy regulators such as ULK1/2 (mammalian Atg1 paralogues), Beclin-1 and ATG16L1 (Kimura, Mandell, et al., 2016). Certain TRIM proteins are in this way important regulators of autophagy, and contribute to the selectivity of autophagy. This has been termed precision autophagy (Kimura et al., 2015).

It has been shown that TRIMs interact with ULK1 and Beclin 1. Of the TRIMs tested, TRIM5α, TRIM17, TRIM22, TRIM49 and TRIM 55, only those with a SPRY domain were able to interact with ULK1 and Beclin 1. TRIM55 do not contain a SPRY domain, and showed no interaction with ULK1 or Beclin 1. Furthermore, they showed that mutations in other parts of the TRIMs did not affect the interaction with Beclin 1. TRIM55 showed no interaction with Beclin-1. Interestingly, TRIMs that bound ULK1 and Beclin 1 could assemble those two into a complex. Even though TRIM55 do not bind to either of the proteins, it has shown to affect autophagy. The same TRIMs were also tested for interaction with the Atg8 proteins, which they all did (Table) (Mandell et al., 2014).

1.3.2 The C-terminal part of TRIMs is important for specific binding to cargos

Each TRIM protein's ability to bind to a specific substrate, lies in their domains at their C-terminal part (Mandell et al., 2014). Specific studies of certain TRIM proteins have revealed

some specific functions for that exact TRIM. One example is TRIM5α. In addition to its N-terminal region containing the RING domain, B-box and the CCD, it has the SPRY domain in its C-terminal region (Campbell et al., 2015). The SPRY domain can, in some cases, recognize and protect the organism from certain viruses. Rhesus macaques have a TRIM5α (rhTRIM5α) that protects them from human immunodeficiency virus type 1 (HIV-1), in which the human TRIM5α only has limited protection. rhTRIM5α also seemed to protect against simian immunodeficiency virus (SIV), but at a lower degree than HIV-1 (Imam et al., 2016; Stremlau et al., 2004). In addition to relevance in cell-autonomous retroviral restriction and its ability to bind p62, the TRIM5α cognate target, the HIV capsid protein p24 has been shown to be removed by autophagy (Mandell et al., 2014).

In another study performed by Kimura and coworkers (2015), they found that TRIM20 was strongly induced by IFN (interferon)- γ, which influences cytokine networks and polarization of immune cells and also induces autophagy. They also found that this TRIM was crucial for IFN-γ-induced autophagy. Another finding was that TRIM20 interacts with ULK1, Beclin-1 (Table), and ATL16L1. TRIM20 binds directly to ULK1 and Beclin-1 simultaneously, and thereby assembles them. These bindings require specific domains that TRIM20 has (B-box and CCD for binding to ULK1, and B-box and CCD or PRY/SPRY domain for Beclin-1 and ATL16L1). Familial Mediterranean fever (FMF) has also been associated with TRIM20, where frequent mutations in its PRY/SPRY domain is detected (Masters, Simon, Aksentijevich, & Kastner, 2009). The PRY/SPRY domain of TRIM20 was shown to bind to the inflammasome components NLRP3, pro-caspase 1, and NLRP1, and deliver them for autophagic degradation. This study also suggested that degradation of TRIM20 happens in the autolysosome together with its bound cargo (Kimura et al., 2015).

In the same study they showed that TRIM21 displays many similarities with TRIM20, but TRIM21 also interacted with p62 and did not require the SPRY domain for binding to GABARAP. The SPRY domain of TRIM21 was shown to interact with IRF3 (IFN regulatory factor 3), and thereby cause autophagic degradation of this activated transcription factor (Kimura et al., 2015).

1.3.3 TRIM23

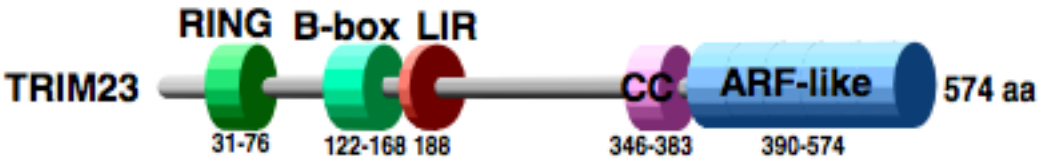

Figure 9: Schematic of TRIM23 domain organization. In the N-terminal there is a RING domain, a B-box and the LIR motif. In the C-terminal there is a coiled-coil (CC) domain and an ARF-like domain.

TRIM23 has been found in many different human tissues at a readily detectable level. TRIM23 has been shown to be involved in autophagy, and also to induce endogenous LC3B. LC3B and p62 are used as marker proteins for monitoring autophagy flux, and are therefore good pinpoints to check other proteins and molecules for involvement in autophagy. Virus-induced autophagy has also been shown to be increased by some TRIM proteins, including TRIM23. In addition to the common domains of TRIM proteins, TRIM23 also contains an ARF (ADP-ribosylation factor) domain in the C-terminal end (Figure 9). The ARF domain has GTPase activity, and has been shown to be important for the interaction with LC3B together with the RING domain. The study performed by Sparrer et al. in 2017 also suggested that this GTPase activity is required for autophagy mediated by TRIM23 (Sparrer et al., 2017). Another finding have suggested that TRIM23 is auto-ubiquitinated, in which this ARF domain is crucial. The mutations of specific binding sites (K402, K425, K446, K458 and K460), where K (lysine) is mutated to R (arginine) also made TRIM23 loose its ability to bind to LC3B. TRIM23 seemed to be recruited to the early autophagosomal membranes by ubiquitin-dependent GTPase activity. TRIM23 also seemed to be dependent of ubiquitination of K27 to be able to hydrolyze GTP (Sparrer et al., 2017). The RING domain is the domain with E3 ligase activity (Hatakeyama, 2017), and has also been a subject in studies. In a study performed by Dawidziak et al. in 2017 they suggested that the RING domain of TRIM23 is catalytically active only in its dimer form (Dawidziak, Sanchez, Wagner, Ganser-Pornillos, & Pornillos, 2017)

In addition to binding to LC3B, TRIM23 has also been shown to interact with TBK1 and p62. These interactions seemed to be stimulated by autophagy activity. Also, TBK1 has been

suggested to be important for TRIM23 in its functions in autophagy, including the phosphorylation of p62 (Sparrer et al., 2017).

TRIM23 has also been linked to other mechanisms and processes in the body. One example is in the process of maturation of adipocytes; fat cells. The precursor cells need upregulation of a transcription factor named PPARγ to differentiate. It seems like TRIM23 present in the precursor cell regulates the level of PPARγ, and thereby allows the cell to mature into an adipocyte (Watanabe et al., 2015).

1.3.4 TRIM31

Figure 10: Schematic of TRIM31 domain organization. The protein contains a RING domain, a B-box and a coiled-coil (CC) domain. Inside the CC domain, two LIRs are proposed present.

TRIM31 is a tissue-specific protein, expressed in association with mitochondria and lysosomes in human colonic and intestinal epithelial cells (Ra et al., 2016). As shown in Figure 10, TRIM31 has a RING domain, a B-box and a coiled-coil (CC) domain. A peptide array performed with this protein has indicated two potential LIR domains located inside the CC domain.

TRIM31 is shown to be involved in different types of cancer. By over-activating the mammalian target of rapamycin complex1 (mTORC1) pathway through negative regulation of the TSC1-TSC2 complex in hepatocellular carcinoma (HCC), TRIM31 promotes tumor growth. TRIM31 is normally expressed in the cytoplasm of healthy hepatocytes, but is significantly upregulated in hepatocarcinoma cells. Also, TRIM31 is expressed at higher levels as the tumor progresses in these patients. The same study by Guo et al. showed that TRIM31 promotes tumor growth, invasion and colony formation when exogenously overexpressed (Guo et al., 2017). TRIM31 is also shown to be upregulated in gastric adenocarcinoma (Sugiura & Miyamoto, 2008). In contrast to the two other cancer types mentioned (HCC and gastric adenocarcinoma), TRIM31

has been suggested to be downregulated in non-small cell lung cancer (NSCLC), indicating it to act as a tumor suppressor for this type of cancer (H. Li et al., 2014)

According to a cDNA screen performed by Sparrer et al., TRIM31 does not impact the lipidation of LC3B (Sparrer et al., 2017). This is also supported by Guo et al. by showing that TRIM31 over-activate the mTORC1 pathway, that further on suppresses autophagy (Guo et al., 2017). In another study by Ra et al. in 2016, TRIM31 is suggested to promote ATG5/ATG7-independent autophagy in intestinal cells. This study also found that TRIM31 is down-regulated in Crohn's disease. Cytosolic proteins and bacteria is recognized by TRIM31 and delivered for autophagic degradation (Ra et al., 2016).

2 Aims of Study

Preliminary work has indicated that TRIM23 and TRIM31 are important in certain aspects of autophagy (Ra et al., 2016; Sparrer et al., 2017). In addition to these studies, peptide arrays have been performed in our lab (G. Evjen and T. Johansen, unpublished), which shows that both TRIM23 and TRIM31 bind GABARAP. The peptide array also showed one potential LIR motif in TRIM23 and two in TRIM31. Because of these results, TRIM23 and TRIM31 may be binding to ATG8s. The main aim of this study were therefore to increase the understanding of TRIM23 and TRIM31 acting in autophagy, moreover binding to the human ATG8 family proteins and if this binding was mediated via the potential LIR domain(s) found in TRIM23 and TRIM31. Secondly, we wanted to determine the degradation pathways of TRIM23 and TRIM31.

3 Materials and Methods

3.1 Materials

The materials used in this thesis are listed in tables. Agar plates and growth medium for bacteria are only mentioned in methods when used.

3.1.1 Plasmids

The plasmids used in this thesis are listed in Table 2.

Table 2: Plasmids used in this thesis.

Plasmid name	Reference	Information
pDONR221 HA TRIM23	(Mandell et al., 2014)	cDNA for TRIM23
pDest-myc TRIM23	Clone HsCD00040302 Harvard PlasmID Repository	cDNA for TRIM23 with myc-tag
pDest-GFP TRIM23	(Mandell et al., 2014)	cDNA for TRIM23 with GFP
pDestmCherry-EYFP TRIM23	A. Jain (unpublished)	cDNA for TRIM23 with double-tag
pDONR221 TRIM31 fusion	(Mandell et al., 2014)	cDNA for TRIM31
pDestmCherry-EYFP p62	T. Lamark unpublished	Mammalian expression vector for double-tagged p62
pDestmCherry-LC3A	(Abudu, 2013)	Mammalian expression vector for mCherry-tagged LC3A
pDestmCherry-LC3B	(Pankiv et al., 2007)	Mammalian expression vector for mCherry-tagged LC3B

pDestmCherry-GABARAP	(Abudu, 2013)	Mammalian expression vector for mCherry-tagged GABARAP

3.1.2 Proteins

The proteins used in this thesis are listed in Table 3.

Table 3: Proteins used in this thesis.

Name	**Reference**	**Information**
pDest15 LC3A	(Pankiv et al., 2007)	Bacterial expression vector to produce GST-tagged LC3A in *E. coli*
pDest15 LC3B	(Pankiv et al., 2007)	Bacterial expression vector to produce GST-tagged LC3B in *E. coli*
pDest15 LC3C	(Jain et al., 2010)	Bacterial expression vector to produce GST-tagged LC3C in *E. coli*
pDest15 GABARAP	(Pankiv et al., 2007)	Bacterial expression vector to produce GST-tagged GABARAP in *E. coli*
pDest15 GABARAP Y49A	Y. P. Abudu (unpublished)	Bacterial expression vector to produce GST-tagged GABARAP Y49A in *E. coli*
pDest15 GABARAP Y49A/F104A	Y. P. Abudu (unpublished)	Bacterial expression vector to produce GST-tagged GABARAP Y49A/F104A in *E. coli*
pDest15 GABARAPL1	(Pankiv et al., 2007)	Bacterial expression vector to produce GST-tagged GABARAPL1 in *E. coli*
pDest15 GABARAPL2	(Pankiv et al., 2007)	Bacterial expression vector to produce GST-tagged GABARAPL2 in *E. coli*

3.1.3 Fusion Protein Tags

The fusion protein tags used in this thesis are listed in Table 4.

Table 4: Fusion protein tags.

Name	Information	Size
Myc	The myc-tag is 10 amino acids long (EQKLISEEDL), and derived from the human c-Myc protein (Jarvik & Telmer, 1998).	1.20 kDa
EGFP	EGFP (enhanced green fluorescent protein) is a mutant from GFP (Green Fluorescent protein) which originally was isolated from the jellyfish *Aequorea victoria*. Excitation maximum of EGFP is 488 nm (Heim, Cubitt, & Tsien, 1995)	~ 29 kDa
mCherry	mCherry was obtained from numerous mutations on the red chromophore of DsRed. Excitation maximum for mCherry is 587 nm (Shaner et al., 2004).	~ 30 kDa
EYFP	EYFP (enhanced yellowish fluorescent protein) is an enhanced version of YFP (yellow fluorescent protein) which again is a variant of GFP (Nagai et al., 2002).	~ 29 kDa
GST	Glutathione S-transferase (GST) was first isolated from *Schistosoma japonicum*. GST	26 kDa

	constitutes of a class of enzymes which utilize glutathione as a substrate (Smith & Johnson, 1988). GST is available from different manufacturers, and is, among other things, used in affinity and purification experiments.	

3.1.4 Oligos

The oligos used in this study are listed in Table 5.

Table 5: Oligos ordered and used in this thesis. All oligos was ordered from ThermoFisher (Invitrogen), and used in mutagenesis and sequencing.

Name	Sequence	Purpose
TRIM31 LIR1, forward	5´-GCAAAGGATCCTCACAGAAGCTGAACTCGCGCATCAAGTCCTAGAGG-3´	Mutagenesis of LIR1 in TRIM31
TRIM31 LIR1, reverse	5´-CCTCTAGGACTTGATGCGCGAGTTCAGCTTCTGTCTAGGATCCTTTGC-3´	Mutagenesis of LIR1 in TRIM31
TRIM31 LIR2, forward	5´-GCAGAAGTGAAGAGGCTCAGTTTGCCAACCCAACCCCTG-3´	Mutagenesis of LIR2 in TRIM31
TRIM31 LIR2, reverse	5´-CAGGGGTTGGGTTGGCAAACTGAGCCTCTTCAGTTTCTGC-3´	Mutagenesis of LIR2 in TRIM31

3.1.5 Primers

The primers used in this thesis are listed in Table 6.

Table 6: Primers used in this thesis.

TRIM31 LIR1 primer, forward	5´-GCAGCAAAAGGAGAAGGAG-3´	Sequencing primer in TRIM31
TRIM31 LIR2 primer, reverse	5´-CATGCTTTTGAAGAATCTG-3´	Sequencing primer in TRIM31

3.1.6 Antibodies

The primary antibodies used in Western blotting in this thesis are listed in Table 7, while the secondary antibodies are listed in Table 8.

Table 7: Primary antibodies for Western blotting

Name	**Producer/catalog number**	**Dilution**
GFP-tag; rabbit	abcam	1:5000
Anti-Proliferating Cell Nuclear Antigen Clone PC10 (PCNA)	DAKO	1:1000

Table 8: Secondary antibodies for Westen blotting.

Name	**Producer/catalog number**	**Dilution**
Anti-Biotin HRP-linked Ab	Cell Signaling	3:4000
HRP Goat Anti-Rabbit IgG	BD Pharmingen™	3:4000
HRP Goat Anti-Mouse Ig	BD Pharmingen™	3:4000

3.1.7 Inhibitors

The inhibitors used in this thesis are listed in Table 9.

Table 9: Inhibitors used in this thesis.

Name	Producer	Working concentration	Information
Bafilomycin A1	Santa Cruz	200 nM	Inhibits vacuolar type H+-ATPase
MG132	Sigma	10 uM	Inhibits proteasome
cOmplete Mini, EDTA-free Protease Inhibitor Cocktail tablets	Roche	1 tablet in 10 mL solution	Inhibit degradation of proteins

3.1.8 Cell lines

The cell lines used in this thesis are listed in Table 10.

Table 10: Cell lines used in this thesis.

Cell line	Organism	Organ	Reference
HeLa	Human	Cerevix	(Lazarou et al., 2015)
HeLa ATG7 knock out	Human	Cerevix	Y. P. Abudu (unpublished)

3.1.9 *E. coli* Strains

The *E. coli* strains used in this thesis are listed in Table 11.

Table 11: *E. coli* strains used in this thesis.

Name	Producer	Information
One Shot OmniMAX 2 T1 phage-resistant cells (DHSa cells)	Bethesda Research Laboratories Inc.	Competent *E. coli* for cloning
BL21 (DE3)	Novagen®	*E. coli* for protein expression

3.1.10 Protein Ladders

Protein ladders used in this thesis are listed in Table 12.

Table 12: Ladders used in this thesis.

Name	Producer	Catalog number
Unstained Protein Standards Broad Range (10-200 kDa)	BioLabs	p7704 S
Biotinylated Protein Ladder	Cell Signaling	7727 L
ProSieve® Quad Color™ Protein Marker	Lonza	193837-BMA
Gel Loading Dye Purple (6x)	BioLabs	B7024S

3.1.11 Plasmid Miniprep

For purifying plasmids, the GenElute™ Plasmid Miniprep kit from Sigma Aldrich was used. The content is listed in Table 13.

Table 13: Solutions used in purification of plasmids. All materials are included in the GenElute™ Plasmid Miniprep kit from Sigma Aldrich (#PLN350). Plasmids have to be prepared and purified from single colonies of *E. coli* for further use in experiments.

Solution name	Purpose
Resuspention Solution added RNase A	Resuspention of the bacteria pellet
Lysis Solution	Lyse the bacteria in the solution to free their proteins
Neutralization/Binding Buffer (S3) for plasmid preparation	Neutralize the lysis solution
Column Preparation Solution	Preparation of columns for an efficient binding of plasmid
Wash Solution (ws) for GenElute™ plasmid prep kits with added ethanol	Washing to optimize purity of the prepared plasmid
Elution Solution (es) for GenElute™ plasmid prep kits	Elution of the pure plasmid and inhibit its degradation when stored

3.1.12 Gel Electrophoresis

Buffers used in this thesis for SDS-PAGE and agarose gel electrophoresis are listen in Table 14.

Table 14: Buffers used in SDS-PAGE.

Method	Buffer	Content
SDS-PAGE gel electrophoresis	4x Separating gel buffer	181.65g Trizma-base 4g SDS dH_2O to 1L pH 8.8, adjusted with HCl
	4x Concentrating gel buffer	60.55g Trizma-base 4g SDS dH_2O to 1L pH 6.8, adjusted with HCl
	10% separating gel	4.9 mL dH_2O 2.5 mL 40% acrylamide (Sigma Aldrich) 2.5 mL separation buffer 100 µL 10% APS (Sigma Aldrich) 10 µL TEMED (Tetramethylethylenediamine) (Sigma Aldrich)
	13% separating gel	4.15 mL dH_2O 3.25 mL 40% acrylamide (Sigma Aldrich) 2.5 mL separation buffer 100 µL 10% APS (Sigma Aldrich) 10 µL TEMED (Tetramethylethylenediamine) (Sigma Aldrich)
	4% concentrating gel	6.4 mL dH_2O 1 mL 40% acrylamide (Sigma Aldrich) 2.5 mL concentrating gel buffer, pH 6.8 100 µL 10% APS (Sigma Aldrich) 10 µL TEMED (Tetramethylethylenediamine) (Sigma Aldrich)
	Electrophoresis buffer	3g Tris-base 14.4g glycin 1g SDS dH_2O to 1L

	2x SDS loading buffer	100 mM Tris/HCl, pH 6.0 20% glycerol 4% SDS 0.2% Brom phenol blue 200 mM DTT
	5x SDS loading buffer	5% DTT 0.02% Bromphenol blue 30% glycerol 10% SDS (Sodium dodecyl sulfate) 3 mM Tris-Cl (pH 6.8)
Agarose gel electrophoresis	20x minigelbuffer	193.76g Tris 27.22g NaOAc 14.9g EDTA-Trihydrate dH_2O to 2 L pH adjusted to 8.0 with acetic acid
	0.7% Agarose gel	0.35g SeaKem agarose 50 mL 1x minigelbuffer
	GelRed staining	GelRed™ Nucleic Acid Stain, 10 000X in water (#41003) from Biotium 0.1 M NaCl

3.1.13 Cell culturing

Materials used in cell culturing in this thesis are listed in Table 15.

Table 15: Materials used in cell culturing.

Product name	**Producer**	**Catalog number or content**	**Purpose**
Dulbecco's Modified Eagle's Medium – low glucose (DMEM)	SIGMA, Life Science	M6046	Supply living cells with nutrition
1x PBS (Phosphate Buffered Saline)	Gibco	0.1 mM Na-phosphate buffer, pH 7.2	Washing

		0.7% NaCl	
Penicillin-Steptomycin	Sigma	P0781-100ML	Hindering contamination of the cells from other bacteria
Fetal bovine serum	Biochrom AG	s0615	Provides nutrient and amino acids to keep cells healthy
Trypsin – EDTA Solution	Sigma	T4049	Detach cells from each other and surface
Dimethyl sulfoxide	Sigma	D5879-1L-M	For freezing cells
Fibronectin Bovine (1:200)	Sigma	F1141	Coating of cells

3.1.14 Gateway Technology – LR Reaction

Buffers used in LR reaction in this thesis are listed in Table 16, and enzymes are listed in Table 17.

Table 16: Buffers used in LR reaction.

Buffer	**Content**	**Purpose**
Tris-EDTA (TE) buffer pH 8.0	10 mM Tris/HCl, pH 8.0 (adjusted with HCl) 1 mM EDTA	Buffer to solubilize and stabilize DNA

Table 17: Enzymes used in LR reaction.

Enzyme name	**Producer**	**Catalog number**	**Purpose**
LR clonase II	Thermo Fisher	11791-100	Enzyme to onset the reaction of vector change in protein
Proteinase K	INVITROGEN	11791-100	Terminate the reaction of vector change in protein

3.1.15 GST Pulldown

Buffers used in GST pulldown in this thesis are listed in Table 18, and other materials are listed in Table 19.

Table 18: Buffers used in GST pulldown assay.

Buffer	Content	Purpose
Lysis buffer	2.5 mL 1M TrisCl, pH 8.0 6.25 mL 2M NaCl 39 mL dH_2O	Lyse *E. coli*
NET-N buffer	20 mM 1M Tris pH 8.0 100 mM 2M NaCl 1 mM 0,5 M EDTA 0,3% NP-40 (Nonidet™ P 40 Substitute) (Sigma Aldrich)	Washing of GST beads and buffer in loading buffer
Lysis buffer added lysozyme and DTT	3,85 mL lysis buffer 4 µL 1M DTT (DL-Dithiothreitol) (Sigma Aldrich) 140 µL lysozyme (10 mg/mL)	Resuspension of *E. coli* with ATG8s pellets to be frozen down
Triton – X100 (vwr)	10 mL Triton – X100 90 mL dH_2O	A non-ionic surfactant and emulsifier detergent
Loading buffer	12 µL NET-N Buffer 15 µL 5x or 2x SDS loading buffer diluted in dH_2O (1:5/1:2) 3 µL 1M DTT	Prepare ATG8 bound GST beads for gel electrophoresis
Coomassie brilliant blue	2g Coomassie Brilliant Blue R-250 (Thermo Scientific) dH_2O to 200 mL	Staining of the gel after gel electrophoresis
Fixation buffer	400 mL MeOH 100 mL HAc 500 mL dH_2O	Fixation of gel before staining with coomassie brilliant blue
Destain I	500 mL Methanol 100 mL Acetic Acid 400 mL dH_2O	Destaining of the gel after staining
Destain II	50 mL MeOH 70 mL HAc dH_2O to 1L	Further destaining the gel after staining and re-hydrate the gel

Table 19: List of materials used in GST pulldown assay.

Product name	Producer	Catalog number	Purpose
Isopropyl β-D-1-thiogalactopyranoside (IPTG)	SIGMA Aldrich	I6758-10G	Induce transcription from promoter to the protein wanted to be expressed from pDest vectors (Noireaux, Bar-Ziv, & Libchaber, 2003)
Glutathione Sepharose™ 4 Fast Flow	GE Healthcare	17-5132-01	GST beads for binding to GST-tagged proteins

3.1.16 Site Directed Mutagenesis and Sequencing

Materials used in site directed mutagenesis and sequencing in this thesis are listed in Table 20.

Table 20: List of materials used in site directed mutagenesis and sequencing.

Product name	Producer	Catalog number	Purpose
10x Cloned Pfu Reaction Buffer	Agilent	206115-51	Buffer containing an optimal concentration of magnesium for PCR
dNTP mix	Sigma Aldrich	D7295	Provides nucleoside triphosphates for transcription of new sequences
Pfu Turbo DNA Polymerase	Agilent	600254-52	A DNA polymerase with proofreading activity
DPNI	NEB	R0176 L	A restriction endonuclease enzyme
BigDye Terminator v3.1 Cycle Sequencing	Thermo Fisher	4337455	Buffer containing enzymes, nucleotides and what else is needed for a

			sanger sequencing reaction

3.1.17 GST-Pulldown Assay with Cell Lysate

Buffers used in GST-pulldown with cell lysate in this thesis are listed in Table 21, while other products are listed in Table 22.

Table 21: Buffers used in GST pulldown assay with cell lysate.

Buffer	**Content**	**Purpose**
RIPA buffer	50 mM Tris, pH. 7,5 150 mM NaCl 1 mM EDTA 1% NP40 0,25% Triton-X dH_2O	Lyse cells
1x PBS-T	75 mL 2 M NaCl 10 mL 1 M Tris-HCl, pH 8.0 1 mL Tween20 dH_2O to 1L	Washing of membrane

Table 22: List of materials used in GST-pulldown assay with cell lysate.

Product name	**Producer**	**Catalog number**	**Purpose**
Metafectene®Pro	Biontex	T040-5.0	A liposome-based transfection reagent
Glutathione Sepharose™ 4 Fast Flow	GE Healthcare	17-5132-01	GST beads for binding to GST-tagged proteins

3.1.18 Western Blot

Materials used in Western blotting in this thesis are listed in Table 23.

Table 23: List of the different materials used in Western blotting.

Product name	Producer	Catalog number or content	Purpose
SuperSignal™ West Femto Maximum Sensitivity	Thermo Scientific	34095	A chemiluminescent substrate in which visualize proteins with HRP tag
5% dried milk solution	GABER SALITER	2g dried milk (Magermilch pulver) 40 mL 1x PBS-T	Block the membrane
0.1% Ponceau staining buffer	Sigma Aldrich	0.5 g Ponceau S 2.5 mL acetic acid 474.5 mL dH_2O	Staining of the membrane
1x PBS-T		75 mL 2 M NaCl 10 mL 1 M Tris-HCl, pH 8.0 1 mL Tween20 dH_2O to 1L	Washing of membrane

3.1.19 Transfection and Analyzing with Confocal Microscopy

Materials used in transfection and analyzing with confocal microscopy in this thesis are listed in Table 24.

Table 24: List of the different materials used in Transfection of cells and visualizing with confocal microscopy.

Product name	Producer	Catalog number	Purpose
Ethanol (70%) diluted in dH_2O			Washing of coverglasses in 24-well dishes

TransIT ®- LT1 Reagent	Mirus	MIR2300	A reagent which provides a high efficiency DNA delivery in mammalian cells
Hanks' Balanced Salt Solution (HBSS)	Sigma	H8264	Starvation media to starve mammalian cells.
Formaldehyde solution (Pfa) 4%, buffered, pH 6.9	Thermo Scientific	1.00496-5000	Fixation of cells
DAPI	Thermo Fisher	62248	Staining of nucleus
Mowiol ®	Merck Millipore	475904-100GM	Preserve and attach cells on coverglasses on coverslips

3.2 Methods

3.2.1 General Methods

3.2.1.1 Plasmid Purification

There are many methods developed for purifying plasmids, and method used is often chosen based on how pure the plasmid has to be in the experiment. Some methods may use a drastic pH, heat or other changes to help purify impurities from the plasmid solution. Different kits are available for purifying plasmids. GenElute™ HP 96-Well Plasmid Miniprep Kit, GenElute™ HP Plasmid Maxiprep Kit, and GenElute™ Plasmid Miniprep Kit are three examples from Sigma Aldrich.

3.2.1.1.1 Protocol

To purify the different plasmids needed, the GenElute™ Plasmid Miniprep Kit from Sigma Aldrich was used with the manufactures protocol. Overnight cultures of *E. coli* harboring the plasmids of interest were grown in ~5 mL TB medium containing antibiotics, kanamycin for proteins in pDONR vector and ampicillin when in pDest vectors, and pelleted in Eppendorf tubes in two turns by centrifugation at 13 000 rpm for one minute each time in a microcentrifuge. The pellets were then re-suspended in 200 µL Resuspension Solution containing RNase A which catalyzes the degradation of RNA, and added 200 µL Lysis Solution to lyse the bacteria containing *Escherichia coli*. The solution was mixed by gently inverting the tubes, and allowed

to clear for 5 minutes. To prepare the cleared lysate, 350 µL Neutralization Solution was added. To enable the column to bind DNA, 500 µL Column Preparation Solution was added to empty columns in new Eppendorf tubes. After adding the DNA solution to the columns, the tubes were centrifuged at 13 000 rmp and flow-through was discarded. Now, when the plasmid DNA should have bound to the column, the columns were washed with 700 µL Wash Solution. The purified DNA in the columns were then moved to new tubes and added 50-100 µL Elution Solution to be detached from the columns by centrifugation (13 000 rpm). The concentrations of the purified plasmids could now be measured by for example Nanodrop, and kept at -20°C until needed.

3.2.1.2 SDS-PAGE Electrophoresis

SDS-PAGE (Sodium Dodecyl Sulfate – PolyAcrylamide Gel Electrophoresis) is a method to separate proteins according to their size. To separate the proteins from each other, they first have to be denatured to their primary structure. This occurs when the proteins are mixed with SDS, which works as a detergent. Bound SDS gives proteins a negative charge. The gel used in this method is based on polyacrylamide. The proteins will move towards the plus pole when the electricity is turned on. The small proteins will move the fastest, because they can fit into any of the pores in the gel, while the larger proteins only have a few pores they fit in to. Upon running the gel, the various proteins are separated by size. With the help of a ladder (a set of proteins with known molecular weights), the size of the different proteins can be estimated. To get visible protein bands, the gel has to be stained with e.g Ponceau or Coomassie Blue or specific bands can be detected by Western blot ("SDS-PAGE (PolyAcrylamide Gel Electrophoresis)," 2001).

3.2.1.3 Agarose Gel Electrophoresis

To verify LR reaction products, agarose gel electrophoresis was run to separate LR product DNA. To prepare DNA for agarose gel electrophoresis, 5 µL DNA (100-200 ng)/H_2O was added 1 µL 6x loading buffer. A 0.7% agarose gel was made by dissolving 0.35 g SeaKem agarose in 50 mL 1x minigelbuffer. The solution was heated in a microwave for some minutes until SeaKem agarose was properly dissolved. The solution was thereafter added to a plate, in which was properly sealed to avoid leakage, and a comb was inserted to make wells. When the gel was solid, the comb was carefully taken out to avoid destroying of the wells. The wells were added 6

μL of the DNA/buffer solution and run at 90 V for 60 minutes. To visualize the bands, the gel was stained with GelRed (1:10 000 in 0.1 M NaCl) for 10-20 minutes. The image was taken by BioDoc-It® 220 Imaging System using a UV lamp.

3.2.1.4 *Spectrophotometry (O.D.)*

Spectrophotometry is a method to measure how much light a solution is absorbing. The method can be used to measure the density of bacterial strains, as a way to follow bacterial growth. The machine is made up of two components; a spectrometer that produces light at any wavelengths, and a photometer that measure the intensity of the light that is not absorbed by the solution. The spectrophotometer gives the absorption in optical density (O.D.), which is in a logarithmic scale. When measuring the density, you need to have a reference solution, preferably the solution that is used as sample buffer, to compare the bacteria culture solution to (Caprette, 1996). Spectrophotometry may also be used to find DNA concentration in a solution. For this, specific instruments are used (e.g. Nanodrop) ("Protein assay technical handbook,").

3.2.1.5 *Transformation of* E. coli

Transformation is the process in which foreign DNA is taken up by a bacterium. The process was first demonstrated by Griffith in 1928 in *Streptococcus pneunomonia* (Griffith, 1928). For transformation to be successful, the bacteria need to be competent. That the bacteria is competent means that it is able to take up the foreign DNA introduced to it at a high, preferably as close to 100% uptake as possible, degree. The principal behind developing competent cells is bacteria is grown overnight and pelletized, re-suspended in method specific solution and frozen down (Chan, Verma, Lane, & Gan, 2013). The competent bacteria can be developed by different methods, some of them being Hanahan's method (Hanahan, 1983), the DMSO method (Chung & Miller, 1988), and the $CaCl_2$ method (Mandel & Higa, 1970). For all these methods, the bacteria is re-suspended in method specific medium and frozen at -80°C. For the transformation, competent cells are mixed with plasmid and kept on ice. For most transformation methods, the cells are then heat-shocked for some seconds before taken back to ice (Chan et al., 2013). DNA is negatively charged, and are not able to enter most bacteria without some help. By shocking the bacteria cells with heat for a few seconds, their membrane is disrupted, and DNA may freely enter the cells (Panja, Saha, Jana, & Basu, 2006). Heat-shock is not used in the DMSO method.

Appropriate growing media (e.g. SOC), which is rich in nutrients and without antibiotics so that the bacteria recovers, is then added to the suspension before growing at 37°C for 1 hour and plated on appropriate agar plates (Chan et al., 2013). Appropriate agar plates are rich in nutrients to favor growth, and contain antibiotics (e.g. kanamycin or ampicillin) in which the transformed bacteria are resistant to. Antibiotics are widely used to avoid the growth of other bacteria which may have contaminated the transformed bacteria.

3.2.1.5.1 Protocol

From LR reaction (described later), 1 μL mutagenesis mixture containing plasmid was added to a 15 mL tube and carefully added 15 μL autoclaved H_2O and 50 μL competent cells (*E. coli* DH5α) from freezer. The tube was kept 20 minutes on ice, thereafter 2 minutes in a warm bath at 37°C. the tube was then brought back on ice, and added 250 μL SOC. After 1 hour at 37°C with shaking, 150 μL of the solution was plated on agar plates containing either kanamycin (for pDONR vectors) or ampicillin (for other vectors).

3.2.1.6 Measuring Protein Concentration

Knowing the protein concentration is very often necessary when using a protein in experiments. There are many different methods (copper-based total protein assays, dye-based total protein assays, fluorescence-based protein detection and other specialty assays) to obtain the protein concentration, and the method is chosen from what experimental procedure the protein is going to be used in. The protein concentration may be obtained by either a UV-Vis spectrophotometer for colorimetric-based assays or a fluorometer for fluorescence-based assays (e.g. Nanodrop) ("Protein assay technical handbook,").

3.3 GST Pulldown

3.3.1 *In vitro* protein-protein interaction assay

Protein-protein interactions are often analyzed *in vitro* to see if there is a direct binding, before performing a binding experiment *in vivo* where also indirect interactions may be detected. The first step is often to express and purify the protein from a chosen bacterium, normally *E. coli.* The purification of the protein may be performed by different methods depending on the further

use of the purified protein and the researcher doing the purification. One method is by cation exchange and gel filtration chromatography (Coyle, Qamar, Rajashankar, & Nikolov, 2002). *E. coli* expressing the protein of interest are lysed in an appropriate buffer and the lysate bound to sepharose beads. When a protein is bound to sepharose beads, proteins in GST vector may be washed without losing the protein. This is an affinity-based method; GST protein from *S. japonicum* is binding with high affinity to the tripeptide glutathione which is covalently bound to the sepharose beads. The beads are not soluble, and only proteins bound to sepharose beads will be left after thoroughly washing. The next stage will then be to perform a binding experiment including the bound protein and another protein or proteins. One method is to perform an *in vitro* transcription and translation of the protein of interest, including a marker to later detect the protein, and add it to bound proteins. A second method is to use extracts from cells transfected with expression vector for the protein of interest, and thereafter bind to proteins bound to beads (Schafer, Seip, Maertens, Block, & Kubicek, 2015). A third method is to detect binding of endogenous from cell extracts using GST pulldown and Western blot detection of the protein of interest.

At last, the binding between the autophagy-related protein and the other protein can be visualized using different methods, depending on the method used for binding. Common is the use of gel electrophoresis (SDS-PAGE, Davidson college). After the gel electrophoresis, if the protein of interest is radioactively labeled, the gel may be dried, incubated with a film to detect radioactivity and visualized in a proper machine. Another way to visualize the binding is to perform western blotting, where antibodies specific to tag or protein of interest are used (Bjørkøy et al., 2009).

3.3.2 Expression and Purification of GST-fusion Proteins from E. coli

From single colonies on agar plates with ampicillin, overnight cultures of pDest15-GST control, pDest15-LC3A, pDest15-LC3B, pDest15-LC3C, pDest15-GABARAP, pDest15-GABARAPL1 and pDest15-GABARAPL2, were made in ~5 mL LB broth containing ampicillin. The overnight cultures were then transferred to bottles containing 100 mL 2x YT broth also containing ampicillin, and grown until OD_{600} was between 0,5 and 0,9. The still growing cultures were then grown at room temperature for approximately 4 hours after addition of IPTG (0,5 mM) to

optimize the protein growth. To pelletize the cultures, they were transferred to centrifuge bottles fitted for Sorvall GSA rotor and kept on ice for some minutes; Centrifugation setting to 10 minutes at 5000 rpm 4°C. Each pellet was re-suspended in 4 mL ice-cold lysis buffer added 1 mM DTT and 10 mg/mL lysozyme. While the suspensions were kept on ice for 20 minutes, they were transferred to tubes that tolerate freezing at -70°C. Three cryon tubes were used for each suspension, containing approximately 1,5 mL of the suspension, and added 150 μL 10% Triton-X100 diluted in dH_2O and mixed gently.

The next day, one lysate from each of the triplets were sonicated (40 seconds on, 10 seconds off, 40% amplitude) and transferred to 2 mL collection tubes. To pelletize the lysate, they were centrifuged 10 minutes (4°C) at high speed in a microcentrifuge. To bind the proteins to GST beads, the supernatant from the lysates were added to 200 μL washed GST beads (in a 50% solution with NET-N), and placed 1 hour in a rotating wheel at 4°C. Now, the beads should have bound the protein in the solution. Washing three times with NET-N buffer would wash away everything that did not bind to the GST beads to get pure proteins bound to beads. To check if the beads and ATG8s had bound, SDS-PAGE gel electrophoresis was performed. In preparation of SDS-PAGE, 10 μL beads with GST fusion protein (50% solution) was added 10 μL 2x gel loading buffer with 20% 1M DTT, boiled for 5-10 minutes and spun down. Beads with proteins in a 50% solution with NET-N buffer were kept in the fridge until needed.

3.3.3 In vitro transcription and translation

To tag a protein to make it possible to detect this exact protein later on for *in vitro* experiments different methods may be used, and many different kits have been developed for this purpose. We have chosen to use the TNT® Coupled Reticulocyte Lysate Systems which is a coupled transcription/translation system for eukaryotic cell-free protein expression. The kit contains TNT® Rabbit Reticulocyte lysate, TNT® Reaction buffer, Amino Acid Mixture (Minus Methionine), ^{35}S methionine, and TNT® T7 RNA Polymerase ("TNT(R) Coupled Reticulocyte Lysate Systems,"). T7 RNA polymerase is a DNA-dependent polymerase, and have a high specificity for its promoter; the T7 promoter. The lysate contains cellular components that are necessary for protein synthesis (e.g. tRNA, ribosomes, amino acids, and initiation, elongation and termination factors). Supplying the translation mix with amino acids is crucial for translation

of the transcribed RNA, and by using an amino acid mixture without methionine, the radioactive ^{35}S-labeled methionine can be used to detect the protein of interest (Sundquist, 2006).

To produce in vitro translated proteins, TNT® T7 Coupled Reticulocyte Lysate System kit was used. 10 µL of in vitro translated proteins were to be used in each pulldown and 3 µL of the proteins were to be used as an indicator for percentage binding of the in vitro translated proteins. This meant that 73 µL assay buffer was needed when seven pulldowns were to be performed. The amount and materials used were calculated from 1 rx, which is shown in Table 25.

Table 25: 1 rx assay buffer for GST pulldowns. To tag the wanted protein with a radioactive tag and bind the protein to GST beads, an assay buffer was made with these different components.

Name	**Amount**
TNT Rabbit Reticulocyte Lysate (RTL)	25 µL
TNT buffer	2 µL
aaMix-Met	1 µL
S^{35}	1 µL
TNT polymerase	1 µL
DNA	1 µg
DNA/H_2O	18 µL
SUM	49 µL

The mix was then incubated in a heat block at 30°C for 90 minutes.

3.3.4 GST-Pulldown Binding Reaction

3 µL of the *in vitro* translation mix was placed in an empty Eppendorf tube and added 15 µL 5x SDS loading buffer in NET-N buffer added 10% 1 M DTT, boiled, spun down and frozen for use as input. The rest of the mix was then added 100 µL NET-N buffer with protease inhibitors for each pulldown and 10 µL empty GST beads, and incubated for 30 minutes at 4°C in a rotating wheel. This was done to avoid nonspecific binding to GST beads later on. To ensure equal amounts of the various GST-fusion proteins in the binding assays, the purified GST-fusion

proteins on beads were run on a test gel. From this gel, 1-10 μL of GST-fusion proteins were added empty beads to a total of 10 μL in a 50% solution, and washed twice with NET-N buffer (supernatant removed after last wash). For the pulldowns, the supernatant (100 μL) from the precleared in vitro translated protein was added to the designated GST-protein beads, and incubated for 1 hour at 4°C and rotation for binding.

After the binding reaction, the beads were washed 5 times with NET-N buffer. In between the washing, the beads were centrifuged at 2500 rpm for one minute to gather the beads at the bottom of the tubes. After the last wash, the buffer was removed in total. The beads were then added a mixture of 10 μL 5x loading buffer in NET-N buffer with 10% 1 M DTT, and boiled for a minimum of 5 minutes to elute the proteins from beads.

3.3.5 Detection of Protein-Protein Interaction

The eluted proteins were separated by SDS PAGE. After gel electrophoresis, the gel stained with Coomassie Blue to detect GST-fusion proteins. The gel was afterwards dried I a gel dryer (BioRad, model 583) and viewed through an autoradiograph (phosphoimaging) to detect radioactive labelled proteins. In this thesis, the Fuji s BAS-5000 from Fujifilm Life Science was used. this is a phosphor imaging system which uses a confocal laser and light-collecting optics to capture radioactivity ("Fujifilm BAS-5000 from FUJIFILM Life Science,").

3.3.6 LR Reaction

3.3.6.1 Gateway Cloning Technology

Gateway cloning technology is a cloning method that allows the transfer of a DNA sequence (usually cDNA of the protein of interest) from a donor vector to different expression vectors by site-specific DNA recombination. The method is based on the bacteriophage λ in *E. coli* and its high specificity in integration and excision in and out of the bacteria DNA. By using two different enzyme mixes, two different reactions may be performed; BP reaction and LR reaction (Reece-Hoyes & Walhout, 2018).

LR reaction uses a mix of phage lambda integrase, *E. coli* integration host factor, and lambda exisionase to recombine *att*L and *att*R sites to create *att*B and *att*P sites. The four *att* sites have a core recognition region approximately 25 base-pairs long, with "arms" in both, one or none on (each) side of this recognition region. The "arms" are the site in which the specific recombination enzymes recognize and interact. In all recognition region, there is a 7 base-pair long asymmetrical overlap, in which the DNA is cut and rejoined. The products of a LR reaction are two plasmids, one that is kanamycin resistant with the toxic ccdB gene and one that is ampicillin resistant. The cDNA of interest is between the two *att*L sites, and ends up in between the two *att*B sites in the expression clone. Examples of plasmids containing *att*R sites are illustrated in Figure 11.

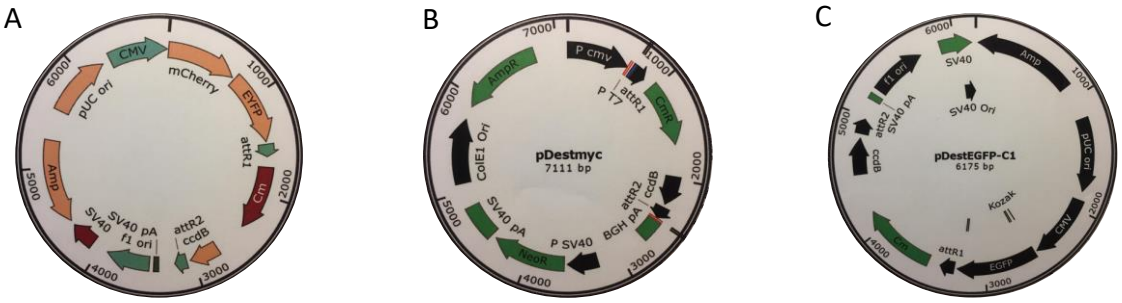

Figure 11: Map over three plasmids containing *att*R sites. pDestmCherry-EYFP (A), pDestmyc (B) and pDestEGFP are plasmids containing *att*R sites.

If pDONR TRIM31 (*att*L) is recombined with pDestmyc (*att*R), two new plasmids are made; pDestmyc-TRIM31 (*att*B) and pDONR containing a toxic gene (*att*P). The new functional plasmid (pDestmyc-TRIM31) will then be the size of pDestmyc without the sequence in between of *att*R sites (~5600 bp) and size of TRIM31 (~1272 bp).

By plating the bacteria with the new vectors on agar plates containing one of these antibiotics, only one of them will survive and grow. Thereby, only the bacteria with the properties of interest will grow and can be studied (Reece-Hoyes & Walhout, 2018).

3.3.6.2 Protocol

To transfer a cDNA insert to another vector, the method of LR reaction is used. The prepared plasmid (50-150 μg/μL) of interest was mixed added 150 μg/μL of the vector and rest up to 8 μL TE-buffer. To start the reaction, 1 μL LR clonase II enzyme was added to the mix and left in room temperature. After one hour, the reaction was stopped with 1 μL proteinase K solution and incubated at 37°C for 10 minutes. To transfer the cDNA inserts with the new vector into bacteria, they were added 50 μL competent cells (*E. coli* DH5α) and left on ice for 20-30 minutes, heat shocked for 2 minutes at 37°C and added 250 μL SOC-media. For transfection into the new competent cells, the mix was incubated for additional one hour at 37°C with shaking and 150 μL was plated on agar plates containing antibiotics. Preparation of plasmids from single colonies as described in "Preparation of Plasmids" were performed and protein concentration was measured for further use in experiments.

3.3.7 Site-Directed Mutagenesis and DNA Sequencing

To alter, mutate, the DNA sequence has been a useful technique in biological research. By mutating specific cDNA sequences in plasmids, the properties of specific sites and domains in the protein may be studied. One method of site-directed mutagenesis is to first run a polymerase chain reaction (PCR) (Carrigan, Ballar, & Tuzmen, 2011). PCR was first developed and discovered by Mullis in 1983 (Mullis et al., 1986), and is a method to amplify a specific sequence or plasmid through temperature specific cycles (Figure 12) (Saiki et al., 1985).

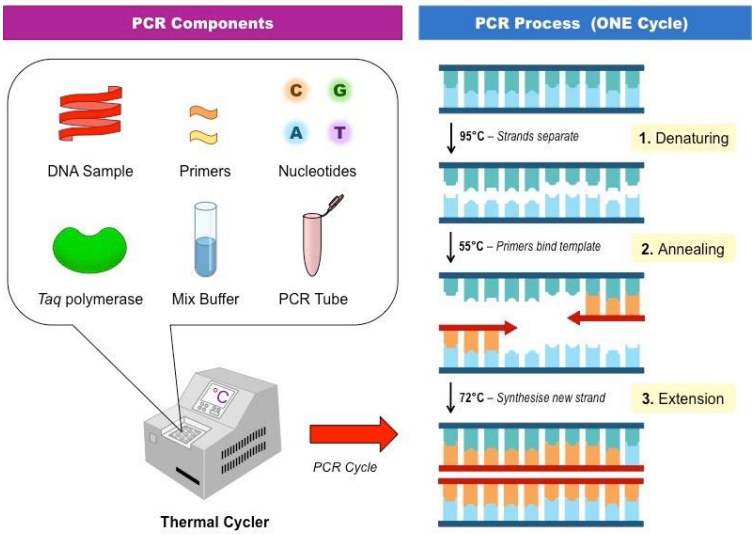

Figure 12: Schematic of one cycle of polymerase chain reaction (PCR) with its components. PCR components are the DNA sample, primers, nucleotides, *Taq* polymerase and a mix buffer, mixed in a PRC tube. Inside the thermal cycler, the DNA is denatured at 95°C, and the strands are separated. The second step, annealing, happens at 55°C and the primers bind template. The temperature is then increased to 72°C where the synthesizing of the new strand happens. Figure is reprinted from ("PCR,").

The temperature and number of cycles may be adjusted to the sequence of interest. Parental DNA is then removed by a restriction enzyme, and transferred into competent cells (Carrigan et al., 2011).

3.3.7.1 Restriction-Enzyme Cutting

Restriction enzymes are defined by which DNA sequence they recognize and cut (Dryden, 2013). The enzymes are divided into four groups (I, II, III and IV) (Roberts et al., 2003). Restriction enzymes cleave double stranded DNA and leave blunt or staggered 5´ and 3´ ends with overhangs in the DNA-strands. Since, restriction enzymes recognize and cleave DNA at specific sites, different enzymes are used in different experimental procedures. Which restriction enzyme to use is also dependent on the DNA and where the cleavage is wanted (Shang et al., 2014).

In this thesis, the restriction enzyme DpnI which targets methylated or hemimethylated DNA sequences in parental DNA (Carrigan et al., 2011; J. Li et al., 2008) was used in site directed mutagenesis.

3.3.7.2 Protocol

For each wanted mutation, 5 µL 10x Pfu reaction buffer, 20 ng template DNA, 125 ng of each of the ordered oligos for the mutation, 1 µL dNTP mix (10 µM), 1 µL Pfu DNA polymerase (2,5 U/µL) and dH_2O until 50 µL were mixed in PCR tubes. Mutagenesis were then performed by running the PCR tubes in a PCR machine with settings:

Cycles	Temperature	Time
1	95°C	30 sec
16-18	95°C	30 sec
	55°C	1 min
	68°C	2 min/kb

After the PCR reaction, Dpn1 were added, and the tubes were left in warm bath (37°C) for one hour. The reaction mix was then transformed into competent *E. coli* cells (DH5α). Thereafter, the cells were grown in SOC medium and plated on proper agar plates. To identify plasmids with correct mutation, mutation target sequence was investigated by DNA sequencing.

3.3.7.3 Protocol for DNA Sequencing

Purified plasmids (200-500 ng) were mixed with 1 µL BigDye, 2 µL primer (10 µM) and dH_2O to a final volume of 10 µL. PCR tubes with this mix were then run on the sequencing program on a PCR machine with these settings:

Cycles	Temperature	Time
1	96°C	1 min
34	96°C	30 sec
	50°C	15 sec
	60°C	4 min

PCR tubes were then delivered for sequencing at the DNA sequencing facility at UiT.

3.3.8 Culturing and Transfection of Mammalian Cells

3.3.8.1 HeLa Cells

HeLa cells are originally obtained from a cervical biopsy of Henrietta Lacks in 1951. This is also the cause of the name; by putting the two first letters of Henrietta Lacks first and last name you get "HeLa". HeLa cells were the first cancer cells to be grown outside of the body, which made these cells so important. The cells grew and proliferated, and are seen as an immortal cell line (Lucey, Nelson-Rees, & Hutchins, 2009).

3.3.8.2 Culture Conditions – Maintenance and Handling of Mammalian Cells

The tissue culture medium is of great importance for maintenance of mammalian cells. Different laboratories have chosen different medium for the culturing (e.g DMEM with 10% FBS, streptomycin and penicillin) that provides nutrients for the growing cells and inhibit contamination (Phelan, 2007). Nutrients needed in a culturing medium for mammalian cells is the twelve essential amino acids, monosaccharides, vitamins (e.g biotin, folate), inorganic ions (e.g sodium, potassium) and trace elements (e.g molybdenum, vanadium) (Z. Yang & Xiong, 2012). Different mammalian cells need different kind of culturing medium. It is important that everything that is used in the handling and maintenance of the cells are sterile, which in some cases means autoclaved. The media used in maintenance of the cells can have an indicator which changes color when pH changes. As the cells grow and reach a high confluency on the surface of the culture flask, they have to be sub-cultured or passaged to avoid reduced mitotic index and cell death. For most mammalian cells, the optimal pH lies between 7.2 and 7.4, and buffers are preferably used in the culturing medium to avoid big pH changes. Even if many use FBS to supply culturing cells with nutrients, other animal serum or serum-free medium are in use. The cultured mammalian cells are incubated in a humidified 37°C, 5% CO_2 incubator, unless otherwise is specified (Phelan, 2007).

3.3.8.3 Splitting of Cells (Cell Passage)

The HeLa cells are immortal, and will grow on some surfaces, e.g plastic bottle surfaces. One of the things that can stop them from multiplying is lack of space. So when the confluence is

between 70% and 80%, they have to be split. To avoid contamination, the cells has to be handled in a biological safety cabinet. The media over the cells were first removed, and the cells were washed with PBS to be sure that the old culture media was properly removed. To this point, it has been important to be careful not to disturb the cells. Then, to separate the cells from each other and from the surface, 0,5 mL (Nunc^{TM} EasYFlask^{TM} 25 cm^2 Nucleon^{TM} Delta Surface) or 1 mL (Nunc^{TM} EasYFlask^{TM} 75 cm^2 Nucleon^{TM} Delta Surface) trypsin was added directly at the cells, and the cells were incubated at 37°C (because trypsin works best at this temperature) until the cells had detached from the flask surface and each other. In the meantime, complete media (DMEM with 10% FBS, streptomycin and penicillin) were added to empty culture bottles. After incubation, complete media were added to deactivate the trypsin and avoid further destroying of the HeLa cells. Here, it was important to make a homogenous solution to have the cells evenly distributed in the solution. Appropriate amount of the homogenous solution was placed into the culture bottles containing complete media (e.g 2:10 and/or 3:10 dilutions) for continuing the culture or for counting and seeding out for experiments. All the media used in splitting of the HeLa cells were pre-warmed to either room temperature or 37°C.

3.3.8.4 Cell Counting

A few microliters of the cell suspension were taken up in a pipette, and the solution placed under the coverglass over the haemocytometer. The haemocytometer was placed under a microscope under 10x objective and 10x ocular. The haemocytometer is divided in many squares (illustrated in Figure 13 A), and the number of cells within sixteen of these squares x10^4 gives the number of cells per mL in the corresponding solution of cells.

A **B**

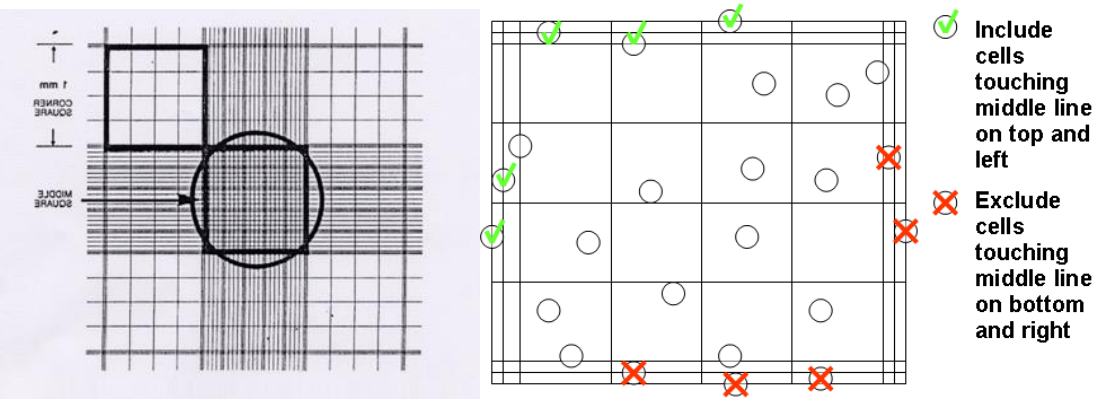

Figure 13: Burkes heamocytometer. A: The big square of heamocytometer, marked with circle, have 25 smaller squares. **B** Enlargement of one of the 25 small squares from A ("Cell counting using a Haemocytometer,"). Pictures are reprinted with permission.

3.3.8.5 Protocol

HeLa cells and HeLa ATG7 KO (knock out) cells were used in this experiment. 24-well dishes were used, and each well were added one coverslip. The wells containing coverslips were then sterilized with ethanol and coated with fibronectin (1:200) to optimize binding of cells. For this, 2 mL PBS, added to each well and added 20 µL fibronectin, and left in room temperature for 20 minutes. 300 000 cells were seeded in each well of the 24-well dish, with 0,5 mL full medium. The next day the cells were transfected using 50 µL DNA mix (DMEM with 1 µL transit LT1 and 200 ng DNA) to 0,5 mL new media without antibiotics .(Table 26). One day later the cells were observed in a fluorescence microscope to determine if the transfection was successful. 22 hours or 46 hours after transfection, the media were changed, and cells in some wells were starved or starved in 0,5 mL HBSS or 0,5 mL HBSS with 200 nM Bafilomycin A1 (Baf):

Table 26: Half of a 24-well dish with indicated treatments of HeLa and HeLa ATG7 knock out cells. Each of the empty spaces indicate a well, whereas half of the wells contained HeLa cells and the other half contained HeLa ATG7 KO cells. Each well was thereafter transfected with indicated plasmid, and treated as indicated after successful transfection.

Protein expression construct	Full media	Starvation media (HBSS)	HBSS + Baf (200 nM)
pDestmCherry-YFP			
pDestmCherry-EYFP TRIM23			
pDestmCherry-EYFP TRIM31			
pDestmCherry-EYFP p62			

3.3.8.6 Fixation and Mounting of Cells for Confocal Fluorescence Microscopy

After washing with ice cold PBS, 0,5 mL 4% PFA was added for fixation and incubated in room temperature for 10 minutes. The wells were thereafter washed twice with PBS and stained with DAPI for 10 minutes to make the nucleus visible in the microscope. For this, each well was added 0,5 mL of diluted DAPI in PBS (1:4000). After this, the cells were again washed twice with PBS. Now, the coverglasses were ready to be mounted on coverslips for microscopy. 10 µL Mowiol* were dripped on the coverslips and the coverglass placed on the drop with the cells facing the Mowiol. Coverslips with attached coverglasses were covered to avoid light from affecting the fluorescence and placed in 4°C over night to dry. The cells were analyzed using a LSM780 Zeiss confocal fluorescence microscope.

To investigate co-localization between TRIM31 and the ATG8s, cells were transfected with expression constructs for both TRIM31 and LC3A/LC3B/GABARAP. The conditions used were full medium, starvation medium (HBSS) and full medium with 200 nM Baf.

* Mowiol solution is made by first adding 6 g Glycerol to a 50 mL disposable conical centrifuge tube, and thereby adding 2.4 g Mowiol. The mixture is stirred and added 6 mL dH_2O. After incubation for 2 hours at room temperature, 12 mL 0.2 M Tris pH 8.5 is added, and incubated at approximately 53°C until Mowiol has dissolved. The mixture was stirred occasionally during this incubation. Thereafter, the mixture was clarified by cetrifugation at 4000-5000 rpm for 20 minutes, and transferred into Eppendorf tubes. Mowiol may now be stored at -20°C for 12 months or at room temperature for one month.

3.3.9 Transfection and analyzing with confocal microscopy

3.3.9.1 Confocal fluorescence Microscopy

Marvin Minsky was the one that originally developed confocal microscopy in the mid 1950s (Minsky, 1988), but the first mechanically scanned image of a cell was not obtained before David Eggers work in 1973 (Davidovits & Egger, 1973). Since then, the confocal microscope has developed into the many we have today. Confocal fluorescence microscopes send light to the specimen in different wavelengths in which excite the fluorophores in the specimen. The fluorophores will then emit fluorescent light and be visible in the microscope. In biological analyzing methods, fluorophores are much used to stain cells and tissues for detection in for example a confocal fluorescence microscope where the specimen (e.g. cells, tissues or protein) is visualized (Thooft, Cassaidy, & VanVeller, 2017). To do this, fluorophores are transfected into living cells directly or proteins containing fluorophores are transfected into the cells. In this manner, the fluorophores are fluorescence tag (e.g. GFP or mCherry). By altering fluorophores, more fluorescence tags are being made (Thooft et al., 2017).

In this thesis, a confocal fluorescence microscope from Zeiss was used to detect fluorescent tagged TRIM23, TRIM31 and ATG8s.

3.3.9.2 Co-localization assay

Transfection, fixation and mounting of cells for confocal fluorescence microscope was performed as described under “3.3.8.5 Protocol” and “3.3.8.6 Fixation and Mounting of Cells for Confocal Fluorescence Microscopy”. To investigate co-localization between TRIM31 and the ATG8s, cells were transfected with expression constructs for both TRIM31 and LC3A/LC3B/GABARAP. The conditions used were full medium, starvation medium (HBSS)

and full medium with 200 nM Baf. 24 hours after transfection the cells were fixated and mounted for confocal fluorescence microscopy.

3.3.10 Western Blot

Western Blot method was first presented by Towbin et al (Towbin, Staehelin, & Gordon, 1979). The method derived from the DNA (Southern) Blotting and RNA (Northern) Blotting, and is for the transfer of proteins from a SDS polyacrylamide gel to an adsorbent membrane (Kurien & Scofield, 2006). Because of the use of antibodies, the method is also called immunoblot. The antibody is used to detect its specific antigen on the membrane, and bind to it. This make it possible, and rather easy, to detect the chosen protein in a large mixture of different proteins. A blocking buffer is used to prevent the unspecific binding of antibodies to the membrane. Also, two antibodies are added to the membrane. The first antibody (primary antibody) is the specific one and work as an anchor for the secondary antibody, which is conjugated to the enzyme Horse Raddish Peroxidase (HRP). By adding the HRP substrate light is produced as a byproduct from the reaction. This light can be detected by luminescent image machines ("Overview of Western Blotting,") and in this way, specific proteins can be detected on the membrane.

3.3.10.1 Protocol

3.3.10.1.1 Transfection of Cells for Western Blot

Before transferring cells to the dish, the wells were coated with fibronectin to ensure that the cells were properly attached. 2 mL PBS with 20 µL fibronectin (Sigma) was added to each dish, and incubated in room temperature for approximately 30 minutes. 300 000 cells were then added to the dishes with DMEM added 10% fetal bovine serum and antibiotics, and grown overnight in 37°C, 5% CO_2. One 60 x 15 mm dish for each pulldown was made. When the cells reached a 70-80% confluency, they were transfected. To transfect the cells, two tubes were made for each dish; one with 300 µL DMEM with serum and 3 µg of the selected DNA, and the other with 300 µL DMEM with serum and 4 µL Metafectene pro. The two mixes were then mixed together and left in room temperature for 20 minutes. The media on the cells were changed to media without antibiotics and added 600 µL of the DNA/Metafectene mix and incubated overnight.

3.3.10.1.2 Western Blotting

The beads from the binding reaction were added SDS-loading buffer with 20% DTT and the bound proteins were separated by SDS-PAGE and transferred to a membrane. After successfully transferring the proteins to the membrane, the membrane was stained with Ponceau S to visualize the amount of loaded proteins. After taking a picture of the membrane, the staining was removed by washing with PBS-T and thereafter blocked with 5% nonfat-dry milk to avoid unwanted binding with antibodies. The membrane was then transferred to a new tube with primary antibody specific to the proteins or their tag diluted in PBS-T, and incubated in 4°C overnight with rotation. To remove excessive antibody, the membrane was washed in PBS-T. The membrane was incubated in room temperature with rotation for 1 hour with secondary antibodies diluted in PBS-T and washed for at least 15 minutes with PBS-T (changed at least 4 times). The protein-bands on the membrane where then visualized by staining with SuperSignal™ West Femto Maximum Sensitivity kit from Thermo Scientific and detected with an imager (ImageQuant™ LAS 4000 from GE Healthcare).

3.3.10.2 Western Blot of Transfected Cells for Degradation Measurements

300 000 cells were seeded out in each well of a 6-well dish. The cells were grown overnight in DMEM with 10% FBS at 37°C and 5% CO_2. To transfect the cells, two tubes were made for each dish; one with 300 µL DMEM with serum and 3 µg of the selected DNA, and the other with 300 µL DMEM with serum and 4 µL Metafectene pro. The two mixes were then mixed together and left in room temperature for 20 minutes. The media on the cells were changed to media without antibiotics and added 600 µL of the DNA/Metafectene mix and incubated overnight. The next day, the cells were treated as indicated in Table 27.

Table 27: 6-well dish with indicated treatment for HeLa cells transfected with expression constructs for GFP-TRIM23 or GFP-TRIM31.

Full medium	Full medium with Baf	Full medium with MG132
HBSS 2-4h	HBSS with Baf 2-4h	HBSS with MG132 2-4h

After treatments (Table 27), the cells were washed with PBS. The cells were thereafter harvested in 40 μL 2x SDS gel loading buffer with 100 mM DTT, boiled, spun down, and separated by SDS-PAGE before Western blotting as described above. An antibody against GFP was used as primary antibody to detect the GFP-fusion proteins.

4 Results

4.1 cDNAs Encoding TRIM23 and TRIM31 were Successfully Transferred into Expression Vectors

To use the TRIM31 cDNA to analyze binding of TRIM31 to ATG8 family proteins, co-localization in cells and lysosomal degradation, Gateway LR reactions were used to generate pDestmyc TRIM31, pDestEGFP TRIM31 and pDestmCherry-EYFP TRIM31 (see Figure 11). Table 28 lists the pDONOR plasmids and the resultant pDest(ination) plasmids. The calculated sizes of the various established plasmids are; pDestmCherry-EYFP (~5300 bp), pDestmCherry-EGFP TRIM31 (~6700 bp), pDestEGFP (~6200 bp), pDestEGFP TRIM31 (~5600 bp),pDestEGFP TRIM31 LIR2 mutant (~5600 bp),pDestEGFP TRIM31 LIR1/LIR2 mutant (~5600 bp), pDestmyc (~7100 bp), pDestmyc TRIM23 (~7400 bp), pDestmyc TRIM31 (~7000 bp), pDestmyc TRIM31 LIR1/LIR2 mutant (~7000 bp), pDestmyc TRIM31 LIR1/LIR2 mutant (~7000 bp). Establishment of correct plasmids was verified by agarose gel electrophoresis (Figure 14).

Table 28: LR reaction to make pDest(ination) clones.

LR reaction	**pDest(ination) plasmids**
pDONR221 TRIM31 fusion + pDestmyc pDONR221 TRIM31 fusion + pDestmCherry-EYFP pDONR221 TRIM31 fusion + pDestEGFP	pDestmyc TRIM31 pDestmCherry-EYFP TRIM31 pDestEGFP TRIM31
pDONR221 TRIM31 LIR2 mutant + pDestmyc pDONR221 TRIM31 LIR2 mutant + pDestEGFP	pDestmyc TRIM31 LIR2 mutant pDestEGFP TRIM31 LIR2 mutant
pDONR221 TRIM31 LIR1/LIR2 mutant + pDestmyc pDONR221 TRIM31 LIR1/LIR2 mutant + pDestEGFP	pDestmyc TRIM31 LIR1/LIR2 mutant pDestEGFP TRIM31 LIR1/LIR2 mutant

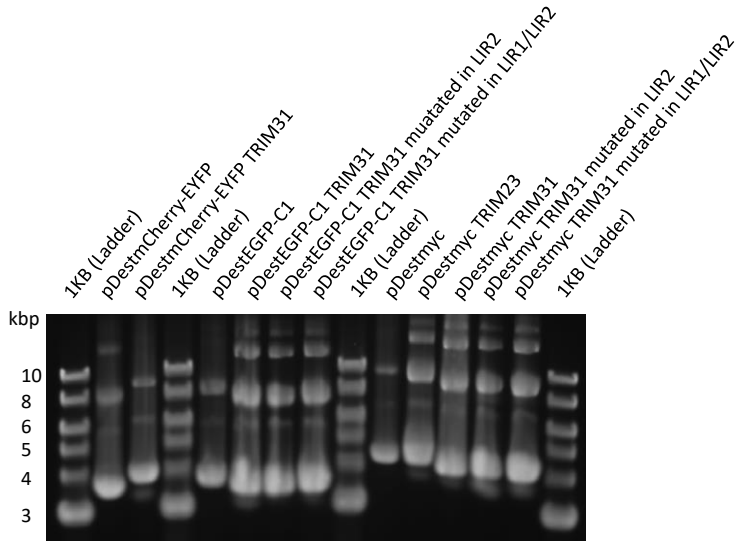

Figure 14: Agarose gel electrophoresis (0.7%) of various TRIM31 pDest(ination) vectors. Some plasmids were made previously to this thesis; pDestmCherry-EYFP, pDestEGFP, pDestmyc and pDestmyc TRIM23. The size of the plasmids must be compared to the other plasmids and not the ladder. The 0.7% agarose gel show the expected size of plasmids compared to each other.

Plasmids are double-stranded, circular DNA molecules and the ladder is linear DNA fragments. The ladder is therefore not an indicator of the specific size of the pDest vectors. Rather, the plasmids were compared to each other, and LR reactions were determined to be successful.

4.2 ATG8s were Successfully Expressed and Purified from *E. coli*

Here, the interactions between ATG8s and TRIM23 and TRIM31 were to be studied. N-terminal GST fusions of the six human ATG8 family proteins LC3A, LC3B, LC3C, GABARAP, GABARAPL1 and GABARAPL2 were therefore expressed using an *E. coli* expression vector. Lysates of the *E.coli* expressing the various ATG8s were sonicated and bound to GST beads, and the GST-ATG8s purified by repeated washing steps. SDS-PAGE gel electrophoresis showed that the ATG8s were successfully expressed and purified (Figure 15). The gel electrophoresis with GST and GST-ATG8 fusion proteins show that the proteins are relatively pure with low levels of other bands seen on the coomassie-stained gel. From the intensity of the bands, the amounts used in GST pulldown were adjusted.

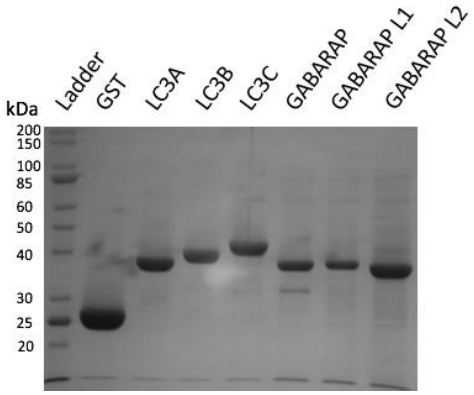

Figure 15: ATG8s were successfully expressed and purified from *E. coli*. SDS-PAGE gel electrophoresis (10%) with GST (empty vector) and GST-ATG8s were run. The same amount of 50% solution beads was loaded in each well lysed in 10 µL 2x gel loading buffer with 20% 1 M DTT.

4.3 TRIM23 binds weakly to the ATG8s

Before the start of this thesis work, a peptide array scan had been performed in our group (Molecular Cancer Research Group; MCRG) (G. Evjen and T. Johansen, unpublished data) (Figure 16) identifying a potential LIR motif in TRIM23 binding to GST-GABARAP. In the peptide array, 20-amino acids long peptides corresponding to the entire amino acid sequence of the protein of interest are spotted on a membrane with each peptide moved a window of 3 amino acids relative to the previous peptide. This way a "peptide walk" is performed where the entire amino acid sequence is covered from the N-terminal end to the C terminus (Johansen et al., 2017). As shown in Figure 16, 5 consecutive peptides gave a positive signal on the array defining the core LIR motif as FVCL. The aromatic position in LIR that binds to the HP (hydrophobic) 1 pocket usually has a tryptophan (W) or a phenylalanine (F) for most proteins, and a few proteins have tyrosine (Y). As the general rule, the consensus of the core LIR motif is (W/F/Y)XX(L/I/V). Acidic amino acids are often seen just N-terminal to the LIR motif (Alemu et al., 2012; Birgisdottir et al., 2013). That these peptides turn out positive does not necessarily mean that the native, folded protein will bind as the motif may be differently exposed or hidden.

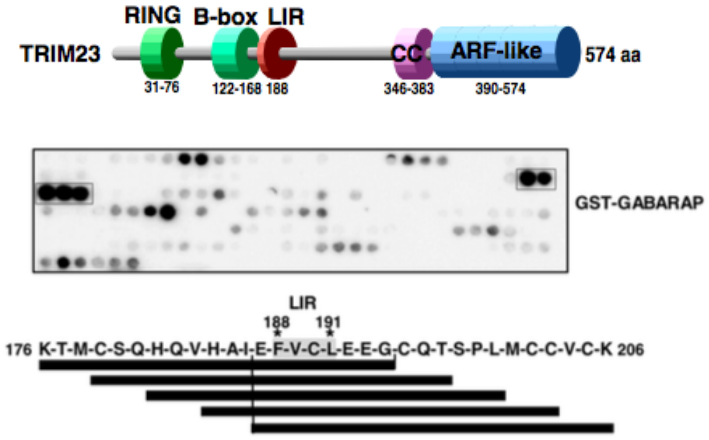

Figure 16: Peptide array scan identified one potential LIR motif in TRIM23. 20-amino acid long peptides covering the entire peptide sequence are spotted on a membrane, moving three amino acids relative to the previous peptide. In the end, the entire sequence of the protein has been spotted on the membrane. Recombinant GST-GABARAP is added to the arrays and an antibody to GST is used to detect bound GST-GABARAP. Dark dots indicate binding, and was detected with anti-GST antibodies. There was found one potential LIR motif in TRIM23 (FVFL) at position 188 to 191.

Therefore, to check if TRIM23 bound any of the mammalian ATG8, GST pulldown was performed. GST fusions of ATG8s (LC3A-C, GABARAP, GABARAPL1 and GABARAPL2) were purified and bound to GST beads. The beads were mixed with *in vitro* translated myc-TRIM23 containing a radioactive tag (^{35}S-methionin). Figure 17A shows the result from one binding assay, which is representative of two independent experiments. Quantification of the bands on the autoradiogram, shows that TRIM23 binds weakly to the ATG8s and are based on both experiments. The results show that TRIM23 bind strongest to GABARAP.

A

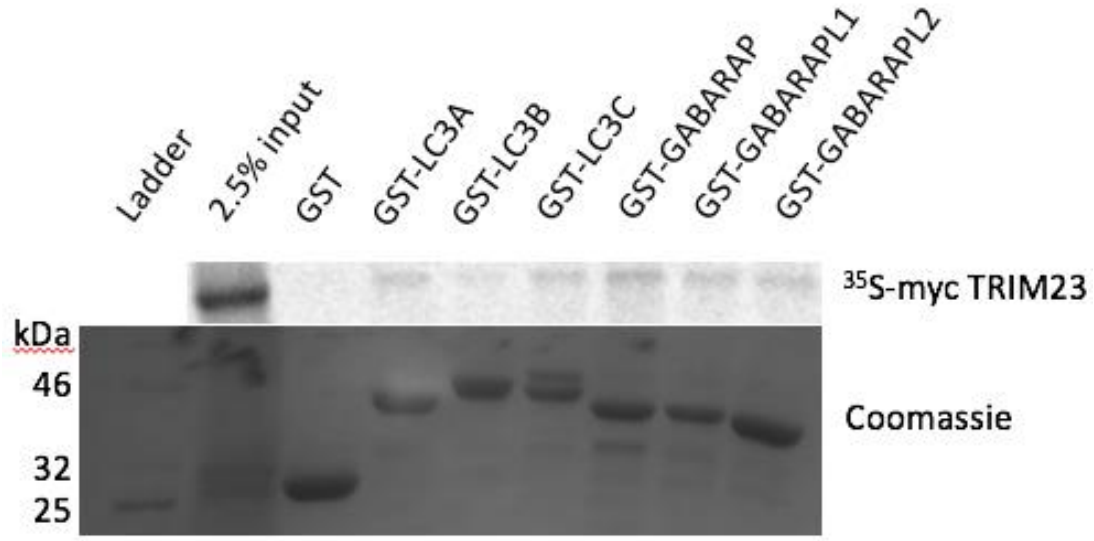

B

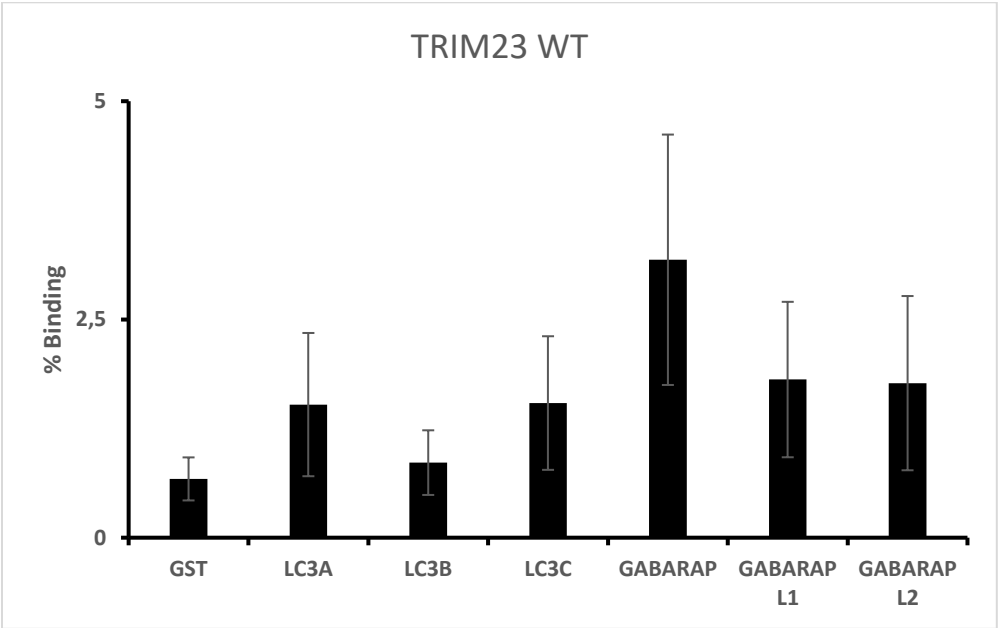

Figure 17: GST Pulldown detected weak binding of GST-ATG8s to myc-TRIM23. The SDS-PAGE gel electrophoresis and autoradiography (A) and percentage binding normalized to input (B) of binding between TRIM23 and each of the six different ATG8s are shown. Autoradiogram and quantification shows that there is weak binding to all ATG8s. The quantifications are based on two individual experiments, and includes the standard deviation.

4.4 TRIM31 Binds strongest to GABARAP and GABARAPL1

A peptide array scan had been performed in our group (Molecular Cancer Research Group; MCRG) (G. Evjen and T. Johansen, unpublished data) (Figure 18) identifying a potential LIR motif in TRIM31 binding to GST-GABARAP. In the peptide array, 20-amino acids long peptides are spotted on a membrane with each peptide moved a window of 3 amino acids relative to the previous peptide until the whole sequence is covered (Johansen et al., 2017). As shown in Figure 18, 6 consecutive peptides gave a positive signal on the array defining the two core LIR motifs as FELL and FQFL. As for peptide array explained for TRIM23 above, the consensus of the LIR domain is (W/F/Y)XX(L/I/V) and binding in a peptide array does not necessarily mean that the binding will happen in the native, folded protein.

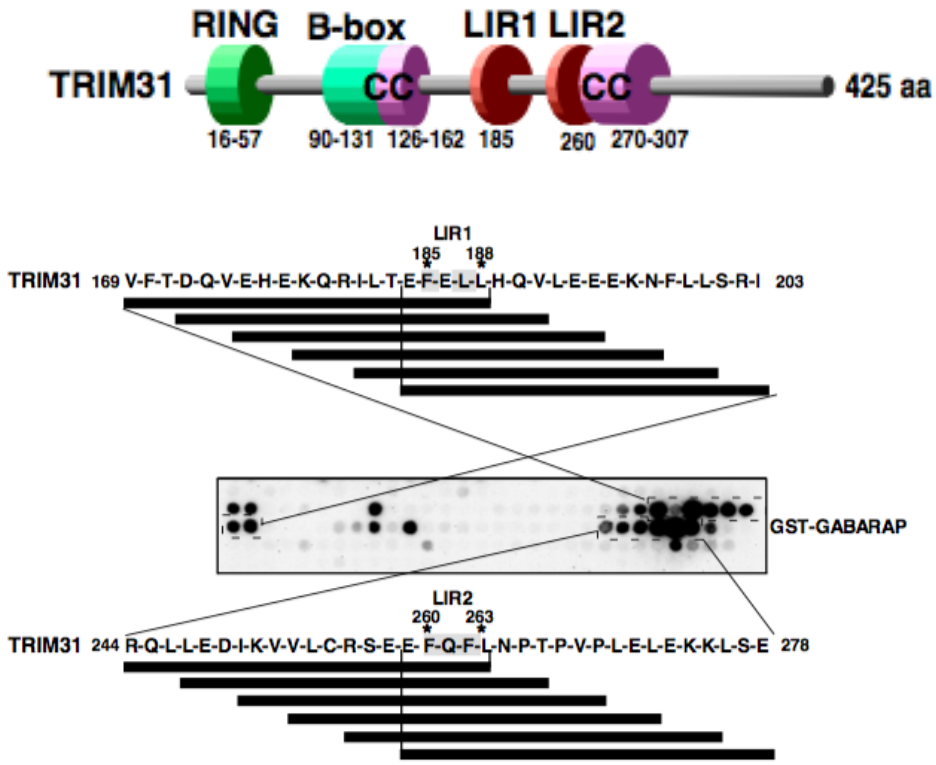

Figure 18: Peptide array scan identified two potential LIR motifs in TRIM31. 20-amino acid long peptides covering the entire protein sequence are spotted on a membrane, moving three amino acids relative to the previous peptide. In the end, the entire sequence of the protein has been spotted on the membrane. Recombinant GST-GABARAP is added to the arrays. Dark dots indicate binding, and was detected with anti-GST antibodies. There was found two potential LIR motifs in TRIM31 (FELL) at position 185 to 155 and (FQFL) 260 to 263.

Therefore, to determine if TRIM31 bound any of the mammalian ATG8s, GST pulldown assays were performed. GST fusions of ATG8s (LC3A-C, GABARAP, GABARAPL1 and GABARAPL2) expressed in *E. coli* were purified on GST beads. The beads were mixed with *in vitro* translated myc-TRIM31 containing a radioactive tag (^{35}S-methionin). Figure 19A shows the result from one binding assay which is representative of three independent experiments, and Figure 19B shows the quantification of the bands on the autoradiogram.

A

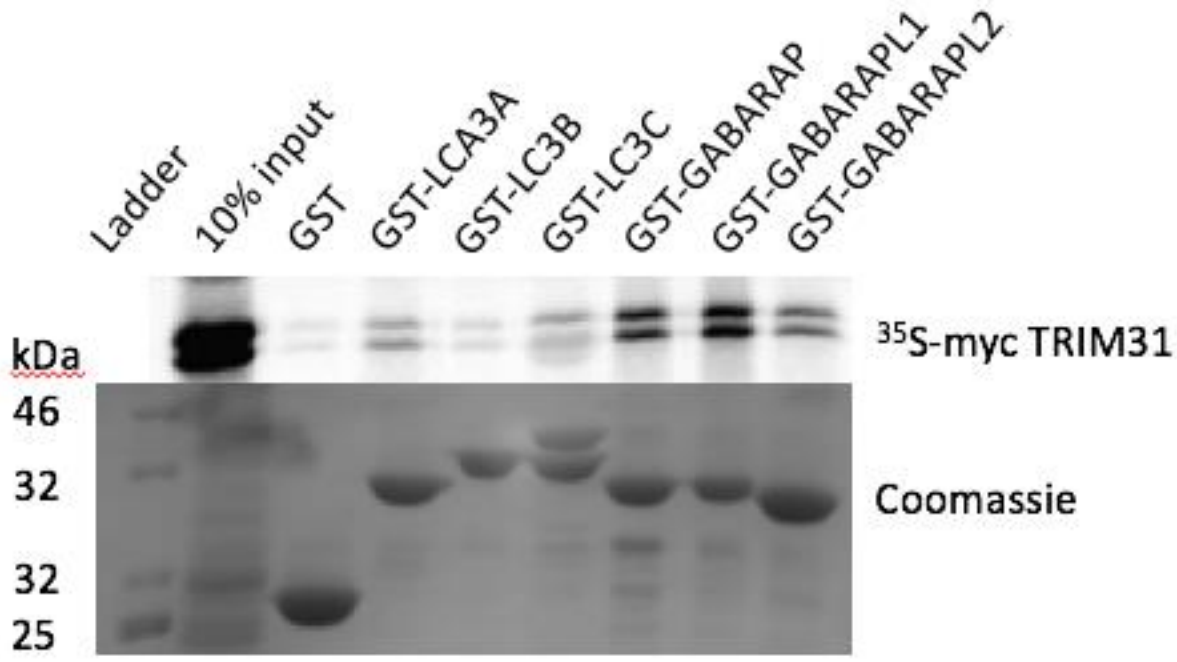

B

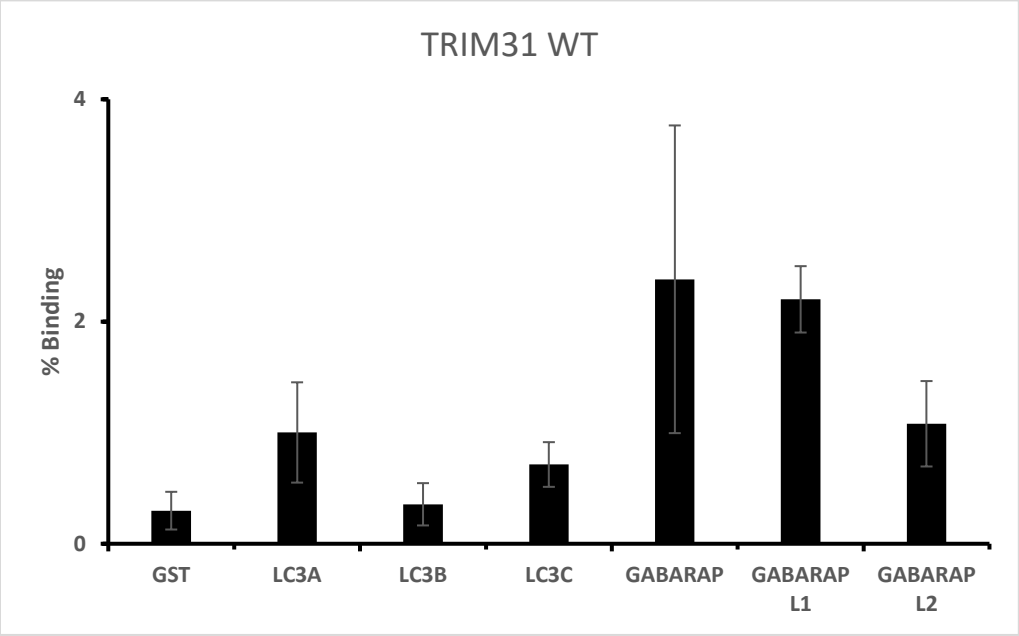

Figure 19: GST Pulldown detect binding of GST-ATG8s to myc-TRIM31. The SDS-PAGE gel electrophoresis and autoradiography (A) and percentage binding normalized to input (B) of binding between TRIM31 and each of the six different ATG8s are shown. From the autoradiogram, ^{35}S methionine-tagged TRIM31 was clearly visible, and quantification shows that there is binding between most ATG8s (LC3A, LC3B, GABARAP, GABARAPL1 and GABARAPL2) and TRIM31. The quantifications based on three independent experiments, and the graphs show the mean values with standard deviation.

The results shown in Figure 19, show that there is binding between myc-TRIM31 and all GST-ATG8s. Quantitation of the myc-TRIM31 bands in three independent experiments showed that GABARAP and GABARAPL1 bound strongest.

Control experiment shows very strong binding of p62 to the ATG8s

From previous research, p62 is known to bind strongly to all ATG8s (Pankiv et al., 2007). p62 was therefore used as a positive control for the GST pulldown assay. Figure 20 shows that in line with the established litterature, p62 displays strong binding to the ATG8s, which is illustrated in Figure 20. This result show that TRIM23 and TRIM31 bind with much lower affinity to the ATG8 proteins than p62. Also, they seem to have a preferance for binding to the GABARAP subfamily, while p62 binds with strong affinity both to the LC3 and the GABARAP subfamilies.

A

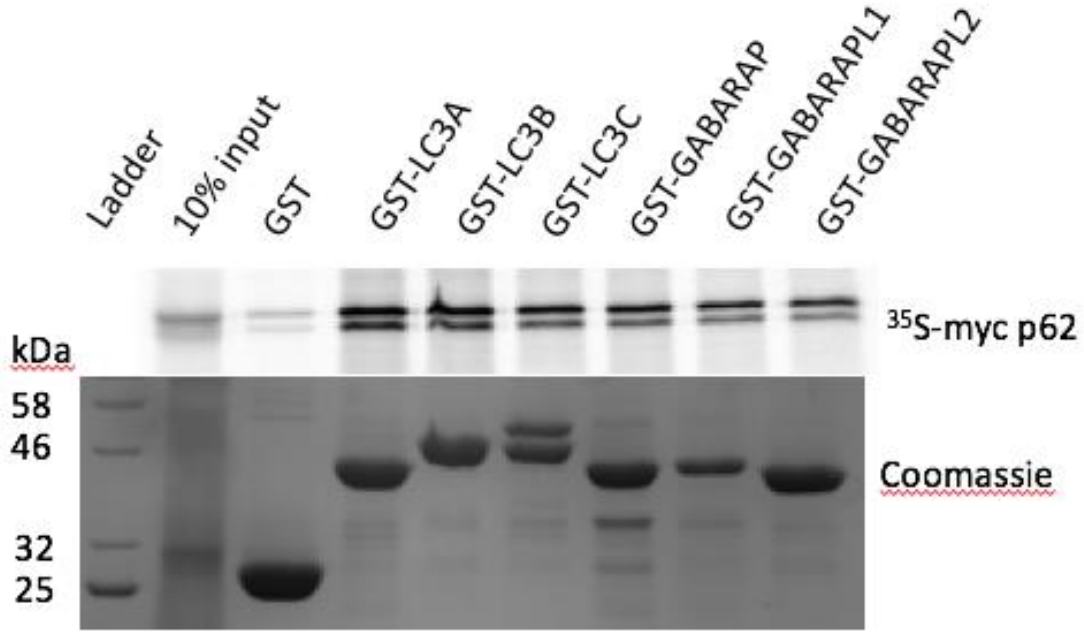

B

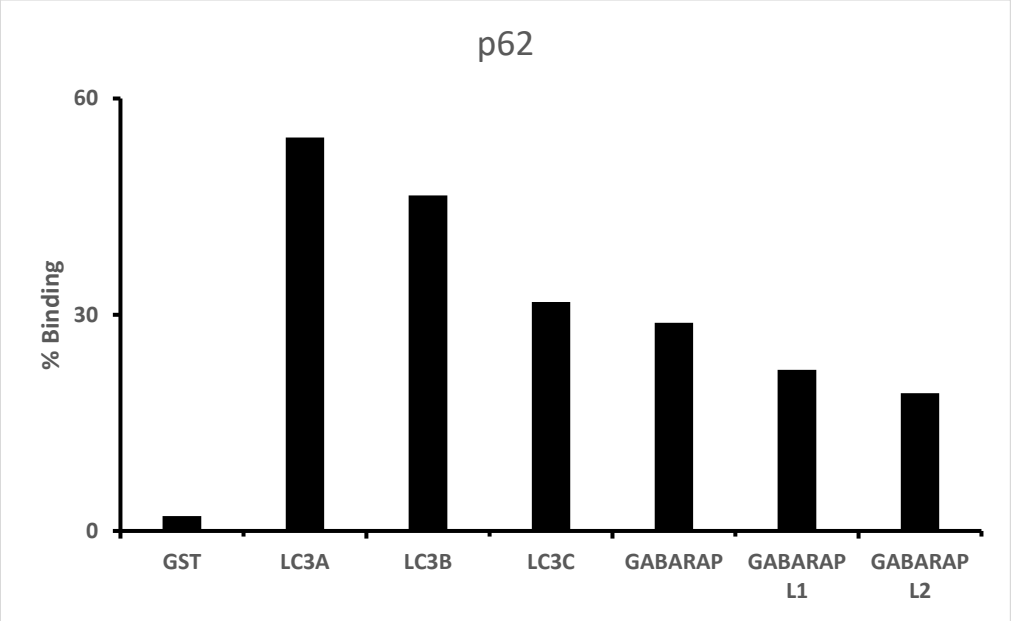

Figure 20: GST Pulldown detect binding of GST-ATG8s to myc-p62. The SDS-PAGE gel electrophoresis and autoradiography (A) and percentage binding normalized to input (B) of binding between p62 and each of the six different ATG8s are shown. From the autoradiogram, ^{35}S methionine-tagged p62 was clearly visible, and quantification shows that there is binding between all ATG8s and p62. The quantifications are based on one experiment.

.

4.5 TRIM23 and TRIM31 Binding to GABARAP is LIR Dependent

Both TRIM23 and TRIM31 bound strongest to GABARAP according to GST pulldown results. To see if the binding of TRIM23 and TRIM31 to ATG8s were LIR-dependent, GABARAP mutated in its key amino acids in LIR docking site (LDS) (Y49A and F104A) were applied in the binding reaction (Behrends, Sowa, Gygi, & Harper, 2010). Y49 bind the first amino acid in the LIR motif, and F104 bind the last amino acid in the core LIR motif. Results are shown in Figure 21 and 22.

A

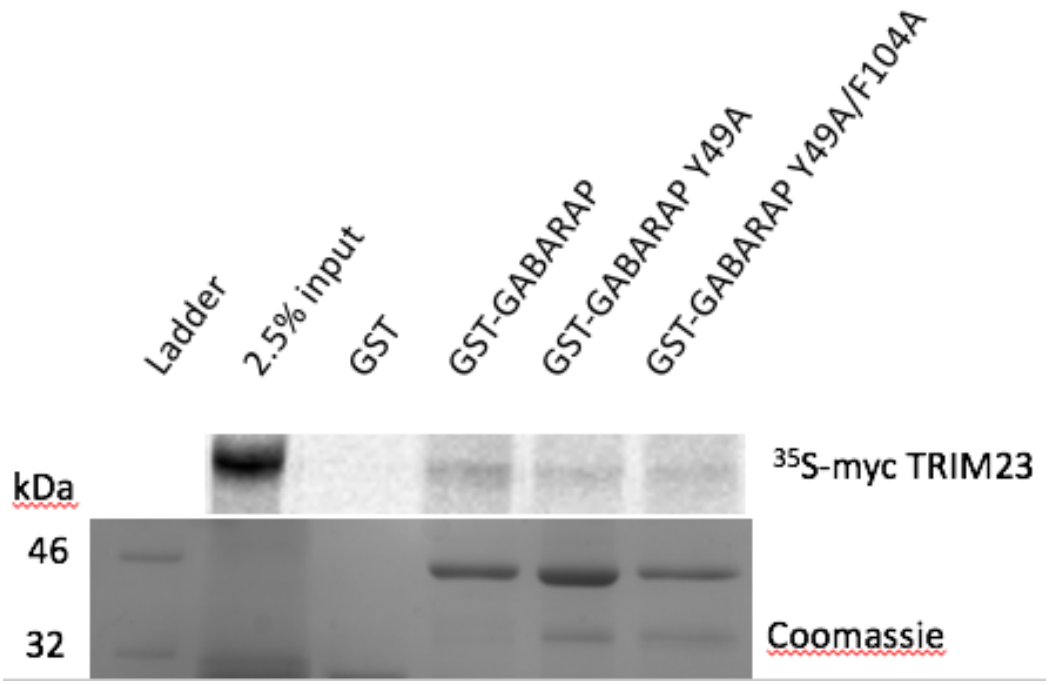

B

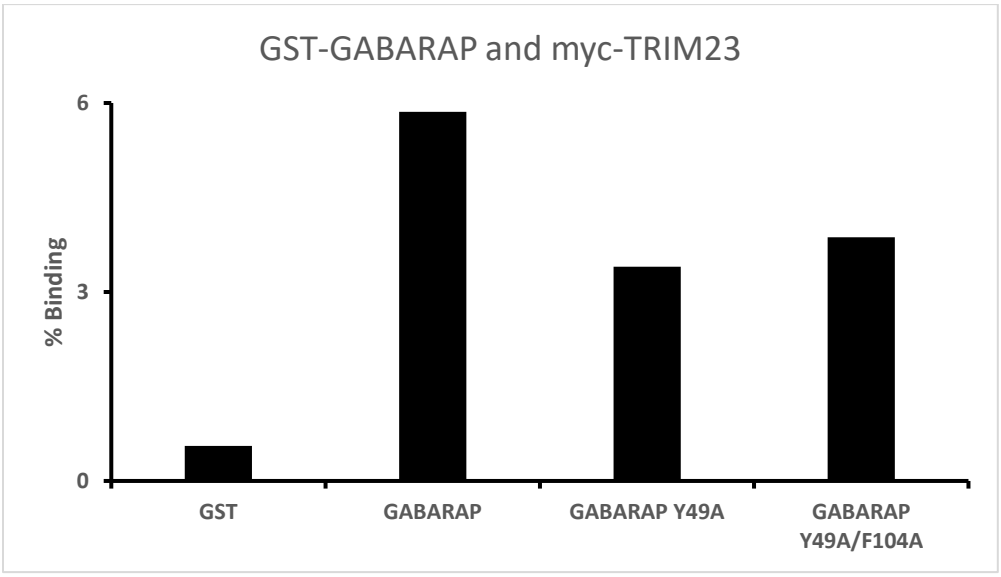

Figure 21: GST pulldown show that binding between GST-GABARAP and myc-TRIM23 is LIR dependent. The SDS-PAGE gel electrophoresis and autoradiography (A) and percentage binding normalized to input (B) of binding between TRIM23 and each of the GABARAPs are shown. From the autoradiogram, ^{35}S methionine-tagged TRIM23 was clearly visible, and quantification shows that there is binding between all three GABARAPs and TRIM23, and that the binding strength decreases for GABARAP Y49A. The quantifications are based on one representative experiment.

Both GABARAP mutants bound weaker to TRIM23 than wild type GABARAP. When adjusted to the amount of GST-proteins used in the binding reaction, quantitations of the myc-TRIM23 bands showed that the binding was reduced to around 50% when using the mutated GABARAP compared to wild type GABARAP. This indicates that the interaction of TRIM23 with GABARAP is LIR dependent.

Next, similar GST-pulldown assays were performed with TRIM31. As displayed in Figure 22, mutation of Y49 in the LIR binding pocket of GABARAP do not reduce binding, while two mutations Y49A and F104A reduced the binding to nearly 50% of the binding of the wild type GABARAP. The Y49A mutation affects binding to the aromatic residue of the LIR motif W/F/Y to hydrophobic pocket 1 (HP1) in the LDS. The F104A mutation affects binding to HP2 of the hydrophobic residues L/I/V of the LIR motif. Hence, TRIM31 binding is affected by the HP2 mutation and not the HP1 mutation alone.

A

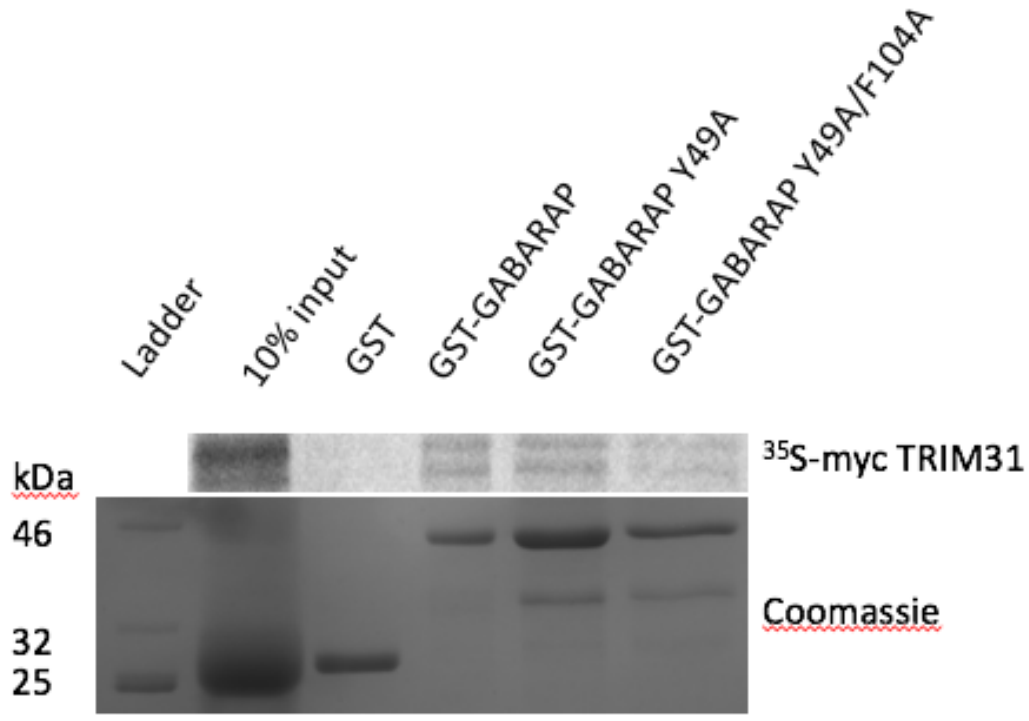

B

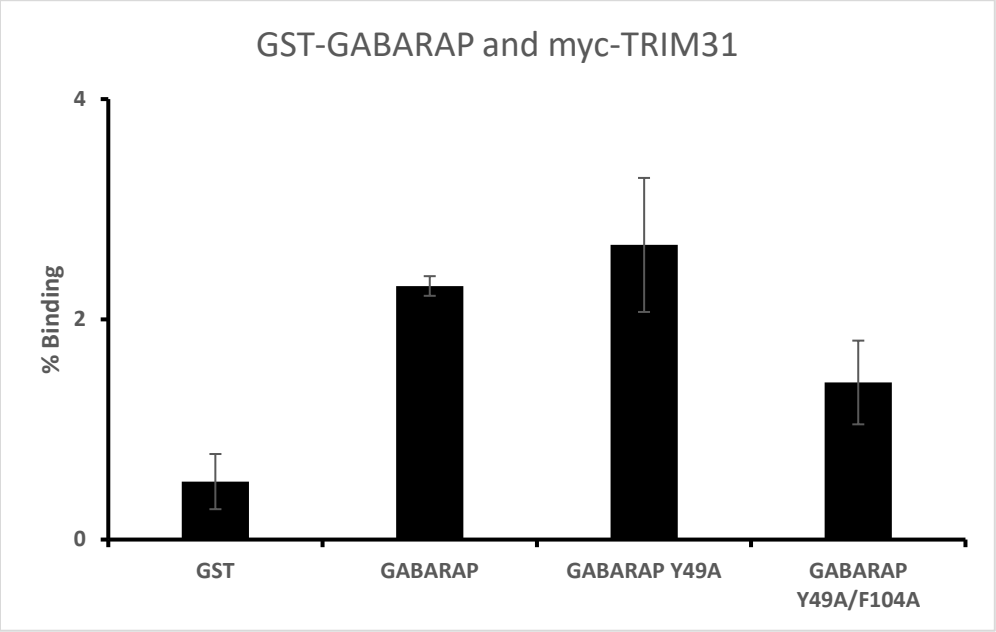

Figure 22: GST pulldown show that binding between GST-GABARAP and myc-TRIM31 is partially LIR dependent. The SDS-PAGE gel electrophoresis and autoradiography (A) and percentage binding normalized to input (B) of binding between TRIM31 and each of the GABARAPs are shown. From the autoradiogram, ^{35}S methionine-tagged myc-TRIM31 was clearly visible, and quantification shows that there is binding between all three GABARAPs and myc-TRIM31, and that the binding strength decreases for GABARAP Y49A/F104A. The quantifications are based on two independent experiments.

4.6 Establishment of TRIM31 Constructs with Mutated LIR Motifs

To further investigate if TRIM31 binding to the ATG8s was LIR dependent, two mutants of TRIM31 were made by site directed mutagenesis; one mutant with a non-functioning LIR2, and one with both LIRs non-functioning. Knowing the position of the LIR motif in the peptide, a two-dimensional peptide array scan can be prepared. 18 amino acids including the potential LIR domain is spotted on a membrane. The wildtype is spotted first to compare binding to. Each position of the 18-mer peptides is replaced with each of the 19 alternative amino acids, ending up with having tested all possible point mutations of the 18-mer peptide. The arrays are then probed with GST-GABARAP, if the first peptide array were tested against GST-GABARAP, and detected with anti-GST antibodies (Johansen et al., 2017). Then, the potential core LIR (W/F/Y)XX(L/I/V) can be mutated in the first and last amino acids. Which amino acid that is replacing these two amino acids is determined based on the peptide array scan and what amino

acids that made the plasmid lose its ability to bind GST-GABARAP. From our accumulated knowledge on studying numerous LIR motifs, we routinely mutate the aromatic and the hydrophobic residues of the core LIR motif W/F/Y XX L/I/V to alanine giving an AXXA motif (Birgisdottir et al., 2013). To verify mutations, samples of the plasmids were sequenced and the successful mutations verified.

TRIM31 wild type sequence with highlighted potential LIR motifs are shown in Figure 23 (LIR1 as FELL and LIR two as FQFL.

```
531     aagcaaaggatcctcacagaatttgaactcctgcatcaagtcctagaggaggagaagaat
         K  Q  R  I  L  T  E  F  E  L  L  H  Q  V  L  E  E  E  K  N
591     ttcctgctatcacggatttactggctgggtcatgagggaacggaagcggggaaacactat
         F  L  L  S  R  I  Y  W  L  G  H  E  G  T  E  A  G  K  H  Y
651     gttgcctccactgagccacagttgaacgatctcaagaagctcgttgattccctgaagacc
         V  A  S  T  E  P  Q  L  N  D  L  K  K  L  V  D  S  L  K  T
711     aagcagaacatgccacccaggcagctgctggaggatatcaaagtcgtcttgtgcagaagt
         K  Q  N  M  P  P  R  Q  L  L  E  D  I  K  V  V  L  C  R  S
771     gaagagtttcagtttctcaacccaacccctgttcctctggaactggagaaaaaactcagt
         E  E  F  Q  F  L  N  P  T  P  V  P  L  E  L  E  K  K  L  S
```

Figure 23: Sequence of TRIM31 wild type with highlighted potential LIR motifs. From peptide array, two potential LIR motifs were detected.

To inactivate the LIR motifs, the first and last amino acid in the core motif was mutated to A (alanine). The planned four mutations in TRIM 31 sequence with highlighted mutated bases and corresponding amino acid are shown in Figure 24.

```
531     aagcaaaggatcctcacagaagctgaactcgcgcatcaagtcctagaggaggagaagaat
         K  Q  R  I  L  T  E  A  E  L  A  H  Q  V  L  E  E  E  K  N
591     ttcctgctatcacggatttactggctgggtcatgagggaacggaagcggggaaacactat
         F  L  L  S  R  I  Y  W  L  G  H  E  G  T  E  A  G  K  H  Y
651     gttgcctccactgagccacagttgaacgatctcaagaagctcgttgattccctgaagacc
         V  A  S  T  E  P  Q  L  N  D  L  K  K  L  V  D  S  L  K  T
711     aagcagaacatgccacccaggcagctgctggaggatatcaaagtcgtcttgtgcagaagt
         K  Q  N  M  P  P  R  Q  L  L  E  D  I  K  V  V  L  C  R  S
771     gaagaggctcagtttgccaacccaacccctgttcctctggaactggagaaaaaactcagt
         E  E  A  Q  F  A  N  P  T  P  V  P  L  E  L  E  K  K  L  S
```

Figure 24: Sequence of TRIM31 with mutated LIR1 and LIR2. The first and last amino acid in the core LIRs changed to alanine are highlighted.

4.6.1 TRIM31 was Successfully Mutated in LIR2

Sequencing results from LIR2 mutation in TRIM31 are shown in Figure 25. Mutated codons and amino acids are highlighted.

664 agccacagttgaacgatctcaagaagctcgttgattccctgaagaccaagcagaacatgcca

P Q L N D L K K L V D S L K T K Q N M P

726 cccaggcagctgctggaggatatcaaagtcgtcttgtgcagaagtgaagaggctcagttt

P R Q L L E D I K V V L C R S E E A Q F

786 gccaacccaacccctgttcctctggaactggagaaaaaactcagtgaagcaaaatcaaga

A N P T P V P L E L E K K L S E A K S R

846 cacgactccatcacagggagcctgaaaaaatcaaagaccaactccaggcskkwtkggt

H D S I T G S L K K S K T N S R X X X

Figure 25: Sequence of the successfully LIR2 mutated TRIM31. Site-directed mutagenesis was performed to construct the TRIM31 LIR2 mutant. The first and last amino acid in the core LIR2 motif was mutated to alanine. Mutated bases and corresponding amino acid are highlighted.

The sequencing results show that the wanted mutations were inserted into pDONR221 TRIM31; F260A/L263A.

4.6.2 TRIM31 was successfully mutated in LIR1 and LIR2

From TRIM31 mutated in LIR2, site-directed mutagenesis was performed to construct a TRIM31 mutated in both LIR1 and LIR2. Sequencing results from LIR1/LIR2 mutation in TRIM31 are shown in Figure 26.

481 caagggctgtacacagggtcgatgtcttcacggaccaggtagaacatgagaagcaaaggatc

R A V H R V D V F T D Q V E H E K Q R I

543 ctcacagaagctgaactcgcgcatcaagtcctagaggaggagaagaatttcctgctatca

L T E A E L A H Q V L E E E K N F L L S

603 cggatttactggctgggtcatgagggaacggaagcggggaaacactatgttgcctccact

R I Y W L G H E G T E A G K H Y V A S T

663 gagccacagttgaacgatctcaagaagctcgttgattccctgaagaccaagcagaacatg

E P Q L N D L K K L V D S L K T K Q N M

723 ccacccaggcagctgctggaggatatcaaagtcgtcttgtgcagaagtgaagaggctcag

P P R Q L L E D I K V V L C R S E E A Q

783 tttgccaacccaacccctgttcctctggaactggagaaaaaactcagtgaagcaaaatca

F A N P T P V P L E L E K K L S E A K S

843 agacacgactccatcacagggagcctgaaaaaattcaaagaccaactccaggctgata

R H D S I T G S L K K F K D Q L Q A D

Figure 26: Sequence of TRIM31 mutated in LIR1 and LIR2. Plasmid from TRIM31 successfully mutated in LIR2 was used in site-directed mutagenesis to develop a new TRIM31 mutant, deficient in both LIR1 and LIR2. The first and last bases and corresponding amino acid in the core LIR motif of both LIR1 and LIR2 are highlighted.

DNA sequencing confirmed the mutations in pDONR221 TRIM31; F185A/L188A and F260A/L263A.

4.7 TRIM31 Binding to LC3A and GABARAP is Dependent on LIR2

After successfully mutating LIR2 and LIR1/LIR2 in TRIM31 and transforming the mutants to pDestmyc expression vector, a new GST pulldown was done to see if the binding to GST-ATG8s was LIR dependent. From the two subfamilies of ATG8s, one of each with the strongest binding according to previous results (GST-LC3A and GST-GABARAP) were tested (Figure 27).

A

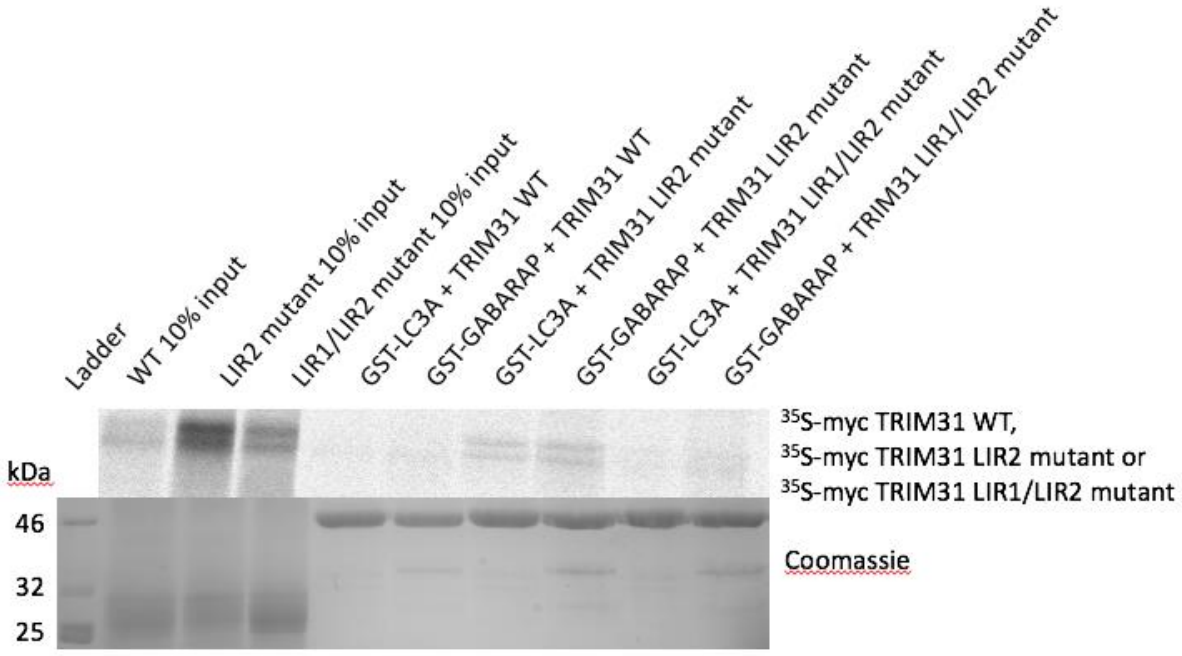

B

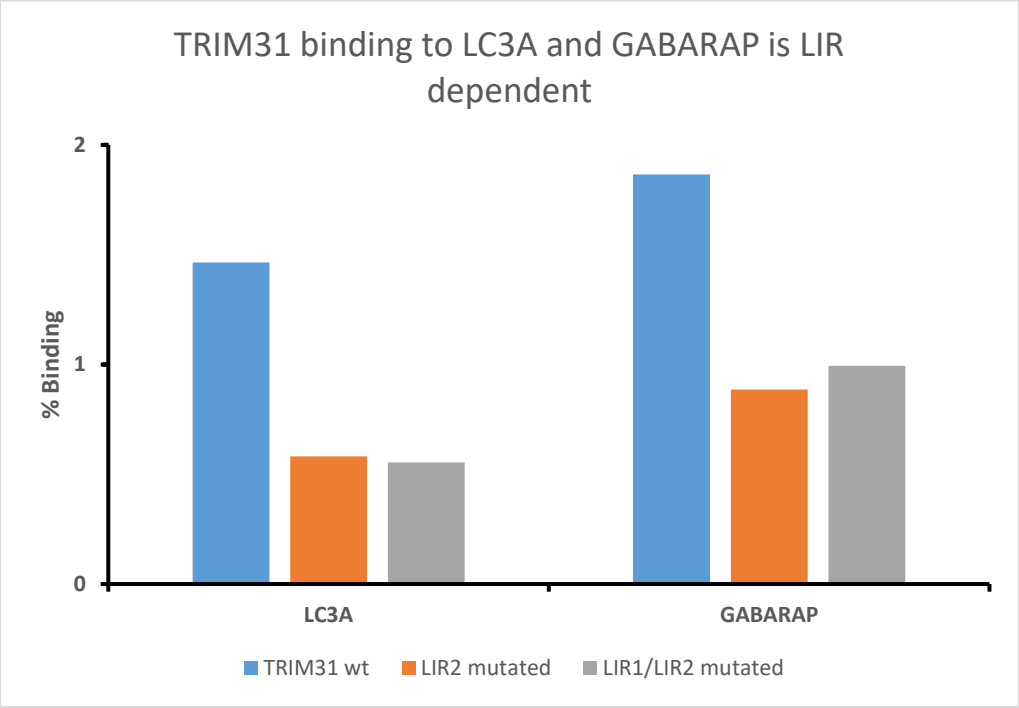

Figure 27: GST pulldown show that binding between GST-LC3A/GST-GABARAP and myc-TRIM31 is mediated by LIR2. The SDS-PAGE gel electrophoresis and autoradiography (A) and percentage binding normalized to input (B) of binding between TRIM31 and each of the two GST fusion ATG8s (GST-LC3A and GST-GABARAP) are shown. From the autoradiogram, the different ^{35}S methionine-tagged TRIM31 were barely visible, but quantification shows that there is binding, and that the binding strength decreases in myc-TRIM31 LIR2 mutant and LIR1/LIR2 mutant. The quantifications are based on one experiment.

Even though the binding of myc-TRIM31 WT was weak, the binding was further reduced when LIR2 or LIR1/LIR2 was mutated. The change in binding strength from myc-TRIM31 mutated in LIR2 and myc-TRIM31 mutated in both LIR1 and LIR2 is not significant, suggesting that LIR2 is the main LIR in TRIM31.

4.8 EGFP TRIM31 co-localize with mCherry LC3A, mCherry LC3B and mCherry GABARAP in HeLa Cells

For further studying the TRIM31 interaction with ATG8s, a co-localization study was performed. HeLa cells were co-transfected with the plasmids pDestmCherry LC3C or pDestmCherry GABARAP and pDestEGFP TRIM31. In addition, LC3B was also included

because of its role as an autophagic marker. The transfected cells were either treated with full medium to monitor normal conditions, starvation medium to induce autophagy or full medium with Baf to inhibit basal autophagy. Baf inhibits the fusion between autophagosomes and lysosomes by inhibiting vacuolar proton ATPase (Yamamoto et al., 1998).

HeLa cells were seeded in a 24-well dish containing coverglasses, and transfected with pDestmCherry LC3A and pDestEGFP TRIM31 plasmids. 22 hours after transfection, cells were treated in full medium, starvation medium and full medium with Baf for 2 hours. The coverglasses containing cells were washed with 1x PBS, fixed with 4% PFA and stained with DAPI. DAPI stains DNA and thereby gives a blue color to the nucleus and was used to detect all cells on the coverglass and not only the transfected cells. The results are illustrated in Figure 28, 29 and 30.

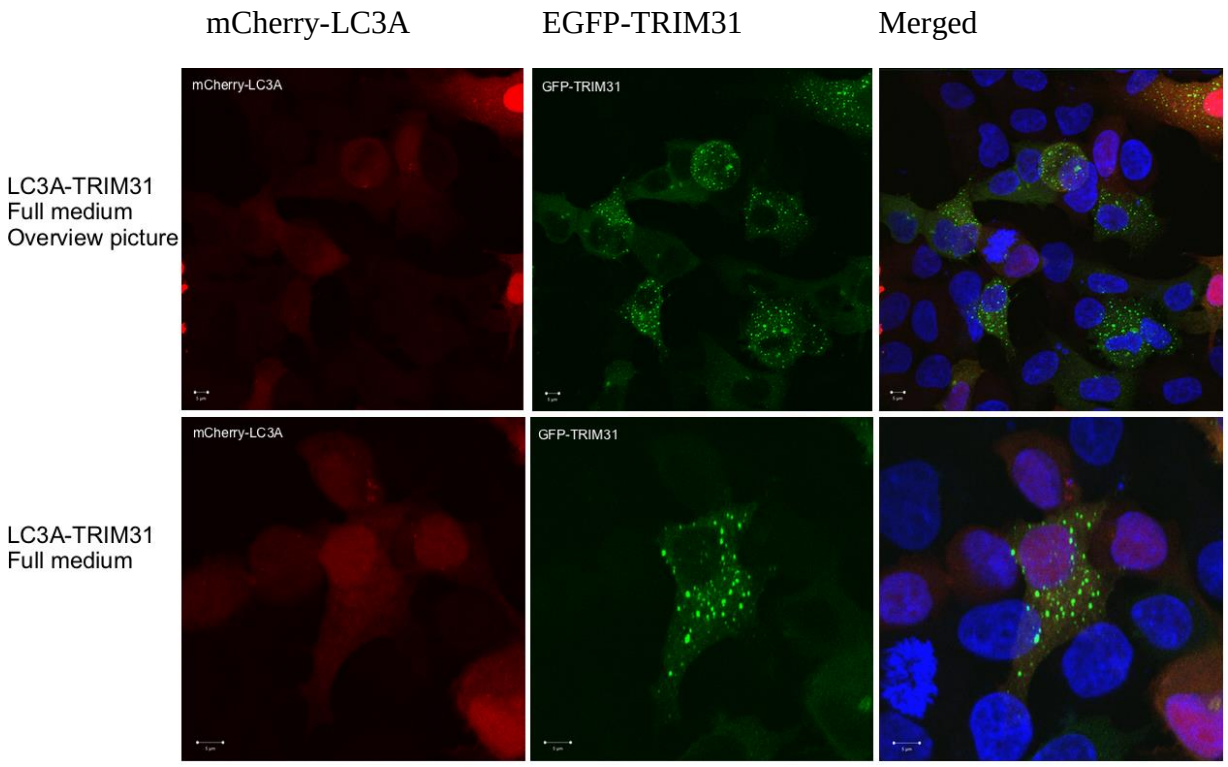

Figure 28: mCherry-LC3A and EGFP-TRIM31 do not co-localize in HeLa cells treated in full medium for 24 hours after transfection. HeLa cells were transfected with pDestmCherry LC3A and pDestEGFP TRIM31 and cultured in normal growth medium (DMEM with 10% FBS), fixed with 4% PFA, stained with DAPI, mounted to coverslips and subjected to confocal fluorescence microscopy.

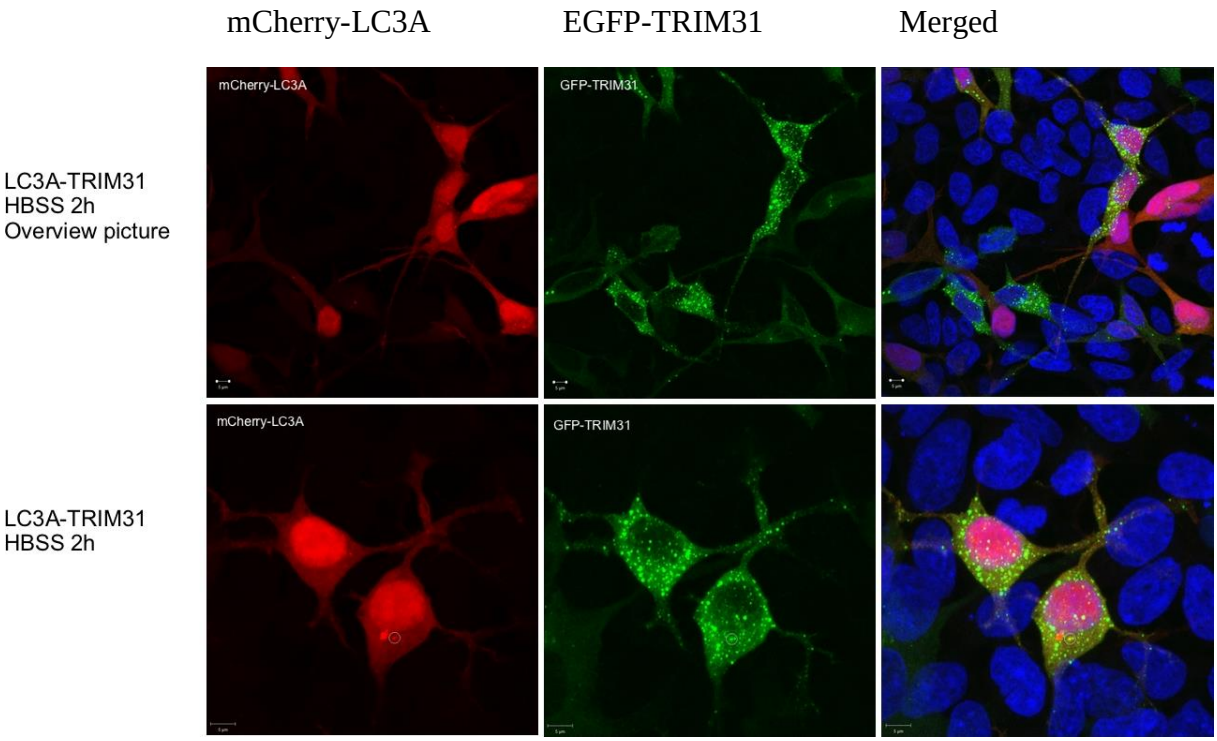

Figure 29: mCherry-LC3A and EGFP-TRIM31 co-localize in HeLa cells when the cells were starved for 2 hours. HeLa cells were transfected with pDestmCherry LC3A and pDestEGFP TRIM31 and starved for 2 hours before they were stained with DAPI and subjected to confocal fluorescence microscopy. One aggregate was found containing both mCherry-LC3A and EGFP-TRIM31, indicated with a circle.

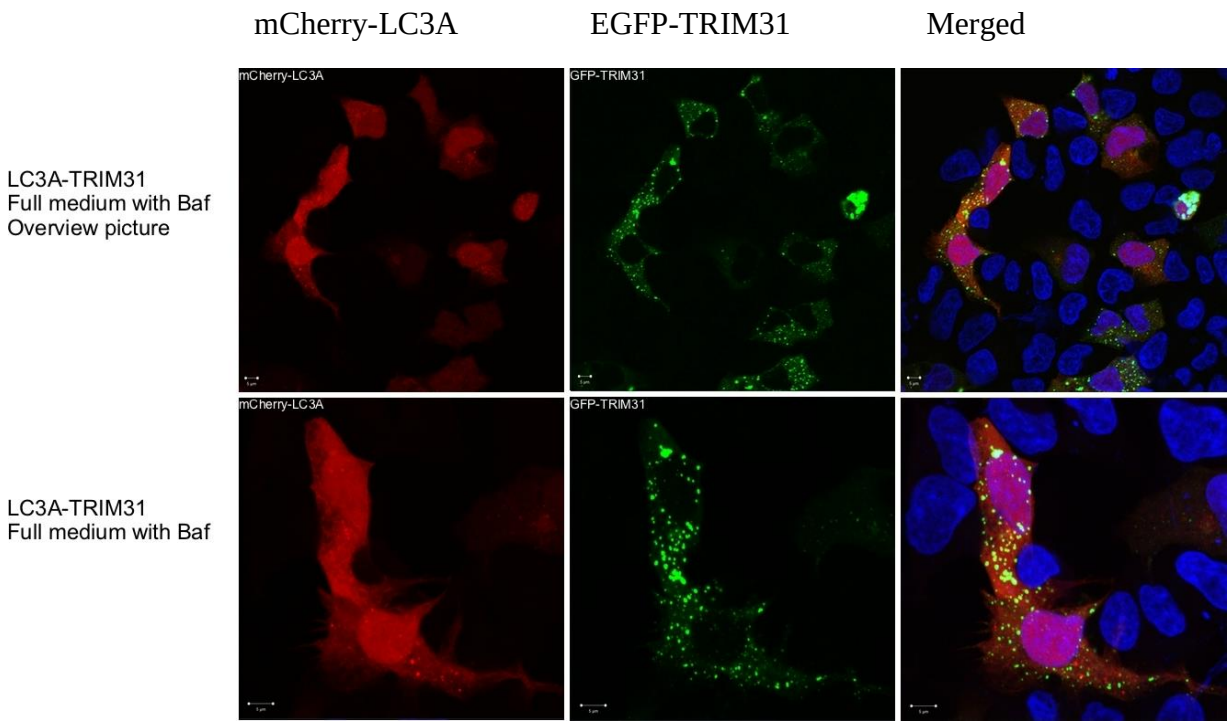

Figure 30: mCherry-LC3A and EGFP-TRIM31 did not co-localize in HeLa cells treated with full medium with Baf for 2 hours. HeLa cells were transfected with pDestmCherry LC3A and pDestEGFP TRIM31 and treated in full medium containing Baf. When studied in confocal fluorescence microscopy, no co-localization between mCherry-LC3A and EGFP-TRIM31 was found.

mCherry-LC3A was overexpressed, present in nucleus as well as in the cytoplasm. EGFP-TRIM31 formed aggregates in the cytoplasm. In full-medium LC3A was mainly diffuse and no clear co-localization with TRIM31 could be observed. However, upon treatment with HBSS, LC3A formed some dots in the cytoplasm (Figure 29), and some of these dots co-localized with the EGFP-TRIM31 aggregates.

As described for HeLa cells transfected with pDestmCherry LC3A and pDestEGFP TRIM31, HeLa cells were seeded in a 24-well dish containing coverglasses. Here, the cells were transfected with pDestmCherry LC3B and pDestEGFP TRIM31 and treated as described in different mediums and atined with DAPI. The results are illustrated in Figure 31, 32 and 33.

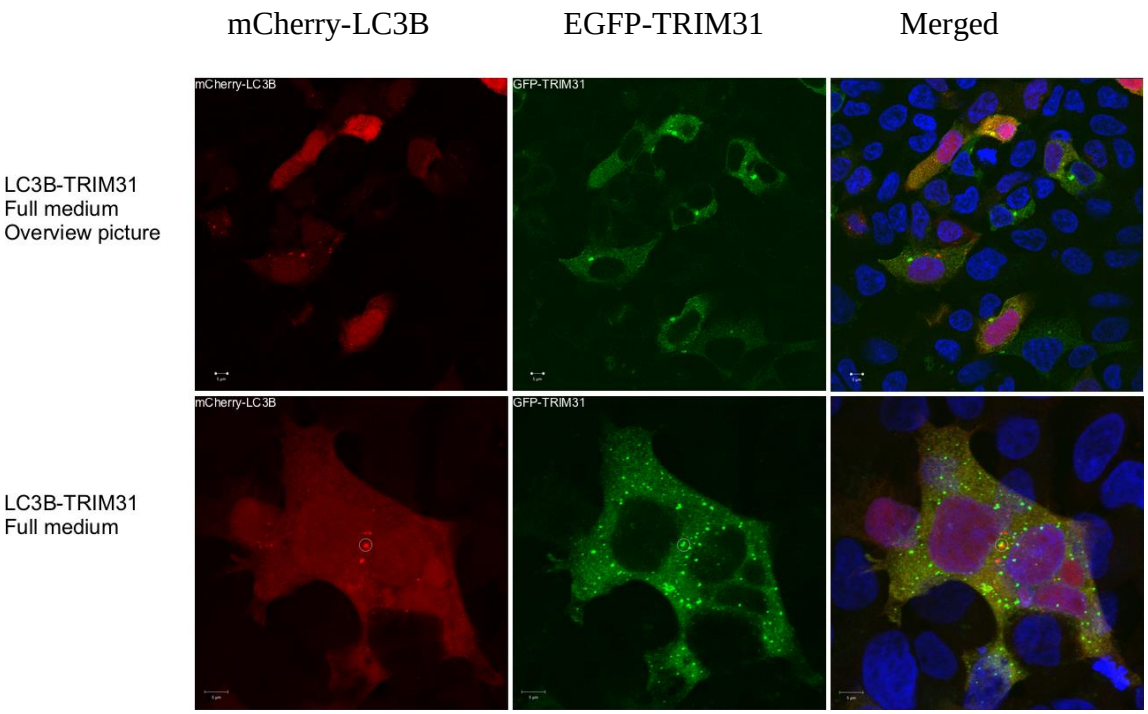

Figure 31: mCherry-LC3B and pDestEGFP-TRIM31 co-localize in HeLa cells treated with full medium. HeLa cells were transfected with pDestmCherry LC3B and pDestEGFP TRIM31 to express mCherry-LC3B and EGFP-TRIM31 and identify co-localization. Co-localization is indicated with a circle.

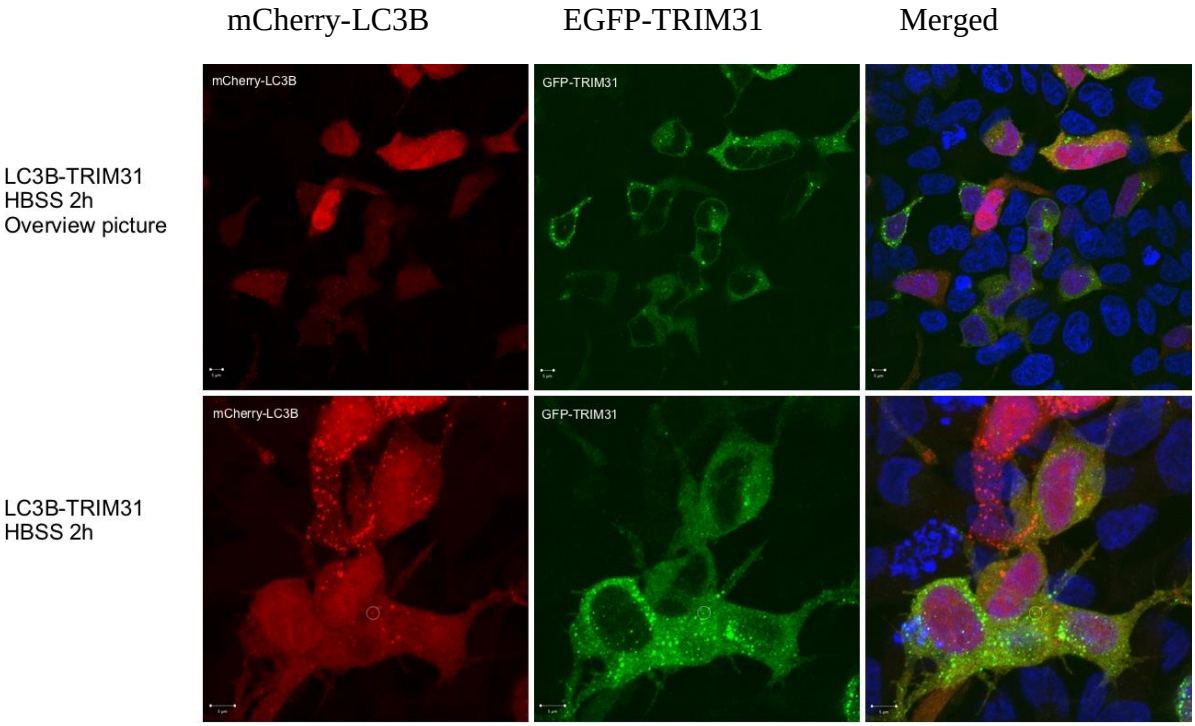

Figure 32: mCherry-LC3B and EGFP-TRIM31 co-localized in starved HeLa cells. HeLa cells were transfected with pDestmCherry LC3B and pDestEGFP TRIM31 and starved for 2 hours. After fixating, staining (with DAPI) and mounting on coverslips, co-localization between mCherry-LC3B and EGFP-TRIM31 (indicated with a circle) was found by viewing the cells in a confocal fluorescence microscope.

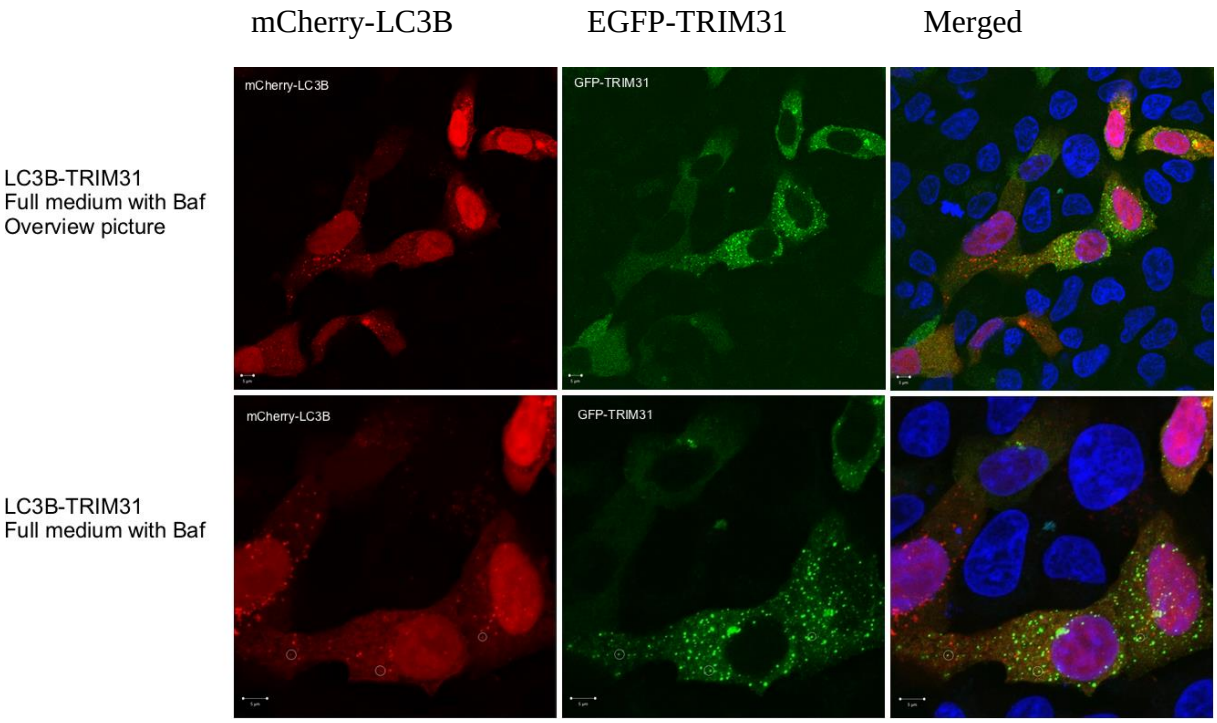

Figure 33: mCherry-LC3B and EGFP-TRIM31 co-localize in HeLa cells treated in full medium added Baf. HeLa cells were transfected with pDestmCherry LC3B and pDestEGFP TRIM31, and treated in full medium with Baf for 2 hours. Using a confocal fluorescence microscope, co-localizations were found and are indicated in the figure with circles.

mCherry-LC3B is present in nucleus as well as the cytoplasm. In full medium it is enriched in a few dots in the cytoplasm, and the amount of dots increases upon starvation. The dots are autophagosomes, as autophagy are induced by starvation. EGFP-TRIM31 formed aggregates in the cytoplasm both in full medium and starvation. TRIM31 aggregates were found to co-localize with LC3B both in full medium and upon starvation.

As described for HeLa cells transfected with pDestmCherry LC3A/B and pDestEGFP TRIM31, cells were transfected with pDestmCherry GABARAP and pDestEGFP TRIM31 and stained with DAPI. The results are illustrated in Figure 34, 35 and 36.

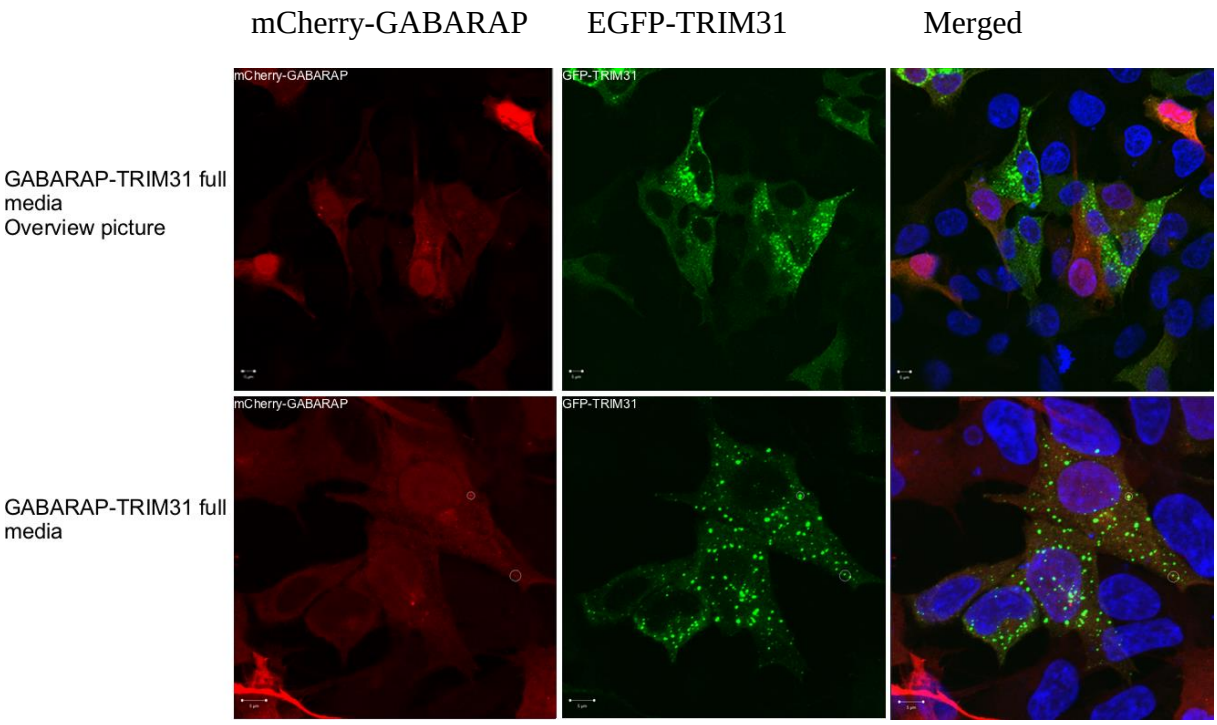

Figure 34: mCherry-GABARAP and EGFP-TRIM31 co-localized in HeLa cells treated in full medium. HeLa cells were transfected with pDestmCherry GABARAP and pDestEGFP TRIM31 and cultured in normal growth medium (DMEM with 10% FBS), fixed with 4% PFA, stained with DAPI, mounted to coverslips and subjected to confocal fluorescence microscopy. Co-localization is indicated with a circle.

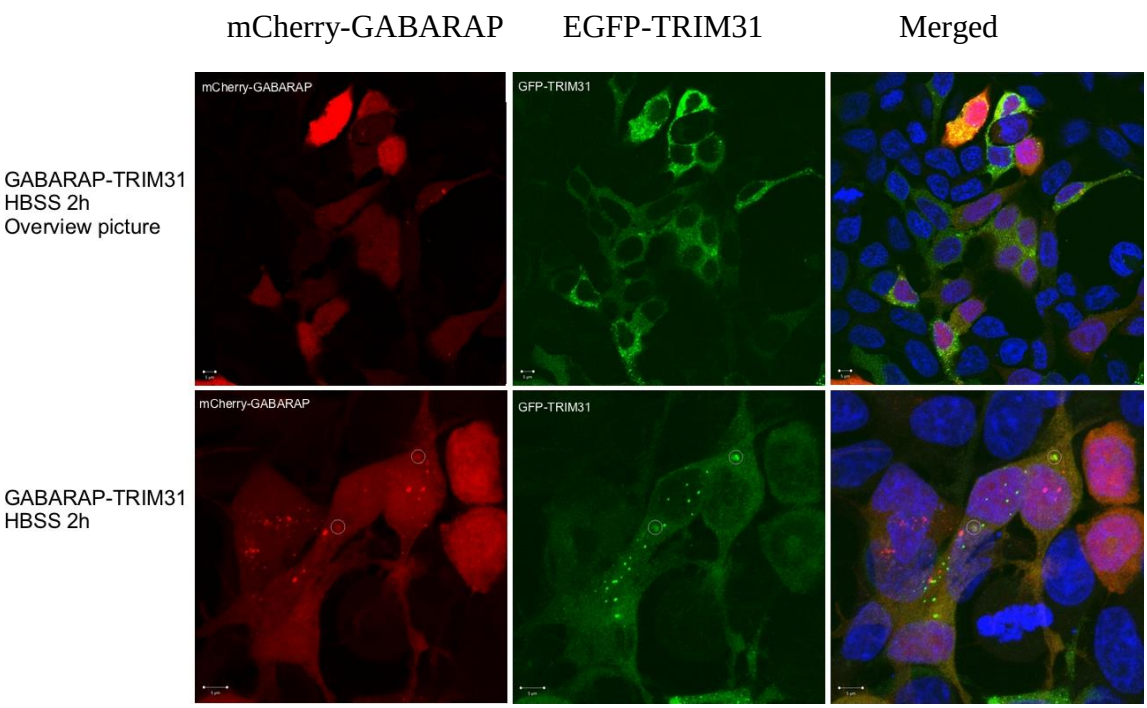

Figure 35: mCherry GABARAP and EGFP-TRIM31 co-localize upon starvation of HeLa cells. HeLa cells were transfected with pDestmCherry GABARAP and pDestEGFP TRIM31 to express the proteins mCherry-GABARAP and EGFP-TRIM31. The cells were starved for 2 hours. Following the method described for mCherry-LC3A and mCherry-LC3B, aggregates containing mCherry-GABARAP and EGFP-TRIM31 were found (indicated with circles).

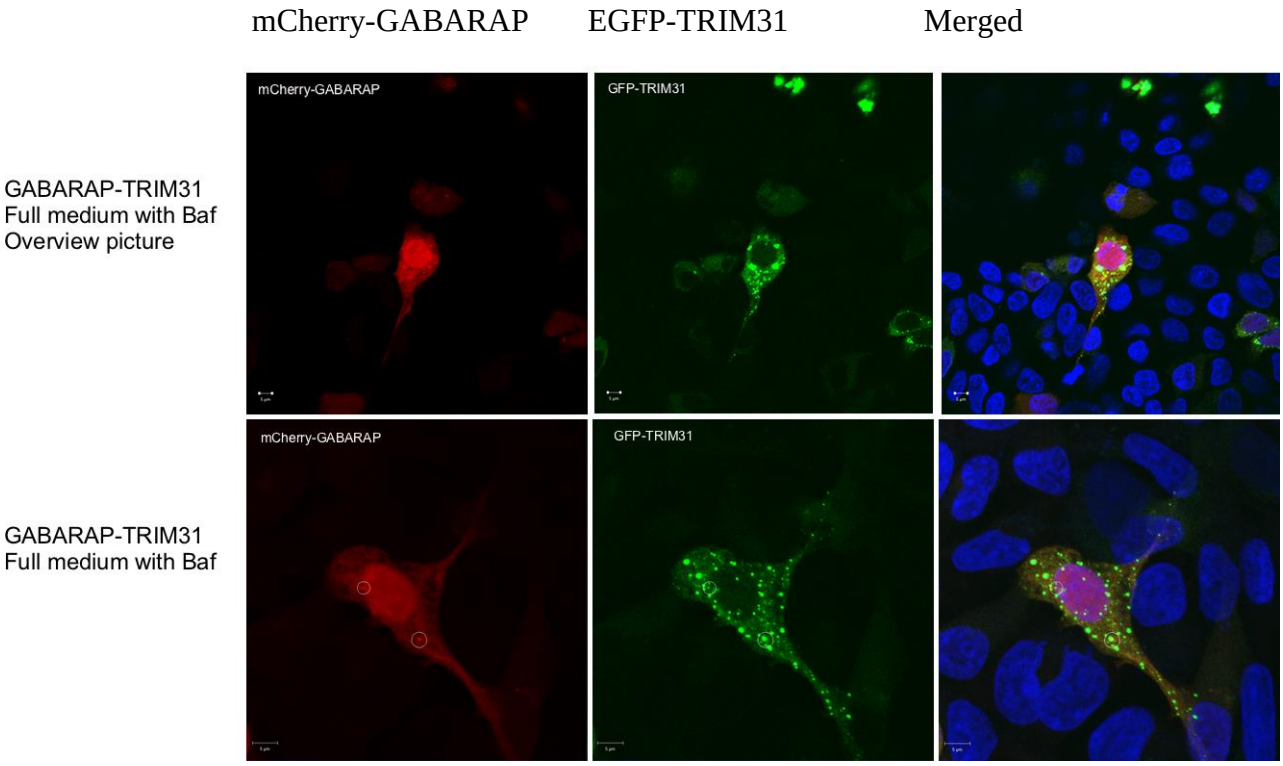

Figure 36: mCherry-GABARAP and EGFP-TRIM31 co-localized in HeLa cells treated with full medium containing Baf. Upon treatment for 2 hours, the cells were fixed, stained with DAPI and mounted on coverslips for confocal microscopy where co-localization were observed (indicated with a circle).

Similar to LC3A and LC3B, mCherry GABARAP was present in nucleus as well as the cytoplasm. Upon starvation, it formed clear cytoplasmic dots. EGFP-TRIM31 formed aggregates in the cytoplasm, as described above. Interestingly, TRIM31 aggregates co-localized with the GABARAP dots both in normal and starved conditions. Together with the GST pulldown results, this suggest that TRIM31 associates with GABARAP.

4.9 TRIM23 and TRIM31 Are Degraded upon Starvation

Proteins involved in autophagy have also been shown in many cases to be degraded with its cargo (Kimura et al., 2015; Liu et al., 2016). To investigate if TRIM23 and TRIM31 were degraded by autophagy or the proteasome, HeLa cells were transfected with pDestEGFP TRIM23 or pDestEGFP TRIM31 and treated with full medium or starvation medium with or without Baf or MG132 for approximately 3 hours. Autophagy is induced by starvation, and Baf inhibits autophagy by inhibiting the fusion between autophagosomes and lysosomes by

inhibiting vacuolar proton ATPase (Yamamoto et al., 1998). MG132 inhibits the proteasome (Ra et al., 2016). The cell lysate was eluted in 2x SDS loading buffer and separated by gel electrophoresis, transferred to a membrane and treated with anti-GFP antibodies to detect the EGFP-TRIM23/31. The protein-bands on the membrane where then visualized and detected as described in methods. To determine if the same amount of cell lysate was loaded to each well, the membrane was again blocked and added anti-PCNA (Anti-proliferating cell nuclear antigen clone PC10) antibody, and secondary antibodies, and staining and detection of bands were again done. The results are illustrated in Figure 37 and 38.

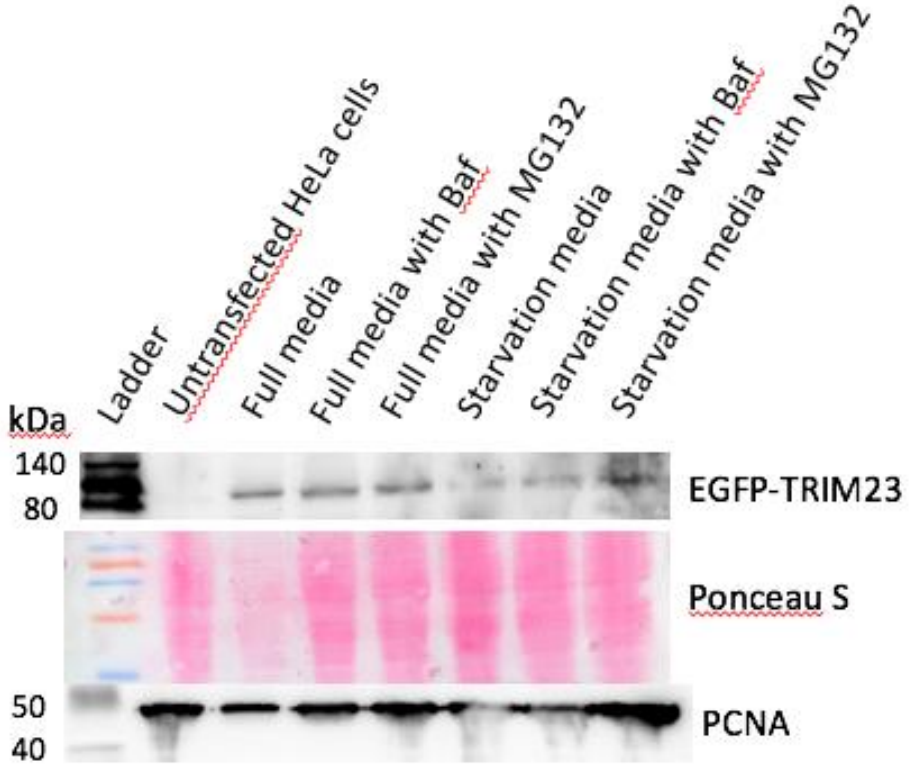

Figure 37: HeLa cells transfected with pDestEGFP TRIM23 and treated with full medium or starvation medium with or without Baf or MG132 shows that EGFP-TRIM23 is degraded upon starvation. HeLa cells were transfected with pDestEGFP TRIM23 and cultured in normal growth medium (DMEM with 10% FBS). The next day, the cells were treated for 3 hours (full media, full media with Baf, full media with MG132, HBSS, HBSS with Baf or HBSS with MG132. GFP and PCNA indicates which antibodies were used during wester blotting. PCNA is a nuclear protein present in all cells and is used as a loading control.

Un-transfected cells were included in the experiment as a negative control. The amount of TRIM23 does not vary between full medium, full medium with Baf and full medium with MG132. When starving the cells, TRIM23 is degraded.

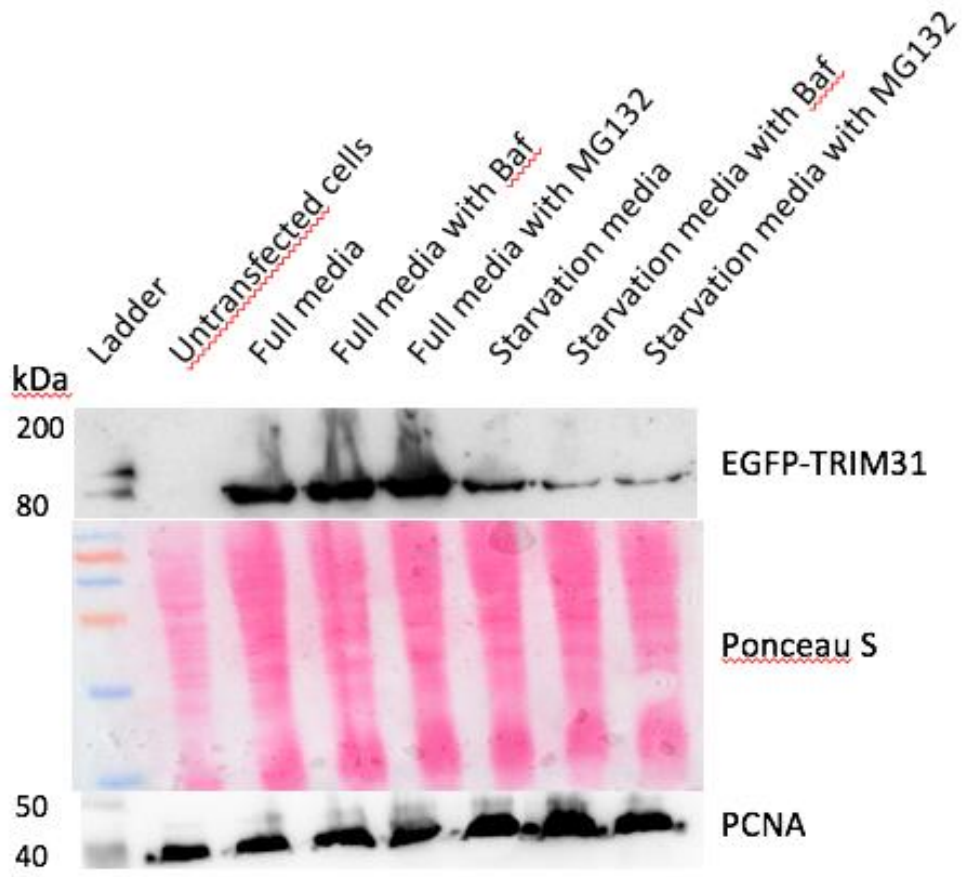

Figure 38: HeLa cells transfected with pDestEGFP TRIM31 and treated with full medium or starvation medium with or without Baf or MG132 shows that EGFP-TRIM31 is degraded during starvation. HeLa cells were transfected with pDestEGFP TRIM31 and cultured in normal growth medium (DMEM with 10% FBS). The next day, the cells were treated for 3 hours (full media, full media with Baf, full media with MG132, HBSS, HBSS with Baf or HBSS with MG132). GFP and PCNA indicates which antibodies were used during Western blotting.

Un-transfected cells were included in the experiment as a negative control. The amount of TRIM31 seems to be a little higher in full medium with Baf/MG132 than in full medium alone. When starving the cells, TRIM31 seems to be degraded, and neither Baf or MG132 seem to stabilize the protein. This is a pattern that can be seen for proteins that are degraded by both pathways (Rodriguez-Muela et al., 2018; Schreiber & Peter, 2014; Scotter et al., 2014; Urushitani, Sato, Bamba, Hisa, & Tooyama, 2010).

4.10 TRIM23 and TRIM31 Are not Degraded by Autophagy in the Double-Tag Assay

To further study if TRIM23 and TRIM31 were degraded by autophagy, experiments using pDestmCherry-EYFP TRIMs were performed. One important hallmark of the lysosomes, is that it has a pH of 5 or lower due to H^+ pumps in the membrane (Alberts et al., 2008). This hallmark can be taken advantage of when using confocal microscopy. While mCherry fusion tags are quite pH stable, the EGFP or EYFP fusion tags are not. In the acidic lysosomes, the EGFP loses its fluorescence, while mCherry maintains its fluorescence until it is proteolytically degraded. Therefore, it is possible to detect degradation of autophagy substrates and autophagy receptors by the lysosome and thereby monitor autophagy (Bjørkøy et al., 2009; Pankiv et al., 2007). pDestmCherry-EYFP plasmid was used as a negative control, and pDestmCherry-EYFP p62 plasmid was used as a positive control. After transfection with the respective plasmid, the HeLa and HeLa ATG7 knock out (KO) cells were treated either in full medium, starvation medium or starvation medium with Baf. Treatment of the cells was done 2 hours before harvesting; 22 or 46 hours after transfection. The cells were then washed, fixed, stained with DAPI, and mounted in mowiol on coverslips. HeLa ATG7 KO cells were included to inhibit autophagy; cells without ATG7 will be deficient in autophagy (Korolchuk, Mansilla, Menzies, & Rubinsztein, 2009).

To see if TRIM23 was degraded by autophagy, pDestmCherry-EYFP TRIM23 was transfected into HeLa (Figure 39) and HeLa ATG7 knock out (Figure 40) cells.

A

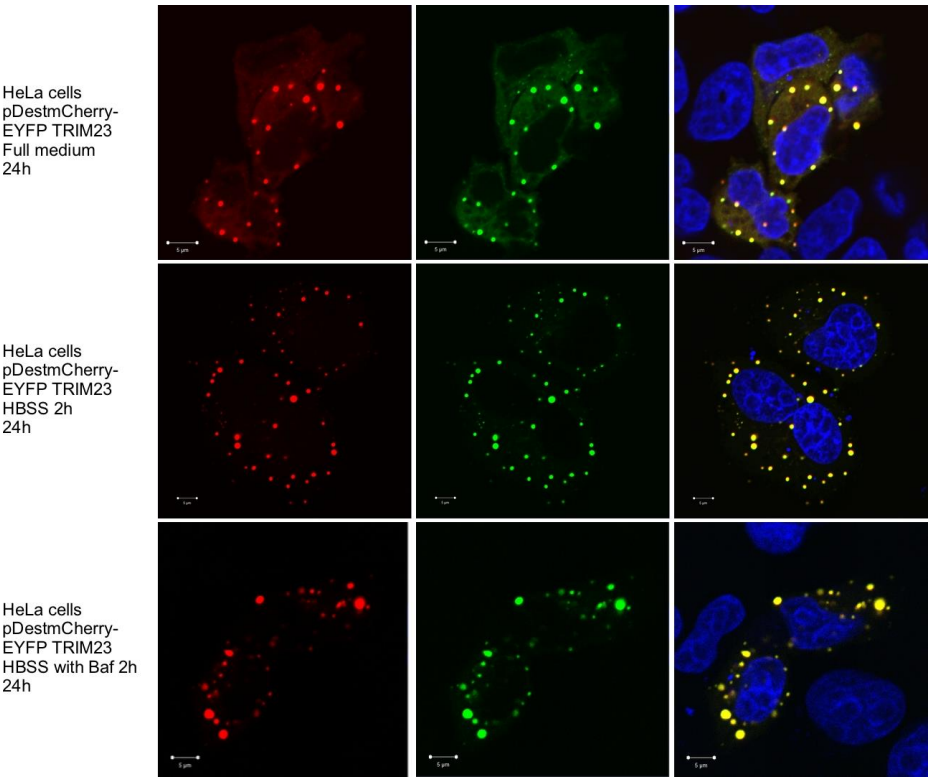
HeLa cells
pDestmCherry-
EYFP TRIM23
Full medium
24h
HeLa cells
pDestmCherry-
EYFP TRIM23
HBSS 2h
24h
HeLa cells
pDestmCherry-
EYFP TRIM23
HBSS with Baf 2h
24h

B

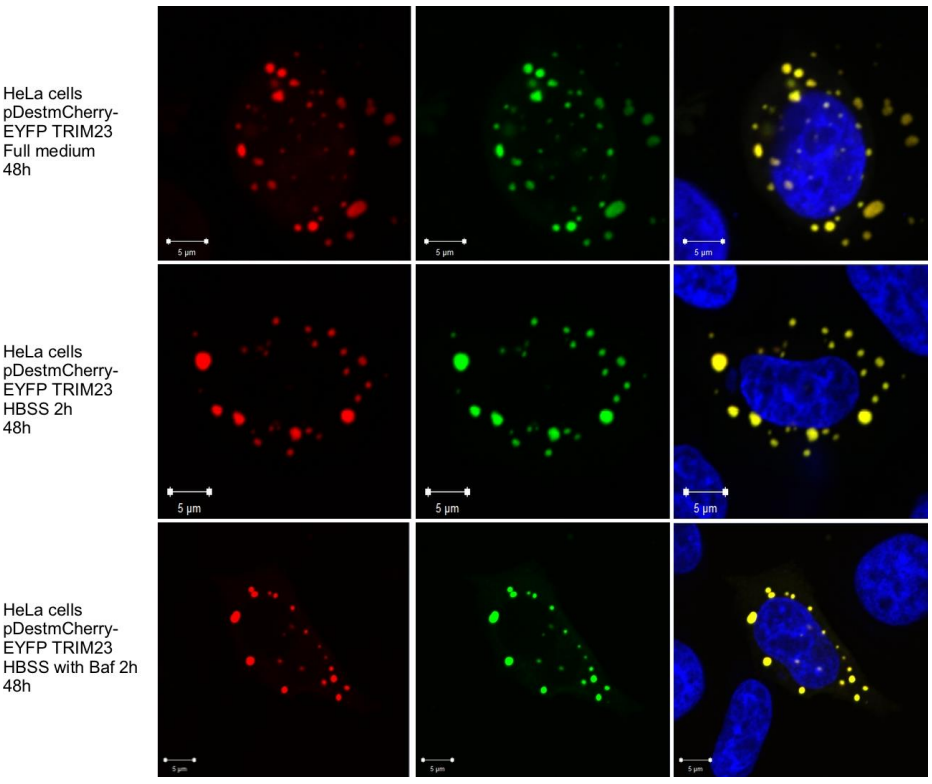
HeLa cells
pDestmCherry-
EYFP TRIM23
Full medium
48h
HeLa cells
pDestmCherry-
EYFP TRIM23
HBSS 2h
48h
HeLa cells
pDestmCherry-
EYFP TRIM23
HBSS with Baf 2h
48h

Figure 39: mCherry-EYFP TRIM23 is not degraded by autophagy. HeLa cells transfected with pDestmCherry-EYFP TRIM23 for 24 (A) and 48 (B) hours and treated with full medium, HBSS or HBSS with Baf for 2 hours, fixed with 4% PFA, stained with DAPI, mounted to coverslips and subjected to confocal fluorescence microscopy. No red-only dots were detected.

A

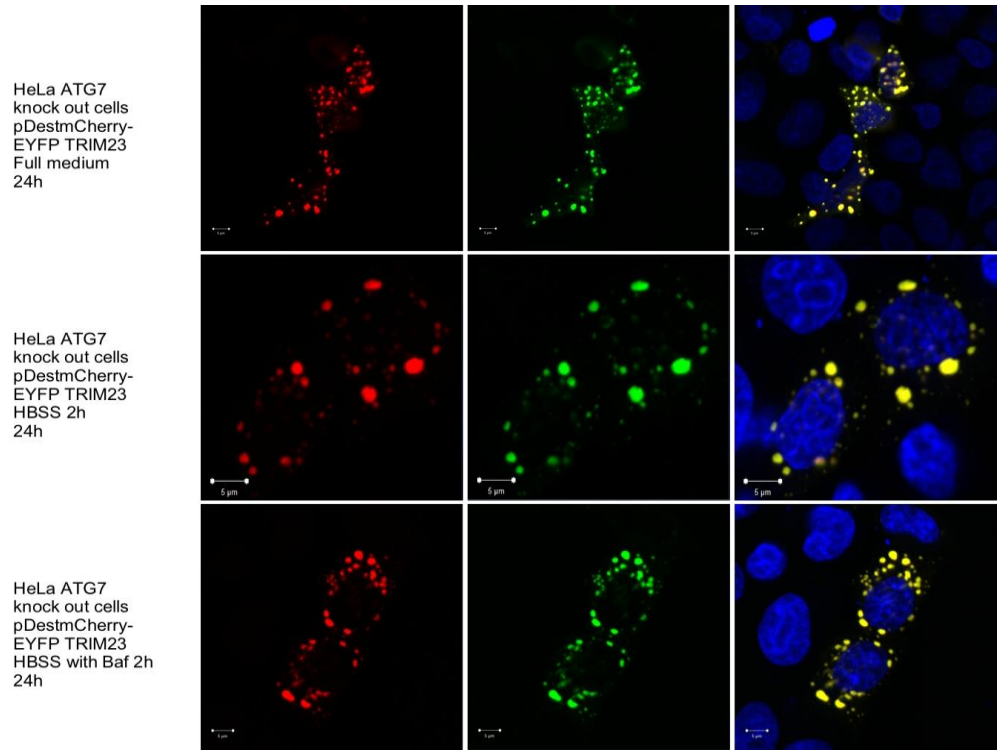

B

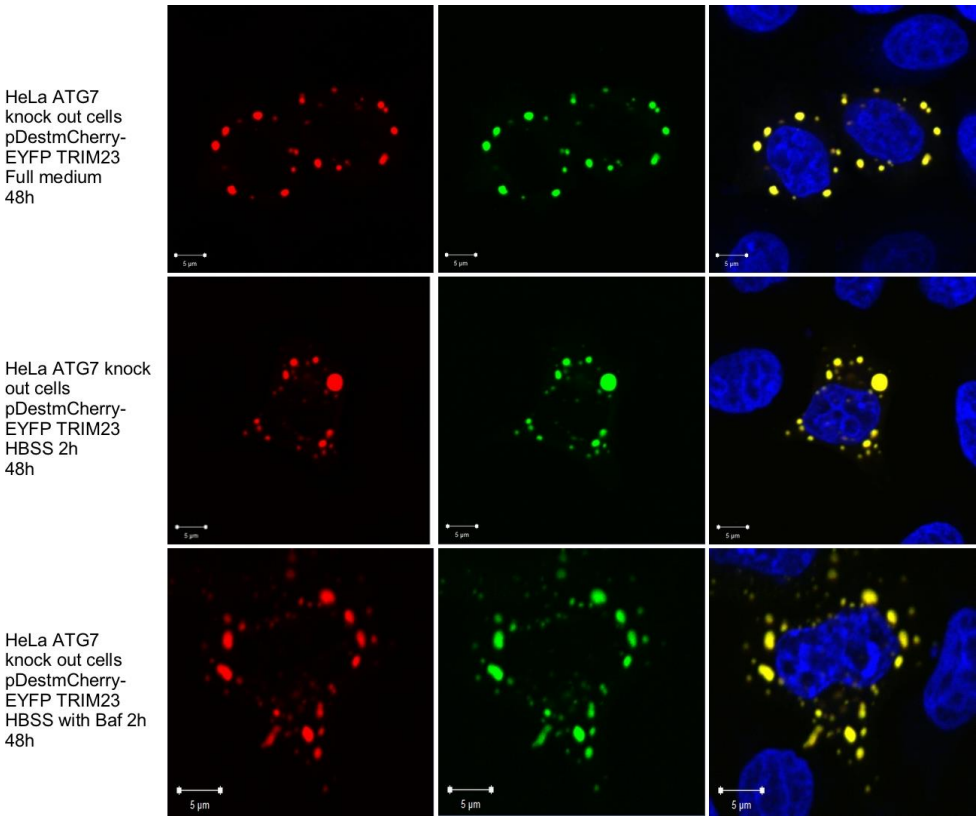

Figure 40: mCherry-EYFP TRIM23 is not degraded by autophagy in HeLa ATG7 knock out cells. HeLa ATG7 knock out cells were transfected with pDestmCherry-EYFP TRIM23 for 24 (A) and 48 (B) hours and treated as indicated for 2 hours. No-red-only dots were found.

mCherry-EYFP TRIM23 makes aggregates in all treatments of HeLa and HeLa ATG7 knock out cells, both in cells harvested 24 hours and 48 hours after transfection. No red-only dots were seen in any treatments.

To further study if TRIM31 was degraded by autophagy, pDestmCherry-EYFP TRIM31 was transfected into HeLa (Figure 41) and HeLa ATG7 knock out (Figure 42) cells.

A

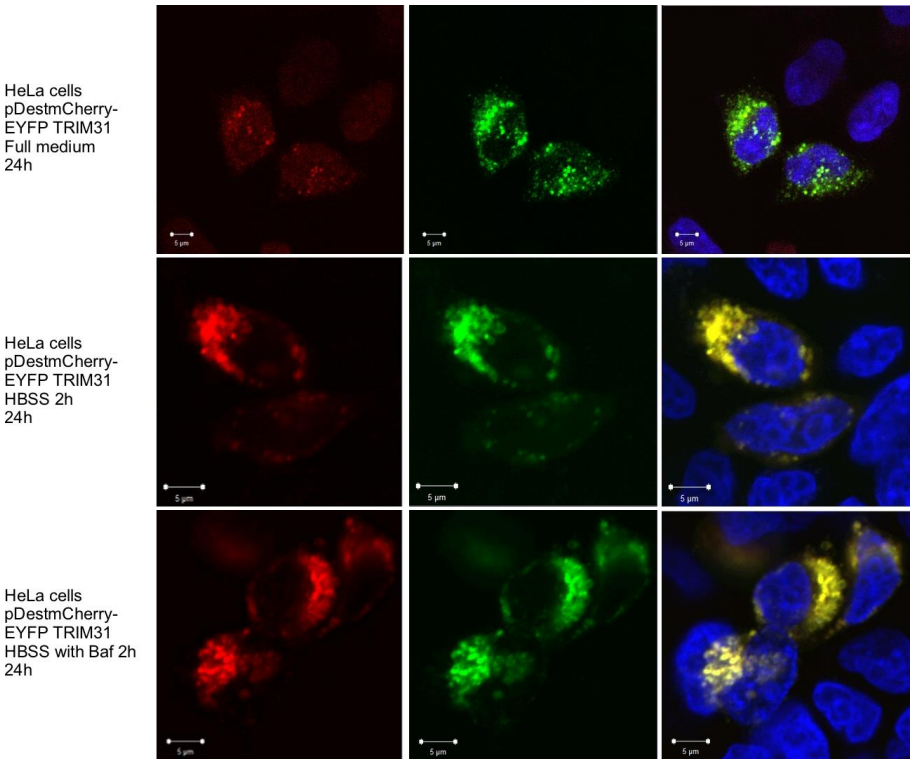
HeLa cells
pDestmCherry-
EYFP TRIM31
Full medium
24h
HeLa cells
pDestmCherry-
EYFP TRIM31
HBSS 2h
24h
HeLa cells
pDestmCherry-
EYFP TRIM31
HBSS with Baf 2h
24h

B

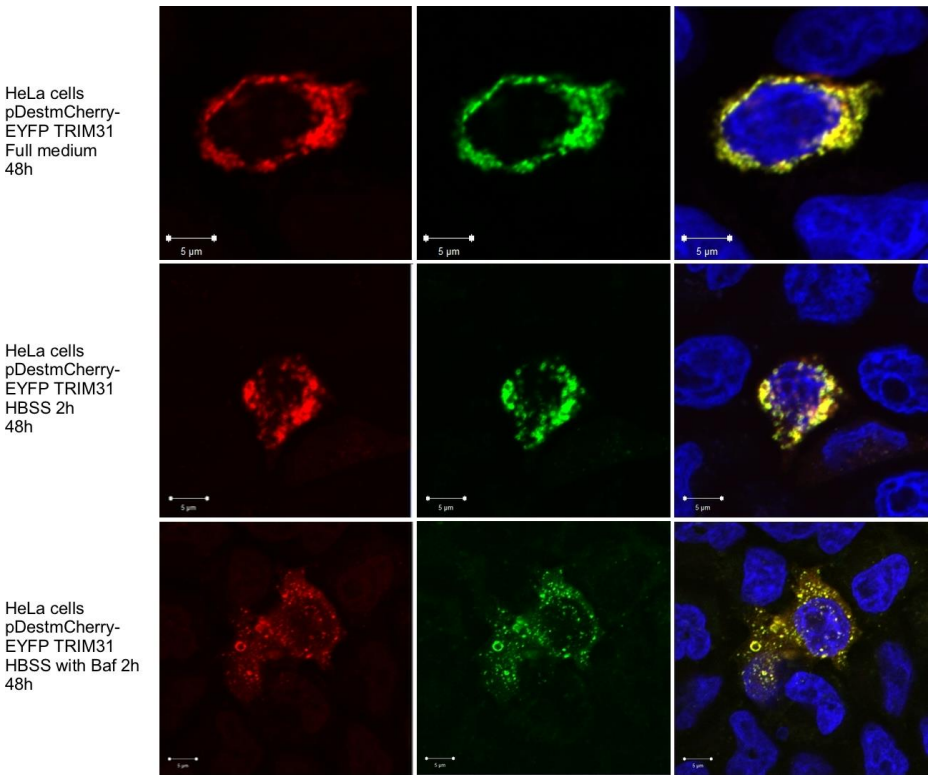
HeLa cells
pDestmCherry-
EYFP TRIM31
Full medium
48h
HeLa cells
pDestmCherry-
EYFP TRIM31
HBSS 2h
48h
HeLa cells
pDestmCherry-
EYFP TRIM31
HBSS with Baf 2h
48h

Figure 41: mCherry-EYFP TRIM31 is not degraded by autophagy in HeLa cells. HeLa cells were transfected with pDestmCherry-EYFP TRIM31 for 24 (A) and 48 (B) hours. Treatments of the HeLa cells are indicated. No red-only dots were detected when viewing the cells in a confocal fluorescence microscope.

A

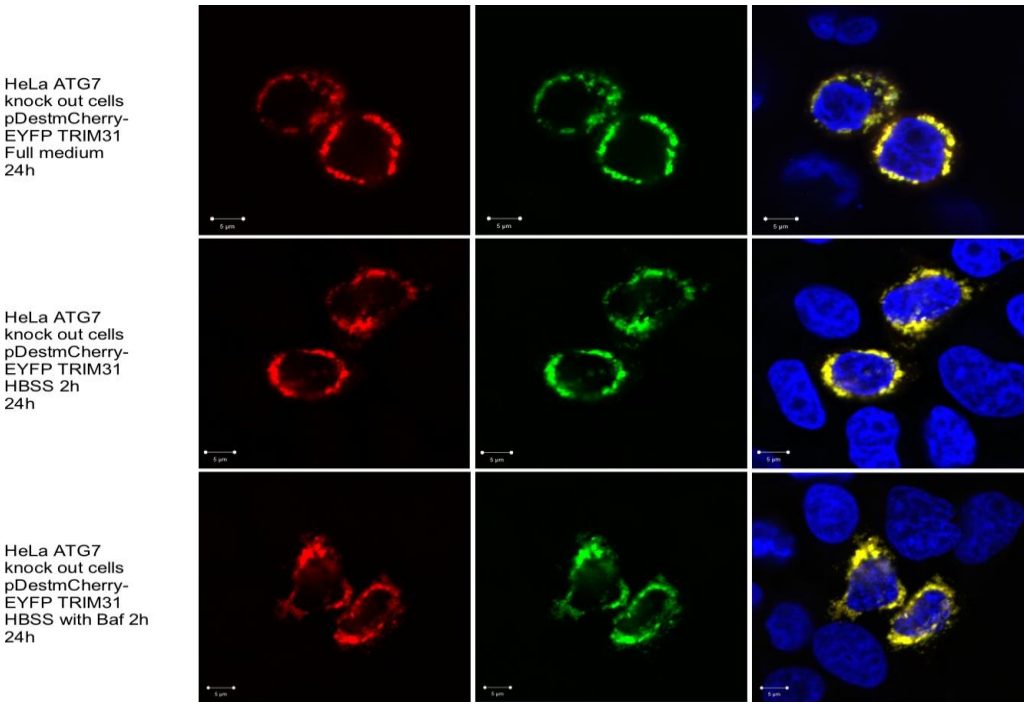

B

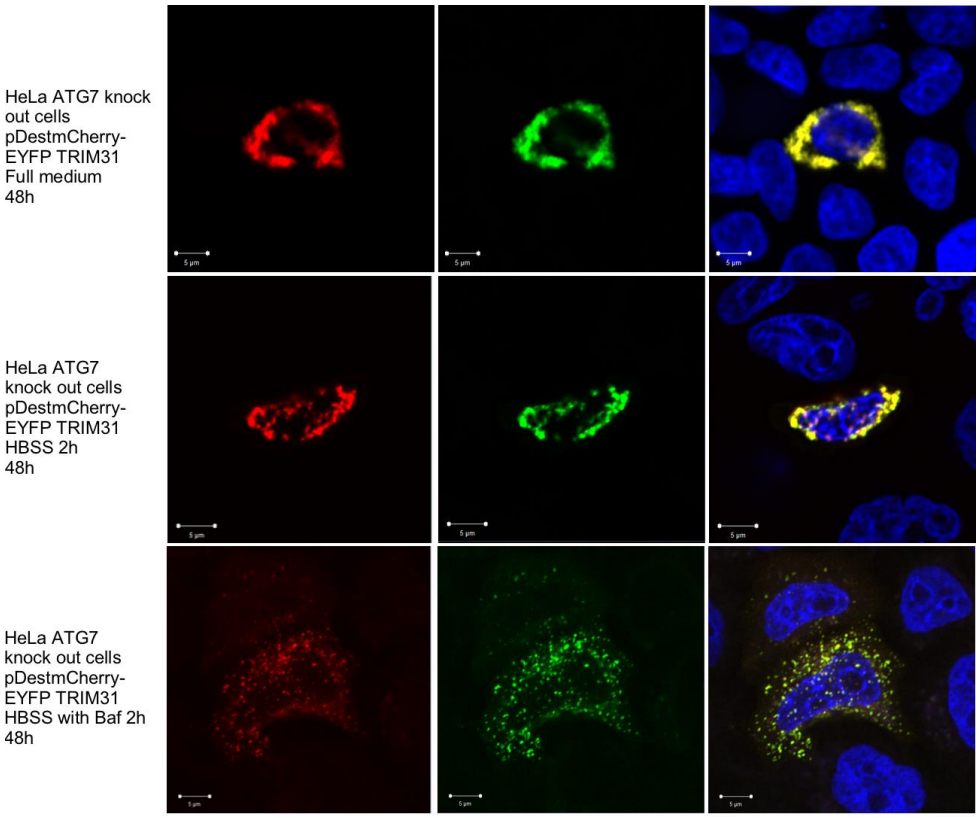

Figure 42: mCherry-EYFP TRIM31 is not degraded by autophagy in HeLa ATG7 knock out cells. HeLa ATG7 knock out cells were transfected with pDestmCherry-EYFP TRIM31 to express mCherry-EYFP TRIM23 for 24 (A) and 48 (B) hours. As before, cells were treated for 2 hours as indicated. No red-only aggregates were detected.

TRIM31 form aggregates, distributed tightly in cytoplasm so TRIM31 look diffusely distributed. No red-only dots were found for any treatments.

<u>Double-tag is diffusely distributed in the whole cell</u>

pDestmCherry-EYFP was transfected into HeLa (Figure 43) and HeLa ATG7 knock out (Figure 44) cells to express mCherry-EYFP. This is used as a control to determine if the double-tag alone could contribute to degradation by autophagy.

A

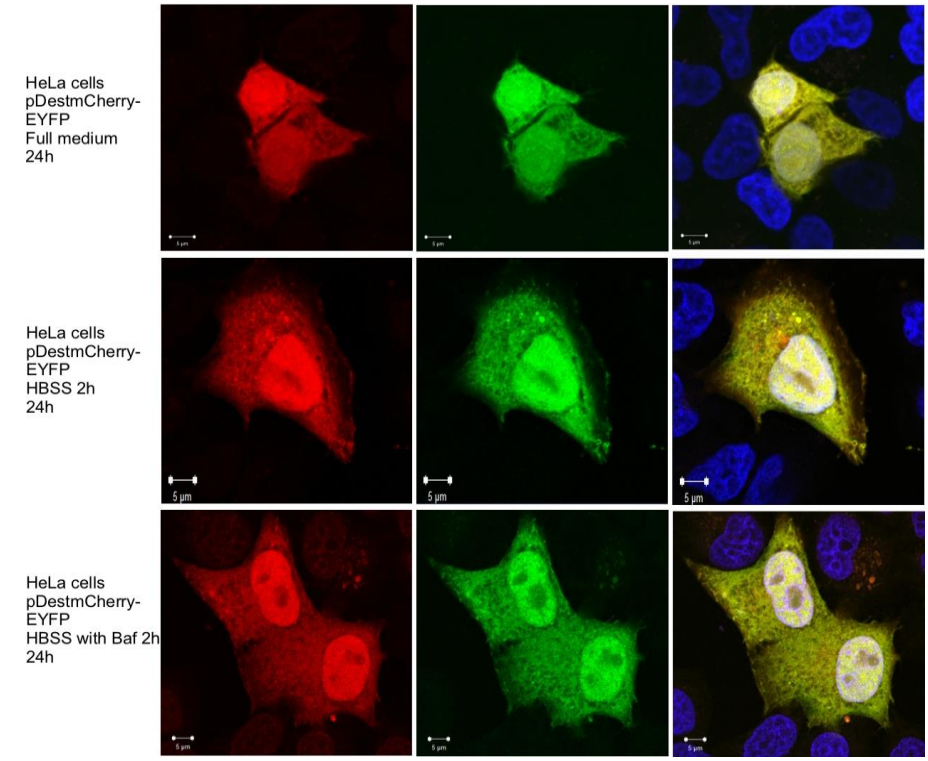
HeLa cells
pDestmCherry-
EYFP
Full medium
24h
HeLa cells
pDestmCherry-
EYFP
HBSS 2h
24h
HeLa cells
pDestmCherry-
EYFP
HBSS with Baf 2h
24h

B

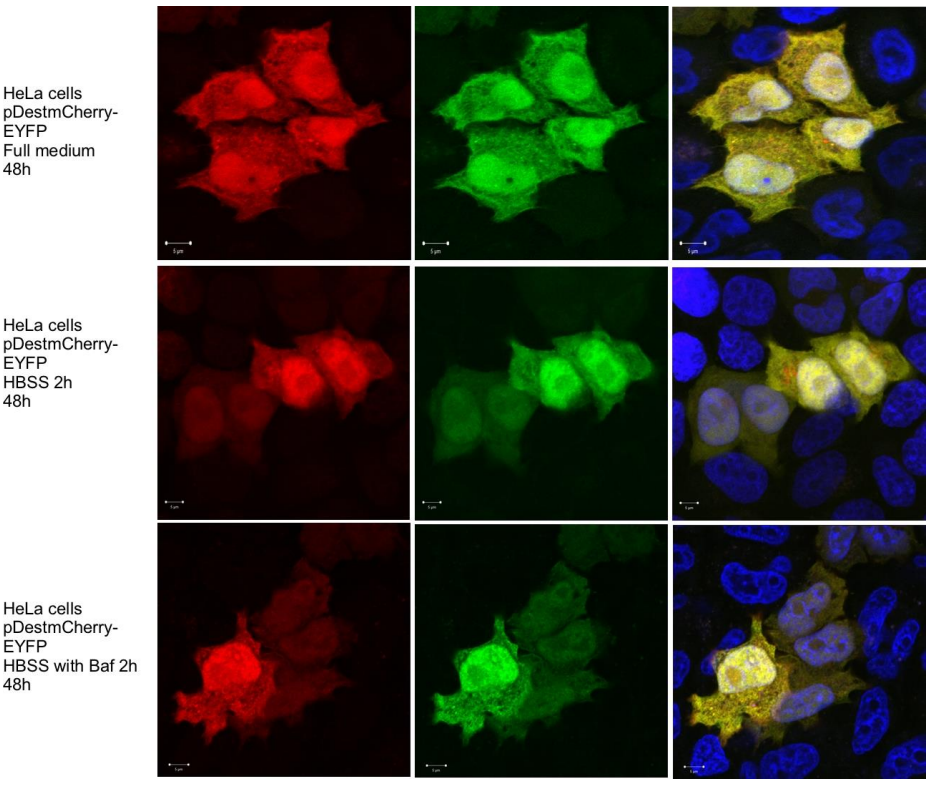
HeLa cells
pDestmCherry-
EYFP
Full medium
48h
HeLa cells
pDestmCherry-
EYFP
HBSS 2h
48h
HeLa cells
pDestmCherry-
EYFP
HBSS with Baf 2h
48h

Figure 43: mCherry-EYFP is diffuse and distributed in nucleus and cytoplasm in HeLa cells. HeLa cells were transfected with pDestmCherry-EYFP for 24 (A) and 48 (B) hours and treated with full medium, HBSS or HBSS with Baf for 2 hours, fixed with 4% PFA, stained with DAPI, mounted to coverslips and subjected to confocal fluorescence microscopy.

A

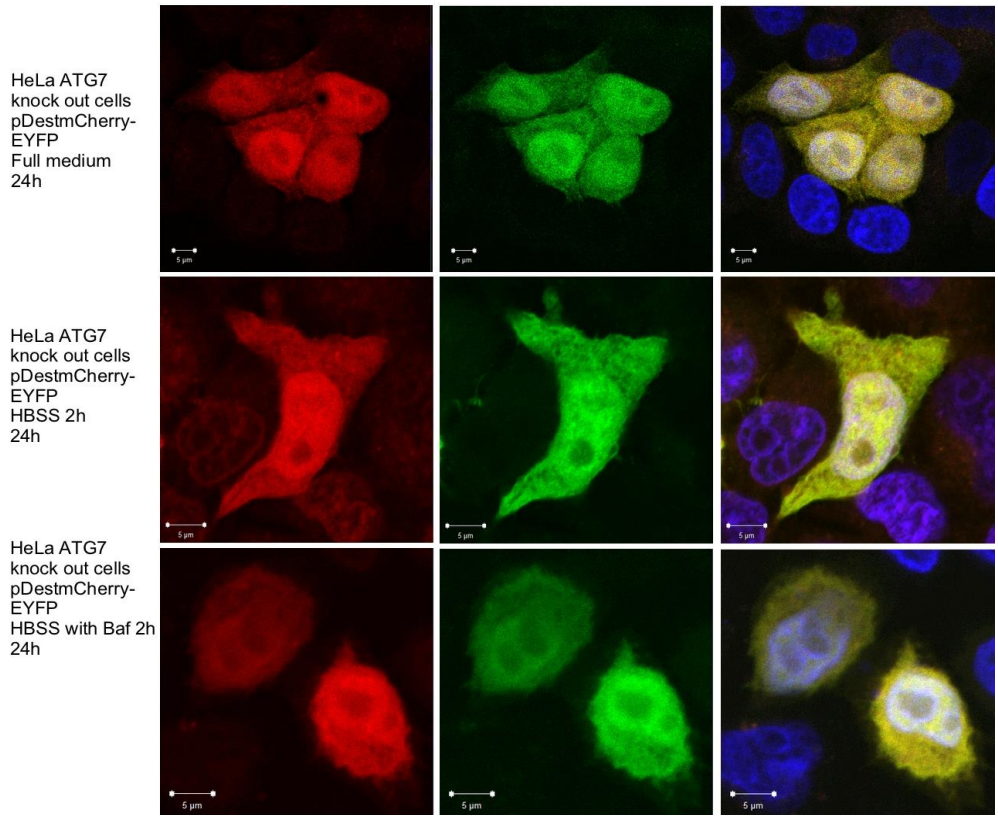

B

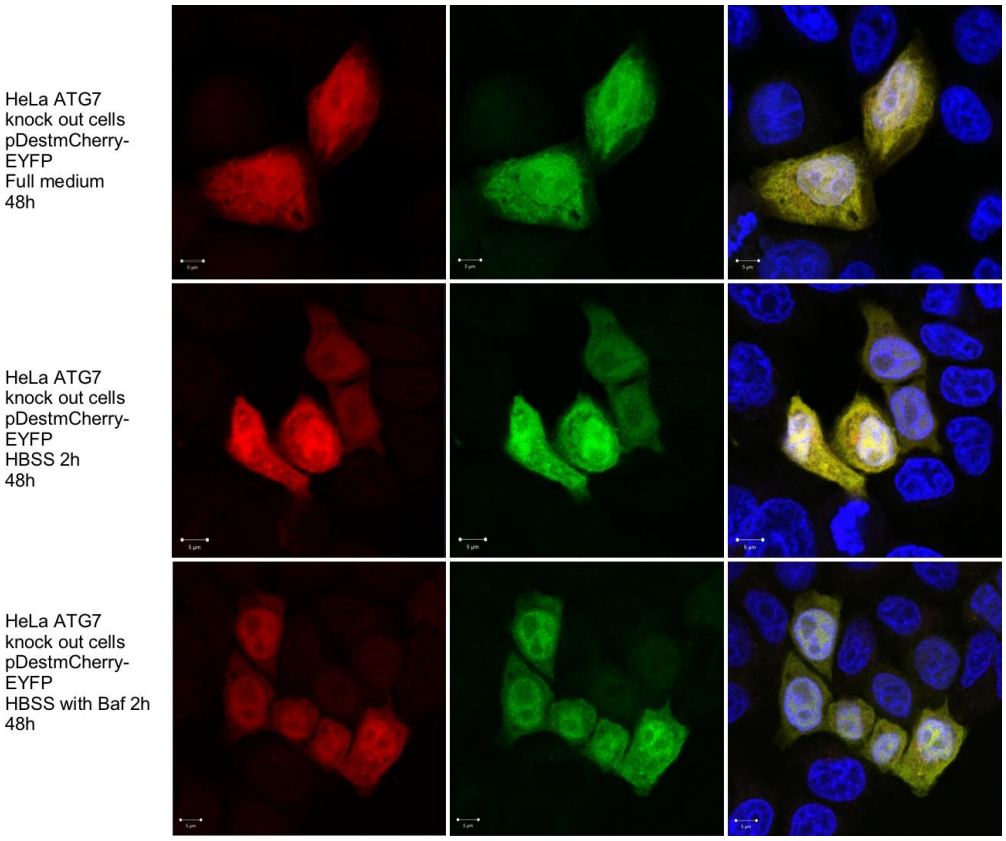

Figure 44: mCherry-EYFP is diffuse and distributed in nucleus and cytoplasm in HeLa ATG7 knock out cells. As for HeLa cells, HeLa ATG7 knock out cells were transfected with pDestmCherry-EYFP for 24 (A) and 48 (B) hours and treated as indicated.

mCherry-EYFP is diffusely distributed in the whole cell in all treatments of HeLa ATG7 KO cells in both the cells harvested after 24 and 48 hours. No red-only dots were detected.

<u>p62 assembles in aggregates and is degraded by autophagy</u>

The double-tagged p62 is used in experiments to check the transfection of the cells. Since p62 is known to be easily transfected into mammalian cells, make aggregates, and is degraded by autophagy, this protein is used as a positive control (Bjorkoy et al., 2005). The same method as described above was used to transfect HeLa (Figure 45) and HeLa ATG7 knock out (Figure 46) cells with pDestmCherry-EYFP p62 and visualize the cells in a confocal microscope.

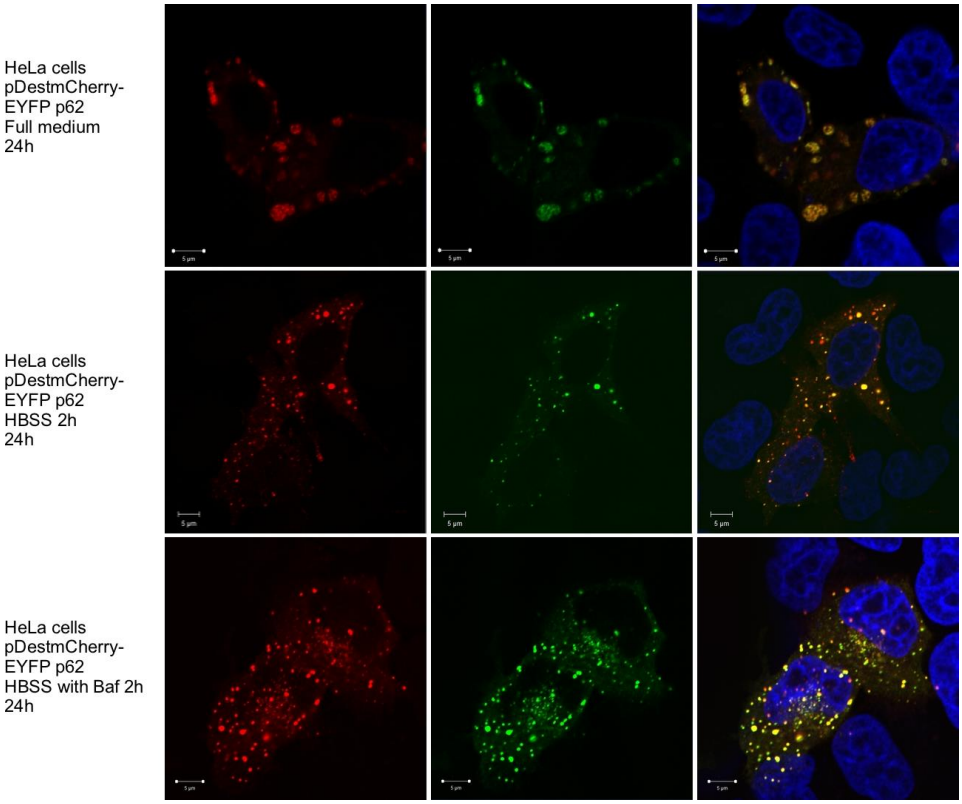

Figure 45: mCherry-EYFP p62 is degraded by autophagy in HeLa cells. HeLa cells were transfected with pDestmCherry-EYFP p62 for 24 hours. Many red-only dots were detected when cells were starved, and only a few were detected when HeLa cells were treated with full medium and with HBSS with Baf.

A

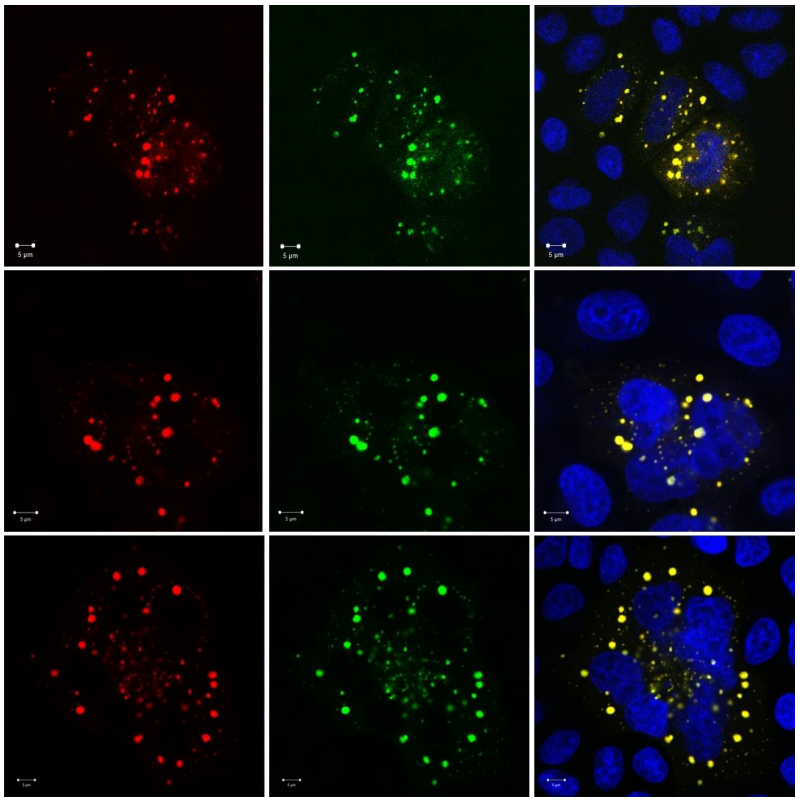
HeLa ATG7 knock out cells pDestmCherry-EYFP p62 Full medium 24h
HeLa ATG7 knock out cells pDestmCherry-EYFP p62 HBSS 2h 24h
HeLa ATG7 knock out cells pDestmCherry-EYFP p62 HBSS with Baf 2h 24h

B

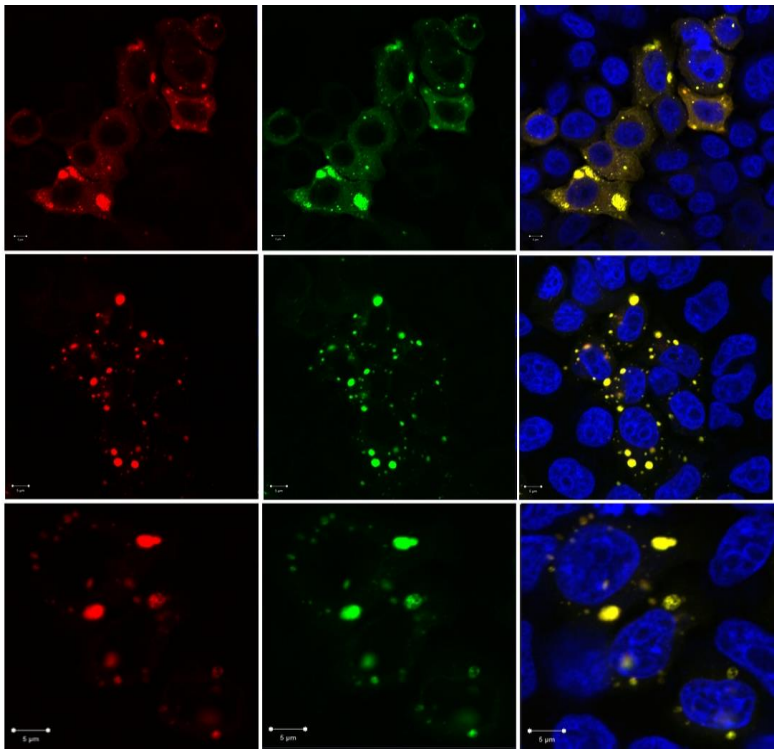
HeLa ATG7 knock out cells pDestmCherry-EYFP p62 Full medium 48h
HeLa ATG7 knock out cells pDestmCherry-EYFP p62 HBSS 2h 48h
HeLa ATG7 knock out cells pDestmCherry-EYFP p62 HBSS with Baf 2h 48h

Figure 46: mCherry-EYFP p62 degradation by autophagy is inhibited in HeLa ATG7 knock out cells. HeLa ATG7 knock out cells were transfected with pDestmCherry-EYFP p62 for 24 (A) and 48 (B) hours and treated as indicated. No red-only dots were detected.

pDestmCherry-EYFP p62 makes aggregates in HeLa and HeLa ATG7 knock out cell in all treatments. In starved HeLa cells, mCherry-EYFP-p62 formed red-only dots. In HeLa ATG7 knock out cells, autophagy is inhibited, and no red-only dots are shown.

5 Discussion and Conclusion

5.1 Both TRIM23 and TRIM31 Bind ATG8 Family Proteins

Many different TRIM proteins have been shown to play a part in autophagy by interacting with autophagy-related proteins (Hatakeyama, 2017). TRIM23 does not only contain a RING domain as most other TRIM proteins, but also an ARF domain which has GTPase activity (Hatakeyama, 2017). Both its E3 ubiquitin ligase and GTPase activity have shown importance in virus-induced autophagy, and the selective autophagy mediated by TBK1 and p62 (Sparrer et al., 2017). The ARF domain has also been shown to induce GFP-LC3B puncta formation (Mandell et al., 2014; Sparrer et al., 2017). TRIM31 is expressed in digestive tissues such as the colon and small intestine in humans (Sugiura & Miyamoto, 2008). Furthermore, TRIM31 makes punctate structures in association with the mitochondria and lysosome, and has been shown to promote lipopolysaccharide dependent autophagy independent of Atg5. TRIM31 also showed a direct binding to PE, and thereby induced autolysosome formation (Ra et al., 2016). In contrast to TRIM23, TRIM31 was shown to not induce GFP-LC3B puncta in the study performed by Sparrer et al. (Sparrer et al., 2017). From peptide arrays of TRIM23 and TRIM31 performed previous to this thesis (unpublished), both proteins were found to bind GABARAP.

Sparrer et al. found that TRIM23 induce GFP-LC3B puncta, both by cDNA screens and *in vivo* experiments (Sparrer et al., 2017). In this study, direct binding between TRIM23 and ATG8s was studied by GST pulldowns. According to the GST pulldown results, there was binding between TRIM23 and ATG8s. The inputs were 2.5%, and the percent binding to ATG8 proteins were adjusted to this in quantifications. It has previously not been known if TRIM23 binds ATG8s. Here, it is shown that there is a weak direct binding to ATG8s with GABARAP binding best of the ATG8s.

When Ra, et at., tried to find co-localization between LC3 and TRIM31 in HeLa cells, they found that there was indeed co-localization. In starved cells, the co-localization increased, and even in normal conditions there were a partly co-localization (Ra et al., 2016). In this study, direct binding between TRIM31 and ATG8s was studied. Results from GST pulldown assay

indicated that there was binding to all ATG8s. To further study these bindings, an *in vivo* study concerning co-localization between EGFP TRIM31 and some mCherry ATG8s were performed. The ATG8s included in this experiment were overexpressed, which may have altered the results. Here, TRIM31 was found to co-localize in most treatments of HeLa cells (full medium, starvation medium and full medium with Baf). More co-localizations were found upon starvation, which supports Ra et al. in their findings that TRIM31 and LC3 are co-localized in cytoplasm, and that there are more co-localization when cells are starved than in normal conditions (Ra et al., 2016). GABARAP also seems to follow this trend, and co-localize with TRIM31 both in full medium and when starved with HBSS for 2 hours.

5.2 LIR Dependent binding

The binding between TRIM31, and possibly also TRIM23, to ATG8s was suggested to be LIR dependent due to mapping of potential LIR motifs by peptide arrays performed before this thesis. By performing GST pulldown with GABARAP mutated in its LIR docking site (LDS), Y49A and F104A (Behrends et al., 2010), one might get an indication if the binding is LIR dependent. This experiment was performed both with TRIM23 and TRIM31. TRIM23 binding to GABARAP Y49A was significantly weaker than GABARAP WT. This indicates that Y49 is important in GABARAPs ability to bind TRIM23. TRIM31 on the other hand, did not get this reduction in binding from GABARAP WT to GABARAP Y49A but did get a reduction with GABARAP Y49A/F104A. This is a trend seen in many LIR interactions; both mutations must be present to inhibit the binding (Behrends et al., 2010).

To further study TRIM31 binding to ATG8s, TRIM31 was mutated in its LIRs (found from peptide array). Two mutants were made by site-directed mutagenesis; TRIM31 LIR2 mutant (F260A/L263A) and TRIM31 LIR1/LIR2 mutant (F185A/L188A/F260A/L263A). GST pulldown with TRIM31 WT, TRIM31 deficient in LIR2 and TRIM31 deficient in LIR1 and LIR2, showed that the binding was LIR dependent. More specific, the results indicated that LIR2 was the binding site for LC3A and GABARAP. Due to shortage of time there was not a possibility to repeat those experiments several times in order to verify this further. It has not been shown before that TRIM31 binds directly to ATG8 proteins via a LIR motif.

5.3 Degradation

It has previously been shown that proteins that bind cargos and deliver them for degradation also are degraded together with its cargo (Kimura et al., 2015; Liu et al., 2016). TRIM31 has previously been suggested to be degraded by the proteasome together with autolysosomes during lipopolysaccharide stimulation. Ra, et al. inhibited the proteasome with MG132, which lead to inhibition of TRIM31 degradation (Ra et al., 2016). In this thesis studying degradation of TRIM23 and TRIM31 was done by Western blot with cell lysates and by confocal fluorescence microscopy of cells transfected with pDestmCherry-EYFP fusion constructs to TRIM23 and TRIM31. Neither TRIM23 or TRIM31 indicated any stabilization by either Baf or MG132. This suggests that both TRIM23 and TRIM31 are degraded by both the lysosome and the proteasome (Rodriguez-Muela et al., 2018; Schreiber & Peter, 2014; Scotter et al., 2014; Urushitani et al., 2010), since both of them clearly are degraded upon starvation. Combined inhibition with simultaneously treatment of Baf and MG132 would reveal if both pathways are involved.

5.4 Future Perspective

TRIM23 and TRIM31 are both likely to be important proteins in autophagy with their E3 ligase activity and GTPase activity in TRIM23. This study showed that TRIM31 bind ATG8s by GST pulldown with *in vitro* translated protein. The binding was also LIR dependent. The binding between ATG8s and TRIM31 should be studied further to determine if both LIR motifs are involved or not in the direct binding. Also, co-localization between TRIM31 and three ATG8s were studied, where the results in this thesis suggest that there is co-localization. This co-localization experiment should be performed again with adjusted levels of ATG8s so that they are not too overexpressed. More GST pulldowns with TRIM23 should be performed to verify the binding. Also, TRIM23 should be included in *in vivo* experiments, to determine if there is binding to ATG8s. Neither TRIM23 or TRIM31 showed to be degraded by autophagy, but were both degraded upon starvation. Since binding to ATG8s often is LIR dependent, the suggested LIR motif from peptide array (G. Evjen and T. Johansen, unpublished) should therefore also be mutated to determine if a potential binding between ATG8s and TRIM23 is LIR dependent. The ARF motif of TRIM23 has also previously been suggested to be important in autophagy, and should also be studied further in experiments concerning TRIM23 and autophagy.

5.5 Conclusion

From the results in this thesis, TRIM23 and TRIM31 bind ATG8 proteins. This binding seems to be LIR-dependent. TRIM31 also co-localize with LC3A, LC3B and GABARAP in cells. Both TRIM23 and TRIM31 are degraded upon starvation. However, whether this degradation was mediated by autophagy or the proteasome, or both, cannot be determined from results in this thesis. TRIM23 and TRIM31 may regulate autophagy processes, and their involvement in autophagy processes should be studied further.

6 References

Abudu, Y. P. (2013). *Studies of the subcellular distribution og human ATG8 family proteins and their role in autophagy.* (Master), The University in Tromsø.

Alberts, B., Johnson, A., Lewis, J., Raff, M., Roberts, K., & Walter, P. (2008). *Molecular Biology of the Cell* (M. Anderson & S. Granum Eds. Fifth edition ed.). New York, USA: Garland Science.

Alemu, E. A., Lamark, T., Torgersen, K. M., Birgisdottir, A. B., Larsen, K. B., Jain, A., . . . Johansen, T. (2012). ATG8 family proteins act as scaffolds for assembly of the ULK complex: sequence requirements for LC3-interacting region (LIR) motifs. *J Biol Chem, 287*(47), 39275-39290. doi:10.1074/jbc.M112.378109

Autophagy. (2013). Retrieved from http://www.amsbio.com/autophagy.aspx

Behrends, C., Sowa, M. E., Gygi, S. P., & Harper, J. W. (2010). Network organization of the human autophagy system. *Nature, 466*(7302), 68-76. doi:10.1038/nature09204

Birgisdottir, A. B., Lamark, T., & Johansen, T. (2013). The LIR motif - crucial for selective autophagy. *J Cell Sci, 126*(Pt 15), 3237-3247. doi:10.1242/jcs.126128

Bjorkoy, G., Lamark, T., Brech, A., Outzen, H., Perander, M., Overvatn, A., . . . Johansen, T. (2005). p62/SQSTM1 forms protein aggregates degraded by autophagy and has a protective effect on huntingtin-induced cell death. *J Cell Biol, 171*(4), 603-614. doi:10.1083/jcb.200507002

Bjørkøy, G., Lamark, T., Pankiv, S., Øvervatn, A., Brech, A., & Johansen, T. (2009). Chapter 12 Monitoring Autophagic Degradation of p62/SQSTM1. *452*, 181-197. doi:10.1016/s0076-6879(08)03612-4

Blandin, G., Marchand, S., Charton, K., Daniele, N., Gicquel, E., Boucheteil, J. B., . . . Richard, I. (2013). A human skeletal muscle interactome centered on proteins involved in muscular dystrophies: LGMD interactome. *Skelet Muscle, 3*(1), 3. doi:10.1186/2044-5040-3-3

Borden, K. L. (2000). RING domains: master builders of molecular scaffolds? *J Mol Biol, 295*(5), 1103-1112. doi:10.1006/jmbi.1999.3429

Campbell, E. M., Weingart, J., Sette, P., Opp, S., Sastri, J., O'Connor, S. K., . . . Bouamr, F. (2015). TRIM5alpha-Mediated Ubiquitin Chain Conjugation Is Required for Inhibition of HIV-1 Reverse Transcription and Capsid Destabilization. *J Virol, 90*(4), 1849-1857. doi:10.1128/JVI.01948-15

Caprette, D. R. (1996, 12.06.2015). Principles of Spectrophotometry. Retrieved from http://www.ruf.rice.edu/~bioslabs/methods/protein/spectrophotometer.html

Carrigan, P. E., Ballar, P., & Tuzmen, S. (2011). Site-directed mutagenesis. *Methods Mol Biol, 700*, 107-124. doi:10.1007/978-1-61737-954-3_8

Cell counting using a Haemocytometer. Retrieved from https://www.phe-culturecollections.org.uk/technical/ccp/cellcounting.aspx

Chan, W. T., Verma, C. S., Lane, D. P., & Gan, S. K. (2013). A comparison and optimization of methods and factors affecting the transformation of Escherichia coli. *Biosci Rep, 33*(6). doi:10.1042/BSR20130098

Chude, C. I., & Amaravadi, R. K. (2017). Targeting Autophagy in Cancer: Update on Clinical Trials and Novel Inhibitors. *Int J Mol Sci, 18*(6). doi:10.3390/ijms18061279

Chung, C. T., & Miller, R. H. (1988). A rapid and convenient method for the preparation and storage of competent bacterial cells. *Nucleic Acids Res, 16*(8), 3580.

Coyle, J. E., Qamar, S., Rajashankar, K. R., & Nikolov, D. B. (2002). Structure of GABARAP in two conformations: implications for GABA(A) receptor localization and tubulin binding. *Neuron, 33*(1), 63-74. doi:10.1016/S0896-6273(01)00558-X

Crighton, D., Wilkinson, S., O'Prey, J., Syed, N., Smith, P., Harrison, P. R., . . . Ryan, K. M. (2006). DRAM, a p53-induced modulator of autophagy, is critical for apoptosis. *Cell, 126*(1), 121-134. doi:10.1016/j.cell.2006.05.034

Cuervo, A. M., & Dice, J. F. (1998). Lysosomes, a meeting point of proteins, chaperones, and proteases. *J Mol Med (Berl), 76*(1), 6-12.

Daido, S., Kanzawa, T., Yamamoto, A., Takeuchi, H., Kondo, Y., & Kondo, S. (2004). Pivotal role of the cell death factor BNIP3 in ceramide-induced autophagic cell death in malignant glioma cells. *Cancer Res, 64*(12), 4286-4293. doi:10.1158/0008-5472.CAN-03-3084

Davidovits, P., & Egger, M. D. (1973). Photomicrography of Corneal Endothelial Cells in vivo. *Nature, 244*(5415), 366-367. doi:10.1038/244366a0

Dawidziak, D. M., Sanchez, J. G., Wagner, J. M., Ganser-Pornillos, B. K., & Pornillos, O. (2017). Structure and catalytic activation of the TRIM23 RING E3 ubiquitin ligase. *Proteins, 85*(10), 1957-1961. doi:10.1002/prot.25348

Demarchi, F., Bertoli, C., Copetti, T., Tanida, I., Brancolini, C., Eskelinen, E. L., & Schneider, C. (2006). Calpain is required for macroautophagy in mammalian cells. *J Cell Biol, 175*(4), 595-605. doi:10.1083/jcb.200601024

Djavaheri-Mergny, M., Amelotti, M., Mathieu, J., Besancon, F., Bauvy, C., Souquere, S., . . . Codogno, P. (2006). NF-kappaB activation represses tumor necrosis factor-alpha-induced autophagy. *J Biol Chem, 281*(41), 30373-30382. doi:10.1074/jbc.M602097200

Dryden, D. T. (2013). The architecture of restriction enzymes. *Structure, 21*(10), 1720-1721. doi:10.1016/j.str.2013.09.009

Freemont, P. S. (2000). Ubiquitination: RING for destruction? *Current Biology, 10*(2), R84-R87. doi:10.1016/s0960-9822(00)00287-6

Fujifilm BAS-5000 from FUJIFILM Life Science. Retrieved from http://www.bio-medicine.org/biology-products/Fujifilm-BAS-5000-from-FUJIFILM--Life-Science-1761-1/

Funderburk, S. F., Wang, Q. J., & Yue, Z. (2010). The Beclin 1-VPS34 complex--at the crossroads of autophagy and beyond. *Trends Cell Biol, 20*(6), 355-362. doi:10.1016/j.tcb.2010.03.002

Fusco, C., Micale, L., Egorov, M., Monti, M., D'Addetta, E. V., Augello, B., . . . Merla, G. (2012). The E3-ubiquitin ligase TRIM50 interacts with HDAC6 and p62, and promotes the sequestration and clearance of ubiquitinated proteins into the aggresome. *PLoS One, 7*(7), e40440. doi:10.1371/journal.pone.0040440

Gallouet, A. S., Ferri, F., Petit, V., Parcelier, A., Lewandowski, D., Gault, N., . . . Romeo, P. H. (2017). Macrophage production and activation are dependent on TRIM33. *Oncotarget, 8*(3), 5111-5122. doi:10.18632/oncotarget.13872

Glick, D., Barth, S., & Macleod, K. F. (2010). Autophagy: cellular and molecular mechanisms. *J Pathol, 221*(1), 3-12. doi:10.1002/path.2697

Griffith, F. (1928). The Significance of Pneumococcal Types. *J Hyg (Lond), 27*(2), 113-159.

Guo, P., Ma, X., Zhao, W., Huai, W., Li, T., Qiu, Y., . . . Han, L. (2017). TRIM31 is upregulated in hepatocellular carcinoma and promotes disease progression by inducing ubiquitination of TSC1-TSC2 complex. *Oncogene*. doi:10.1038/onc.2017.349

Hanahan, D. (1983). Studies on transformation of Escherichia coli with plasmids. *J Mol Biol, 166*(4), 557-580.

Hatakeyama, S. (2017). TRIM Family Proteins: Roles in Autophagy, Immunity, and Carcinogenesis. *Trends Biochem Sci, 42*(4), 297-311. doi:10.1016/j.tibs.2017.01.002

Heim, R., Cubitt, A. B., & Tsien, R. Y. (1995). Improved green fluorescence. *Nature, 373*(6516), 663-664. doi:10.1038/373663b0

Hoyer-Hansen, M., Bastholm, L., Szyniarowski, P., Campanella, M., Szabadkai, G., Farkas, T., . . . Jaattela, M. (2007). Control of macroautophagy by calcium, calmodulin-dependent kinase kinase-beta, and Bcl-2. *Mol Cell, 25*(2), 193-205. doi:10.1016/j.molcel.2006.12.009

Imam, S., Talley, S., Nelson, R. S., Dharan, A., O'Connor, C., Hope, T. J., & Campbell, E. M. (2016). TRIM5alpha Degradation via Autophagy Is Not Required for Retroviral Restriction. *J Virol, 90*(7), 3400-3410. doi:10.1128/JVI.03033-15

Jain, A., Lamark, T., Sjottem, E., Larsen, K. B., Awuh, J. A., Overvatn, A., . . . Johansen, T. (2010). p62/SQSTM1 is a target gene for transcription factor NRF2 and creates a positive feedback loop by inducing antioxidant response element-driven gene transcription. *J Biol Chem, 285*(29), 22576-22591. doi:10.1074/jbc.M110.118976

Jarvik, J. W., & Telmer, C. A. (1998). Epitope tagging. *Annu Rev Genet, 32*, 601-618. doi:10.1146/annurev.genet.32.1.601

Johansen, T., Birgisdottir, A. B., Huber, J., Kniss, A., Dotsch, V., Kirkin, V., & Rogov, V. V. (2017). Methods for Studying Interactions Between Atg8/LC3/GABARAP and LIR-Containing Proteins. *Methods Enzymol, 587*, 143-169. doi:10.1016/bs.mie.2016.10.023

Johansen, T., & Lamark, T. (2011). Selective autophagy mediated by autophagic adapter proteins. *Autophagy, 7*(3), 279-296. doi:10.4161/auto.7.3.14487

Jung, C. H., Ro, S. H., Cao, J., Otto, N. M., & Kim, D. H. (2010). mTOR regulation of autophagy. *FEBS Lett, 584*(7), 1287-1295. doi:10.1016/j.febslet.2010.01.017

Kabeya, Y., Mizushima, N., Ueno, T., Yamamoto, A., Kirisako, T., Noda, T., . . . Yoshimori, T. (2000). LC3, a mammalian homologue of yeast Apg8p, is localized in autophagosome membranes after processing. *EMBO J, 19*(21), 5720-5728. doi:10.1093/emboj/19.21.5720

Khan, M. M., Strack, S., Wild, F., Hanashima, A., Gasch, A., Brohm, K., . . . Rudolf, R. (2014). Role of autophagy, SQSTM1, SH3GLB1, and TRIM63 in the turnover of nicotinic acetylcholine receptors. *Autophagy, 10*(1), 123-136. doi:10.4161/auto.26841

Kimura, T., Jain, A., Choi, S. W., Mandell, M. A., Johansen, T., & Deretic, V. (2016). TRIM-Directed Selective Autophagy Regulates Immune Activation. *Autophagy*, 0. doi:10.1080/15548627.2016.1154254

Kimura, T., Jain, A., Choi, S. W., Mandell, M. A., Schroder, K., Johansen, T., & Deretic, V. (2015). TRIM-mediated precition autophagy targets cytoplasmic regulators of innate immunity. *The Journal of Cell Biology, 210*(6), 973-989.

Kimura, T., Jia, J., Claude-Taupin, A., Kumar, S., Choi, S. W., Gu, Y., . . . Deretic, V. (2017). Cellular and molecular mechanism for secretory autophagy. *Autophagy*, 1-2. doi:10.1080/15548627.2017.1307486

Kimura, T., Jia, J., Kumar, S., Choi, S. W., Gu, Y., Mudd, M., . . . Deretic, V. (2017). Dedicated SNAREs and specialized TRIM cargo receptors mediate secretory autophagy. *EMBO J, 36*(1), 42-60. doi:10.15252/embj.201695081

Kimura, T., Mandell, M., & Deretic, V. (2016). Precision autophagy directed by receptor regulators - emerging examples within the TRIM family. *J Cell Sci, 129*(5), 881-891. doi:10.1242/jcs.163758

Klionsky, D. J. (2005). The molecular machinery of autophagy: unanswered questions. *J Cell Sci, 118*(Pt 1), 7-18. doi:10.1242/jcs.01620

Klionsky, D. J., Cregg, J. M., Dunn, W. A., Jr., Emr, S. D., Sakai, Y., Sandoval, I. V., . . . Ohsumi, Y. (2003). A unified nomenclature for yeast autophagy-related genes. *Dev Cell, 5*(4), 539-545. doi:10.1016/s1534-5807(03)00296-x

Knaevelsrud, H., & Simonsen, A. (2010). Fighting disease by selective autophagy of aggregate-prone proteins. *FEBS Lett, 584*(12), 2635-2645. doi:10.1016/j.febslet.2010.04.041

Korolchuk, V. I., Mansilla, A., Menzies, F. M., & Rubinsztein, D. C. (2009). Autophagy inhibition compromises degradation of ubiquitin-proteasome pathway substrates. *Mol Cell, 33*(4), 517-527. doi:10.1016/j.molcel.2009.01.021

Kumar, S., Chauhan, S., Jain, A., Ponpuak, M., Choi, S. W., Mudd, M., . . . Deretic, V. (2017). Galectins and TRIMs directly interact and orchestrate autophagic response to endomembrane damage. *Autophagy*, 1-2. doi:10.1080/15548627.2017.1307487

Kunz, J. B., Schwarz, H., & Mayer, A. (2004). Determination of four sequential stages during microautophagy in vitro. *J Biol Chem, 279*(11), 9987-9996. doi:10.1074/jbc.M307905200

Kurien, B. T., & Scofield, R. H. (2006). Western blotting. *Methods, 38*(4), 283-293. doi:10.1016/j.ymeth.2005.11.007

Lamb, C. A., Yoshimori, T., & Tooze, S. A. (2013). The autophagosome: origins unknown, biogenesis complex. *Nat Rev Mol Cell Biol, 14*(12), 759-774. doi:10.1038/nrm3696

Lazarou, M., Sliter, D. A., Kane, L. A., Sarraf, S. A., Wang, C., Burman, J. L., . . . Youle, R. J. (2015). The ubiquitin kinase PINK1 recruits autophagy receptors to induce mitophagy. *Nature, 524*(7565), 309-314. doi:10.1038/nature14893

Levine, B., & Klionsky, D. J. (2004). Development by Self-Digestion. *Developmental Cell, 6*(4), 463-477. doi:10.1016/s1534-5807(04)00099-1

Levine, B., & Kroemer, G. (2008). Autophagy in the pathogenesis of disease. *Cell, 132*(1), 27-42. doi:10.1016/j.cell.2007.12.018

Li, H., Zhang, Y., Zhang, Y., Bai, X., Peng, Y., & He, P. (2014). TRIM31 is downregulated in non-small cell lung cancer and serves as a potential tumor suppressor. *Tumor Biology, 35*(6), 5747-5752. doi:10.1007/s13277-014-1763-x

Li, J., Li, C., Xiao, W., Yuan, D., Wan, G., & Ma, L. (2008). Site-directed mutagenesis by combination of homologous recombination and DpnI digestion of the plasmid template in Escherichia coli. *Anal Biochem, 373*(2), 389-391. doi:10.1016/j.ab.2007.10.034

Lippai, M., & Low, P. (2014). The role of the selective adaptor p62 and ubiquitin-like proteins in autophagy. *Biomed Res Int, 2014*, 832704. doi:10.1155/2014/832704

Liu, W. J., Ye, L., Huang, W. F., Guo, L. J., Xu, Z. G., Wu, H. L., . . . Liu, H. F. (2016). p62 links the autophagy pathway and the ubiqutin-proteasome system upon ubiquitinated protein degradation. *Cell Mol Biol Lett, 21*, 29. doi:10.1186/s11658-016-0031-z

Lucey, B. P., Nelson-Rees, W. A., & Hutchins, G. M. (2009). Henrietta Lacks, HeLa cells, and cell culture contamination. *Arch Pathol Lab Med, 133*(9), 1463-1467. doi:10.1043/1543-2165-133.9.1463

Majeski, A. E., & Dice, J. F. (2004). Mechanisms of chaperone-mediated autophagy. *Int J Biochem Cell Biol, 36*(12), 2435-2444. doi:10.1016/j.biocel.2004.02.013

Mandel, M., & Higa, A. (1970). Calcium-dependent bacteriophage DNA infection. *J Mol Biol, 53*(1), 159-162.

Mandell, M. A., Jain, A., Arko-Mensah, J., Chauhan, S., Kimura, T., Dinkins, C., . . . Deretic, V. (2014). TRIM proteins regulate autophagy and can target autophagic substrates by direct recognition. *Dev Cell, 30*(4), 394-409. doi:10.1016/j.devcel.2014.06.013

Mandell, M. A., Jain, A., Kumar, S., Castleman, M. J., Anwar, T., Eskelinen, E.-L., . . . Deretic, V. (2016). TRIM17 contributes to autophagy of midbodies while actively sparing targets from degradation. doi:10.1242/jcs.190017

Mandell, M. A., Jain, A., Kumar, S., Castleman, M. J., Anwar, T., Eskelinen, E. L., . . . Deretic, V. (2017). Correction: TRIM17 contributes to autophagy of midbodies while actively sparing other targets from degradation. *J Cell Sci, 130*(6), 1194. doi:10.1242/jcs.202499

Mandell, M. A., Kimura, T., Jain, A., Johansen, T., & Deretic, V. (2015). TRIM proteins regulate autophagy: TRIM5 is a selective autophagy receptor mediating HIV-1 restriction. *Autophagy, 10*(12), 2387-2388.

Martens, S. (2016). No ATG8s, no problem? How LC3/GABARAP proteins contribute to autophagy. *J Cell Biol, 215*(6), 761-763. doi:10.1083/jcb.201611116

Masters, S. L., Simon, A., Aksentijevich, I., & Kastner, D. L. (2009). Horror autoinflammaticus: the molecular pathophysiology of autoinflammatory disease (*). *Annu Rev Immunol, 27*, 621-668. doi:10.1146/annurev.immunol.25.022106.141627

Meley, D., Bauvy, C., Houben-Weerts, J. H., Dubbelhuis, P. F., Helmond, M. T., Codogno, P., & Meijer, A. J. (2006). AMP-activated protein kinase and the regulation of autophagic proteolysis. *J Biol Chem, 281*(46), 34870-34879. doi:10.1074/jbc.M605488200

Mills, K. R., Reginato, M., Debnath, J., Queenan, B., & Brugge, J. S. (2004). Tumor necrosis factor-related apoptosis-inducing ligand (TRAIL) is required for induction of autophagy during lumen formation in vitro. *Proc Natl Acad Sci U S A, 101*(10), 3438-3443. doi:10.1073/pnas.0400443101

Minsky, M. (1988). Memoir on inventing the confocal scanning microscope. *Scanning, 10*(4), 128-138. doi:10.1002/sca.4950100403

Mizushima, N. (2007). Autophagy: process and function. *Genes Dev, 21*(22), 2861-2873. doi:10.1101/gad.1599207

Modulators of Autophagy Signaling. Retrieved from https://www.bio-connect.nl/modulators-of-autophagy-signaling/cnt/page/4444

Mullis, K., Faloona, F., Scharf, S., Saiki, R., Horn, G., & Erlich, H. (1986). Specific enzymatic amplification of DNA in vitro: the polymerase chain reaction. *Cold Spring Harb Symp Quant Biol, 51 Pt 1*, 263-273.

Nagai, T., Ibata, K., Park, E. S., Kubota, M., Mikoshiba, K., & Miyawaki, A. (2002). A variant of yellow fluorescent protein with fast and efficient maturation for cell-biological applications. *Nat Biotechnol, 20*(1), 87-90. doi:10.1038/nbt0102-87

Nazarko, V. Y., & Zhong, Q. (2013). ULK1 targets Beclin-1 in autophagy. *Nat Cell Biol, 15*(7), 727-728. doi:10.1038/ncb2797

Nguyen, T. N., Padman, B. S., Usher, J., Oorschot, V., Ramm, G., & Lazarou, M. (2016). Atg8 family LC3/GABARAP proteins are crucial for autophagosome-lysosome fusion but not autophagosome formation during PINK1/Parkin mitophagy and starvation. *J Cell Biol, 215*(6), 857-874. doi:10.1083/jcb.201607039

Noda, N. N., Kumeta, H., Nakatogawa, H., Satoo, K., Adachi, W., Ishii, J., . . . Inagaki, F. (2008). Structural basis of target recognition by Atg8/LC3 during selective autophagy. *Genes Cells, 13*(12), 1211-1218. doi:10.1111/j.1365-2443.2008.01238.x

Noguchi, K., Okumura, F., Takahashi, N., Kataoka, A., Kamiyama, T., Todo, S., & Hatakeyama, S. (2011). TRIM40 promotes neddylation of IKKgamma and is downregulated in gastrointestinal cancers. *Carcinogenesis, 32*(7), 995-1004. doi:10.1093/carcin/bgr068

Noireaux, V., Bar-Ziv, R., & Libchaber, A. (2003). Principles of cell-free genetic circuit assembly. *Proc Natl Acad Sci U S A, 100*(22), 12672-12677. doi:10.1073/pnas.2135496100

Ohsumi, Y. (2014). Historical landmarks of autophagy research. *Cell Res, 24*(1), 9-23. doi:10.1038/cr.2013.169

Overview of Western Blotting. Retrieved from https://www.thermofisher.com/no/en/home/life-science/protein-biology/protein-biology-learning-center/protein-biology-resource-library/pierce-protein-methods/overview-western-blotting.html

Panja, S., Saha, S., Jana, B., & Basu, T. (2006). Role of membrane potential on artificial transformation of E. coli with plasmid DNA. *J Biotechnol, 127*(1), 14-20. doi:10.1016/j.jbiotec.2006.06.008

Pankiv, S., Clausen, T. H., Lamark, T., Brech, A., Bruun, J. A., Outzen, H., . . . Johansen, T. (2007). p62/SQSTM1 binds directly to Atg8/LC3 to facilitate degradation of ubiquitinated protein aggregates by autophagy. *J Biol Chem, 282*(33), 24131-24145. doi:10.1074/jbc.M702824200

PCR. Retrieved from http://ib.bioninja.com.au/standard-level/topic-3-genetics/35-genetic-modification-and/pcr.html

Phelan, M. C. (2007). Basic techniques in mammalian cell tissue culture. *Curr Protoc Cell Biol, Chapter 1*, Unit 1 1. doi:10.1002/0471143030.cb0101s36

Pickart, C. M. (2001). Mechanisms underlying ubiquitination. *Annu Rev Biochem, 70*, 503-533. doi:10.1146/annurev.biochem.70.1.503

Pineda, C. T., & Potts, P. R. (2015). Oncogenic MAGEA-TRIM28 ubiquitin ligase downregulates autophagy by ubiquitinating and degrading AMPK in cancer. *Autophagy, 11*(5), 844-846. doi:10.1080/15548627.2015.1034420

Protein assay technical handbook. Retrieved from http://assets.thermofisher.com/TFS-Assets/LSG/brochures/protein-assay-technical-handook.pdf

Pyo, J. O., Jang, M. H., Kwon, Y. K., Lee, H. J., Jun, J. I., Woo, H. N., . . . Jung, Y. K. (2005). Essential roles of Atg5 and FADD in autophagic cell death: dissection of autophagic cell death into vacuole formation and cell death. *J Biol Chem, 280*(21), 20722-20729. doi:10.1074/jbc.M413934200

Ra, E. A., Lee, T. A., Won Kim, S., Park, A., Choi, H. J., Jang, I., . . . Park, B. (2016). TRIM31 promotes Atg5/Atg7-independent autophagy in intestinal cells. *Nat Commun, 7*, 11726. doi:10.1038/ncomms11726

Reece-Hoyes, J. S., & Walhout, A. J. M. (2018). Gateway Recombinational Cloning. *Cold Spring Harb Protoc, 2018*(1), pdb top094912. doi:10.1101/pdb.top094912

Reef, S., Zalckvar, E., Shifman, O., Bialik, S., Sabanay, H., Oren, M., & Kimchi, A. (2006). A short mitochondrial form of p19ARF induces autophagy and caspase-independent cell death. *Mol Cell, 22*(4), 463-475. doi:10.1016/j.molcel.2006.04.014

Ribeiro, C. M., Sarrami-Forooshani, R., Setiawan, L. C., Zijlstra-Willems, E. M., van Hamme, J. L., Tigchelaar, W., . . . Geijtenbeek, T. B. (2016). Receptor usage dictates HIV-1 restriction by human TRIM5alpha in dendritic cell subsets. *Nature, 540*(7633), 448-452. doi:10.1038/nature20567

Roberts, R. J., Belfort, M., Bestor, T., Bhagwat, A. S., Bickle, T. A., Bitinaite, J., . . . Xu, S. Y. (2003). SURVEY AND SUMMARY: A nomenclature for restriction enzymes, DNA methyltransferases, homing endonucleases and their genes. *Nucleic Acids Research, 31*(7), 1805-1812.

Rodriguez-Muela, N., Parkhitko, A., Grass, T., Gibbs, R. M., Norabuena, E. M., Perrimon, N., . . . Rubin, L. L. (2018). Blocking p62/SQSTM1-dependent SMN degradation ameliorates Spinal Muscular Atrophy disease phenotypes. *J Clin Invest*. doi:10.1172/JCI95231

Rogov, V., Dotsch, V., Johansen, T., & Kirkin, V. (2014). Interactions between autophagy receptors and ubiquitin-like proteins form the molecular basis for selective autophagy. *Mol Cell, 53*(2), 167-178. doi:10.1016/j.molcel.2013.12.014

Saiki, R., Scharf, S., Faloona, F., Mullis, K., Horn, G., Erlich, H., & Arnheim, N. (1985). Enzymatic amplification of beta-globin genomic sequences and restriction site analysis for

diagnosis of sickle cell anemia. *Science, 230*(4732), 1350-1354. doi:10.1126/science.2999980

Sarkar, S., Floto, R. A., Berger, Z., Imarisio, S., Cordenier, A., Pasco, M., . . . Rubinsztein, D. C. (2005). Lithium induces autophagy by inhibiting inositol monophosphatase. *J Cell Biol, 170*(7), 1101-1111. doi:10.1083/jcb.200504035

Schafer, F., Seip, N., Maertens, B., Block, H., & Kubicek, J. (2015). Purification of GST-Tagged Proteins. *Methods Enzymol, 559*, 127-139. doi:10.1016/bs.mie.2014.11.005

Schreiber, A., & Peter, M. (2014). Substrate recognition in selective autophagy and the ubiquitin-proteasome system. *Biochim Biophys Acta, 1843*(1), 163-181. doi:10.1016/j.bbamcr.2013.03.019

Scotter, E. L., Vance, C., Nishimura, A. L., Lee, Y. B., Chen, H. J., Urwin, H., . . . Shaw, C. E. (2014). Differential roles of the ubiquitin proteasome system and autophagy in the clearance of soluble and aggregated TDP-43 species. *J Cell Sci, 127*(Pt 6), 1263-1278. doi:10.1242/jcs.140087

SDS-PAGE (PolyAcrylamide Gel Electrophoresis). (2001). Retrieved from http://www.bio.davidson.edu/courses/genomics/method/sdspage/sdspage.html

Shaner, N. C., Campbell, R. E., Steinbach, P. A., Giepmans, B. N., Palmer, A. E., & Tsien, R. Y. (2004). Improved monomeric red, orange and yellow fluorescent proteins derived from Discosoma sp. red fluorescent protein. *Nat Biotechnol, 22*(12), 1567-1572. doi:10.1038/nbt1037

Shang, Y., Zhang, N., Zhu, P., Luo, Y., Huang, K., Tian, W., & Xu, W. (2014). Restriction enzyme cutting site distribution regularity for DNA looping technology. *Gene, 534*(2), 222-228. doi:10.1016/j.gene.2013.10.054

Shashkova, S., & Leake, M. C. (2017). Single-molecule fluorescence microscopy review: shedding new light on old problems. *Biosci Rep, 37*(4). doi:10.1042/BSR20170031

Shibata, M., Sato, T., Nukiwa, R., Ariga, T., & Hatakeyama, S. (2012). TRIM45 negatively regulates NF-kappaB-mediated transcription and suppresses cell proliferation. *Biochemical and Biophysical Research Communications, 423*(1), 104-109. doi:10.1016/j.bbrc.2012.05.090

Shpilka, T., Weidberg, H., Pietrokovski, S., & Elazar, Z. (2011). Atg8: an autophagy-related ubiquitin-like protein family. *Genome Biol, 12*(7), 226. doi:10.1186/gb-2011-12-7-226

Smith, D. B., & Johnson, K. S. (1988). Single-step purification of polypeptides expressed in Escherichia coli as fusions with glutathione S-transferase. *Gene, 67*(1), 31-40. doi:10.1016/0378-1119(88)90005-4

Sparrer, K. M. J., Gableske, S., Zurenski, M. A., Parker, Z. M., Full, F., Baumgart, G. J., . . . Gack, M. U. (2017). TRIM23 mediates virus-induced autophagy via activation of TBK1. *Nat Microbiol, 2*(11), 1543-1557. doi:10.1038/s41564-017-0017-2

Stremlau, M., Owens, C. M., Perron, M. J., Kiessling, M., Autissier, P., & Sodroski, J. (2004). The cytoplasmic body component TRIM5alpha restricts HIV-1 infection in Old World monkeys. *Nature, 427*(6977), 848-853. doi:10.1038/nature02343

Sugiura, T., & Miyamoto, K. (2008). Characterization of TRIM31, upregulated in gastric adenocarcinoma, as a novel RBCC protein. *J Cell Biochem, 105*(4), 1081-1091. doi:10.1002/jcb.21908

Sundquist, T. (2006). Optimize Your TNT(R) Reticulocyte Systems Reaction *American Medical Association*.

Thooft, A. M., Cassaidy, K., & VanVeller, B. (2017). A Small Push-Pull Fluorophore for Turn-on Fluorescence. *J Org Chem, 82*(17), 8842-8847. doi:10.1021/acs.joc.7b00939

TNT(R) Coupled Reticulocyte Lysate Systems. Promega.

Tomar, D., Prajapati, P., Sripada, L., Singh, K., Singh, R., Singh, A. K., & Singh, R. (2013). TRIM13 regulates caspase-8 ubiquitination, translocation to autophagosomes and activation during ER stress induced cell death. *Biochim Biophys Acta, 1833*(12), 3134-3144. doi:10.1016/j.bbamcr.2013.08.021

Tomar, D., & Singh, R. (2014). TRIM13 regulates ubiquitination and turnover of NEMO to suppress TNF induced NF-kappaB activation. *Cell Signal, 26*(12), 2606-2613. doi:10.1016/j.cellsig.2014.08.008

Tomar, D., Singh, R., Singh, A. K., Pandya, C. D., & Singh, R. (2012). TRIM13 regulates ER stress induced autophagy and clonogenic ability of the cells. *Biochimica et Biophysica Acta (BBA) - Molecular Cell Research, 1823*(2), 316-326. doi:10.1016/j.bbamcr.2011.11.015

Towbin, H., Staehelin, T., & Gordon, J. (1979). Electrophoretic transfer of proteins from polyacrylamide gels to nitrocellulose sheets: Procedure and some applications. *Proc. Natl. Acad. Sci. USA, 76*(9), 4350-4354.

Tsuboyama, K., Koyama-Honda, I., Sakamaki, Y., Koike, M., Morishita, H., & Mizushima, N. (2016). The ATG conjugation systems are important for degradation of the inner

autophagosomal membrane. *Science, 354*(6315), 1036-1041. doi:10.1126/science.aaf6136

Tsukada, M., & Ohsumi, Y. (1993). Isolation and characterization of autophagy-defective mutants of Saccharomyces cerevisiae. *FEBS Letters, 333*(1,2), 169-174.

Urushitani, M., Sato, T., Bamba, H., Hisa, Y., & Tooyama, I. (2010). Synergistic effect between proteasome and autophagosome in the clearance of polyubiquitinated TDP-43. *J Neurosci Res, 88*(4), 784-797. doi:10.1002/jnr.22243

van Beek, N., Klionsky, D. J., & Reggiori, F. (2018). Genetic aberrations in macroautophagy genes leading to diseases. *Biochim Biophys Acta, 1865*(5), 803-816. doi:10.1016/j.bbamcr.2018.03.002

Wang, Y., Li, Y., Qi, X., Yuan, W., Ai, J., Zhu, C., . . . Liu, M. (2004). TRIM45, a novel human RBCC/TRIM protein, inhibits transcriptional activities of ElK-1 and AP-1. *Biochem Biophys Res Commun, 323*(1), 9-16. doi:10.1016/j.bbrc.2004.08.048

Watanabe, M., Takahashi, H., Saeki, Y., Ozaki, T., Itoh, S., Suzuki, M., . . . Hatakeyama, S. (2015). The E3 ubiquitin ligase TRIM23 regulates adipocyte differentiation via stabilization of the adipogenic activator PPARgamma. *Elife, 4*, e05615. doi:10.7554/eLife.05615

Xie, Z., & Klionsky, D. J. (2007). Autophagosome formation: core machinery and adaptations. *Nat Cell Biol, 9*(10), 1102-1109. doi:10.1038/ncb1007-1102

Yamamoto, A., Tagawa, Y., Yoshimori, T., Moriyama, Y., Masaki, R., & Tashiro, Y. (1998). Bafilomycin A1 Prevents Maturation of Autophagic Vacuoles by Inhibiting Fusion between Autophagosomes and Lysosomes in Rat Hepatoma Cell Line, H-4-II-E Cells. *Cell Structure and Function, 23*(1), 33-42. doi:10.1247/csf.23.33

Yang, Y., Fiskus, W., Yong, B., Atadja, P., Takahashi, Y., Pandita, T. K., . . . Bhalla, K. N. (2013). Acetylated hsp70 and KAP1-mediated Vps34 SUMOylation is required for autophagosome creation in autophagy. *Proc Natl Acad Sci U S A, 110*(17), 6841-6846. doi:10.1073/pnas.1217692110

Yang, Z., & Xiong, H.-R. (2012). Culture Conditions and Types of Growth Media for Mammalian Cells. doi:10.5772/52301

Zhang, J., Johnson, J. L., He, J., Napolitano, G., Ramadass, M., Rocca, C., . . . Catz, S. D. (2017). Cystinosin, the small GTPase Rab11, and the Rab7 effector RILP regulate intracellular trafficking of the chaperone-mediated autophagy receptor LAMP2A. *J Biol Chem*. doi:10.1074/jbc.M116.764076